Functional characterization of the alveolins, a family of cytoskeleton proteins of malaria parasites

Fatimah Al-Khattaf

Supervisor: Dr Johannes Dessens

Department of Pathogen and Molecular Biology

Faculty of Infectious and Tropical Diseases

London School of Hygiene and Tropical Medicine

March 2016

Thesis submitted for the degree of Doctor of Philosophy

Dedication

الى امى الحبيبه فعلت المستحيل لاحقق ما رددتى لى بغرفه الطوراى" انا ام الدكتوره "نعم الان تحقق لك ما رغبتى به لك الفضل وما فعلت الا القليل بحقك فابقى راضيه ولا تفخرى بانك ام الدكتوره بل لى الفخر ان تكونى لى اما يااغلى ما فقدت فى حياتى رحمه الله عليك

Acknowledgements

Publications

1. F.S.Al-Khattaf, A.Z. Tremp & J.T. Dessens (2015) *Plasmodium* alveolins possess distinct but structurally and functionally related multi-repeat domains. *Parasitology Research* **115**: 631-639

2. A.Z. Tremp, F.S. Al-Khattaf & J.T. Dessens (2014) Distinct temporal recruitment of *Plasmodium* alveolins to the subpellicular network. *Parasitology Research* **113**: 4177-4188

Declaration

I, Fatimah Al-Khattaf, have read and understood the School's definition of plagiarism and cheating given in the Research Degrees Handbook. I declare that this thesis is my own work and that I have acknowledged all results and quotations from the published or unpublished work of other people. I have read and understood the School's definition and policy on the use of third parties (either paid or unpaid) who have contributed to the preparation of this thesis by providing copy editing and proofreading services. I declare that no changes to the intellectual content or substance of this thesis were made as a result of this advice and that I have fully acknowledged all such contributions.

Signed: Date:

Abstract

Malaria remains one of the most serious infectious parasitic diseases in humans. A shared cellular feature of the motile and invasive stages (zoites) of malaria parasites is the presence of a unique cortical cytoskeletal structure named the subpellicular network (SPN), which forms an internal cytoskeletal basket providing mechanical strength to the cell. Malaria parasites have three distinct zoite stages: the merozoite (blood stage); the ookinete (early mosquito stage); and the sporozoite (late mosquito and liver stage).

A family of intermediate filament proteins, named alveolins, comprise main building blocks of the SPN. Several *Plasmodium* alveolins have been shown to be differentially expressed across zoite stages, and to have functionally equivalent and essential roles involved in parasite morphogenesis, tensile strength, motility and infectivity. In this thesis, genetically altered parasite lines expressing disrupted, fluorescent protein-tagged or mutated alveolins were generated in the mouse malaria model *P. berghei*, to further characterize select alveolin family members with respect to their life stage expression, subcellular localization and trafficking, and their contribution to parasite development, infectivity and mosquito transmission. Through structure-function analysis, the contributions of conserved cysteine motifs to alveolin function and post-translational lipid modification (palmitoylation) were also investigated.

Re-examination of the alveolin repertoire identified 13 alveolin family members whose conserved 'alveolin' domains possess tandem repeats of typically 12 amino acids. The results show two alveolins, IMC1c and IMC1e, to be expressed in all three zoite stages and to be essential for blood stage parasite development. Moreover, IMC1c and IMC1e display different temporal recruitment to the SPN. By contrast, the alveolin IMC1d is expressed only in ookinetes and is functionally dispensable. We show that the cysteine motif in the alveolin IMC1c is the site of S-palmitoylation, but is functionally redundant. By contast, the cysteine motifs of IMC1a are important for sporozoite development and infectivity. The combined results suggest that while alveolins have a shared core architecture and overall cytoskeletal function,

differences in life stage expression, protein expression level, recruitment to the SPN, and palmitoylation status ensure that each family member makes a unique contribution to parasite development.

Table of contents

List of figures

List of tables

Abbreviations

μg	Microgram
μl	Microlitre
μM	Micromolar
°C	Degree Celsius
ABE	acyl-biotin exchange
Bis-Tris	2-[bis(2-hydroxyethyl)amino]-2-(hydroxymethyl)propane-1,3-diol
BLAST	*Basic Local Alignment Search Tool*
BSA	Bovine serum albumin
Bp	Base pair
2-BMP	2-bromopalmitate
CSP	Circumsporozoite protein
C-terminus/terminal	Carboxy-terminus/terminal
CTRP	Circumsporozoite protein (CSP) and thrombospondin-related adhesive protein (TRAP)-related protein
dH$_2$O	Distilled water
DAPI	4´,6-diamidino-2-phenylindole
DNA	Deoxyribonucleic acid
dNTP	Deoxyribonucleotide triphosphate
dATP	Deoxyadenosine triphosphate
dTTP	Deoxythymidine triphosphate
dGTP	Deoxyguanosine triphosphate
dCTP	Deoxycytidine triphosphate
DMSO	Dimethyl sulfoxide
DOZI	Development of zygote inhibited
ECP	Egress cysteine protease
EDTA	Ethylene diamine tetraacetic acid

ER	Endoplasmic reticulum
EGFP	Enhanced green fluorescent protein
EGTA	Ethylene glycol tetraacetic acid
FBS	Fetal bovine serum
g	Gram
g	G-force
G2	Glycine at position 2
GAP	Glideosome-associated protein
GFP	Green fluorescent protein
GMB	Gametocyte maintenance buffer
h	Hours
HCl	Hydrochloric acid
hDHFR	Human dehydrofolate reductase
HMM	Hidden Markov Model
HAM	Hydroxylamine
HRP	Horse radish peroxidase
IgG	Immunoglobulin G
IMC	Inner membrane complex
IMP	Intramembranous particle
i.p.	Intraperitoneal
ISP	IMC sub-compartment protein
kb	Kilobase
kDa	Kilodalton
KO	Knock-out
L	Litre
LB	Luria Broth
M	Molar
MAEBL	Merozoite AMA1-EBL-like protein
MAOP	Membrane attack ookinete protein
min	Minute

ml	Millilitre
m*M*	Millimolar
mRNA	Messenger RNA
MTIP	Myosin tail interacting protein
MTOC	Microtubule-organizing centre
nm	Nanometre
ng	Nanogram
NaOH	Sodium hydroxide
NaCl	Sodium chloride
N-terminus/terminal	Amino-terminus/terminal
PAGE	Polyacrylamide gel electrophoresis
*Pb*DHFR	*Plasmodium berghei* dehydrofolate reductase
PBS	Phosphate buffered saline
PCR	Polymerase chain reaction
PCRMP	*Plasmodium* cysteine repeat modular protein
PV	Parasitophorous vacuole
PVDF	Polyvinylidene fluoride
PATs	palmitoyl-S-acyl-transferases
RBC	Red blood cell
RNA	Ribonucleic acid
RPMI medium	Roswell Park Memorial Institute medium
RT-PCR	Reverse transcription PCR
SDS	Sodium dodecyl sulfate
SEM	Standard error of the mean
SIAP	Sporozoite invasion-associated protein
SOAP	Secreted ookinete adhesive protein
SOC	Super optimal broth with glucose
SPN	Subpellicular network
TE	Tris EDTA
TRAP	Thrombospondin-related adhesive protein

TREP	TRAP-related protein
Tris	Tris(hydroxymethyl)aminomethane
u	units
UV	Ultraviolet
UTR	Untranslated region
WARP	von Willebrand factor A domain-related protein
WT	Wildtype

Chapter 1

General Introduction

1.1. Malaria

Humans have been subjected to malaria for thousands of years without knowing the causative agent. This was the case until 1880 when the military physician Alphonse Laveran observed crescent shaped bodies in a blood specimen collected from a soldier who had a fever characterised with intervals of periodic remission (Sherman, 2005). Today, malaria is still considered one of the most threatening infectious parasitic diseases in humans. According to the latest estimates, 214 million new cases of malaria occurred worldwide in 2015, and the disease caused an estimated 438,000 deaths, mainly in children under five (306,000). The burden is heaviest in Africa, where an estimated 90% of all malaria deaths occur (WHO, 2015).

Malaria is caused by parasites belonging to the genus *Plasmodium,* which in turn belongs to the phylum Apicomplexa that includes many protozoan parasites that cause other diseases of medical and veterinary importance (e.g. cryptosporidiosis, toxoplasmosis, coccidiosis) (Blader *et al.,* 2015). The Apicomplexa are unicellular and obligate endoparasites of animals. The name Apicomplexa is derived from the Latin words *apex* (top) and *complexus* (infolds) and refers to specialized subcellular structures that are found at the anterior end of the parasite (the 'apical complex'). There are more than 100 species of *Plasmodium* that infect several animal species such as reptiles, birds, and various mammals including rodents, monkeys and primates. Five species of *Plasmodium* have been identified to infect humans in nature: *Plasmodium falciparum*, *P. vivax*, *P. malariae*, *P. ovale* and *P. knowlesi.* The most widespread and deadliest of the human malaria species is *P. falciparum*.

The malaria parasite is naturally transmitted to people by the bite of mosquitoes belonging to genus *Anopheles*. Parasite reproduction in the red blood cell (RBC) causes clinical symptoms such as fever and headache. These symptoms are usually mild and sometimes difficult to diagnose as malaria. In the absence of appropriate treatment, severe and life-threatening complications can develop like anaemia, organ failure and cerebral malaria. Vector control is the main way of preventing and reducing malaria transmission, with insecticide-treated mosquito nets and indoor residual spraying being amongst the most effective. This is however under

threat from the increased incidence and spread of insecticide resistance. Likewise, the development and spread of antimalarial drug resistance, in particular resistance to artemisinin - a key compound of the best available medicines - threatens progress in malaria control. Hence, significant efforts are needed for the development of new and effective strategies to combat malaria.

1.2. The *Plasmodium* life cycle

The life cycle of malaria parasites includes a vertebrate host and an insect vector (Fig. 1.1). For human and murine malaria species female *Anopheles* mosquitoes constitute the vector. Transmission starts when during blood feeding on a parasite-infected host, mosquitoes ingest gametocytes - sexual stage precursor cells that circulate in the blood stream (Step 1, Fig. 1.1). The ingestion of gametocytes by the mosquito leads to their progession to mature sex cells (gametogenesis): a female gametocyte develops into a single macrogamete, while a male gametocyte develops into eight microgametes. Gametogenesis is triggered by a number of environmental factors in the mosquito midgut such as drop in temperature, as well as rise in pH or a gametocyte-activating factor (xanthurenic acid) that is present in the mosquito (Arai *et al.*, 2001; Billker *et al.*, 1997). Within a day, the fertilized female gametes (zygotes) transform into elongated and motile ookinetes (Step 2, Fig. 1.1). These move through the mosquito's midgut epithelium to avoid digestion with the blood meal. On the hemocoel side of the midgut epithelium, ookinetes round up and transform into young oocysts. These oocyst grow and differentiate over a 2-3 week period resulting in the formation of hundreds of daughter cells per oocyst: the sporozoites (Step 3, Fig. 1.1). After egress from the oocyst, sporozoites migrate to and invade the insect's salivary glands, from where they are transmitted to a new host by mosquito bite. Initially, sporozoites infect and multiply in liver cells, culminating in up to 10,000 daughter merozoite per infected hepatocyte (Step 4, Fig. 1.1). These are released into the bloodstream where they infect RBCs and multiply to form new merozoites through a process called erythrocytic schizogony (16-32 merozoites per infected RBC) (Step 5, Fig. 1.1). Released merozoites infect new RBCs, causing much of the clinical manifestations of the disease. Some of

the infected RBCs leave the cycle of asexual multiplication: rather than replicating, the merozoite in these cells develops into a male or female gametocyte to allow the next round of parasite transmission.

It is notable to mention that in the case of *P. vivax* and *P. ovale* infections of the liver, parasites can develop into dormant forms (hypnozoites) that can stay inactive for years causing disease relapse when reactivated.
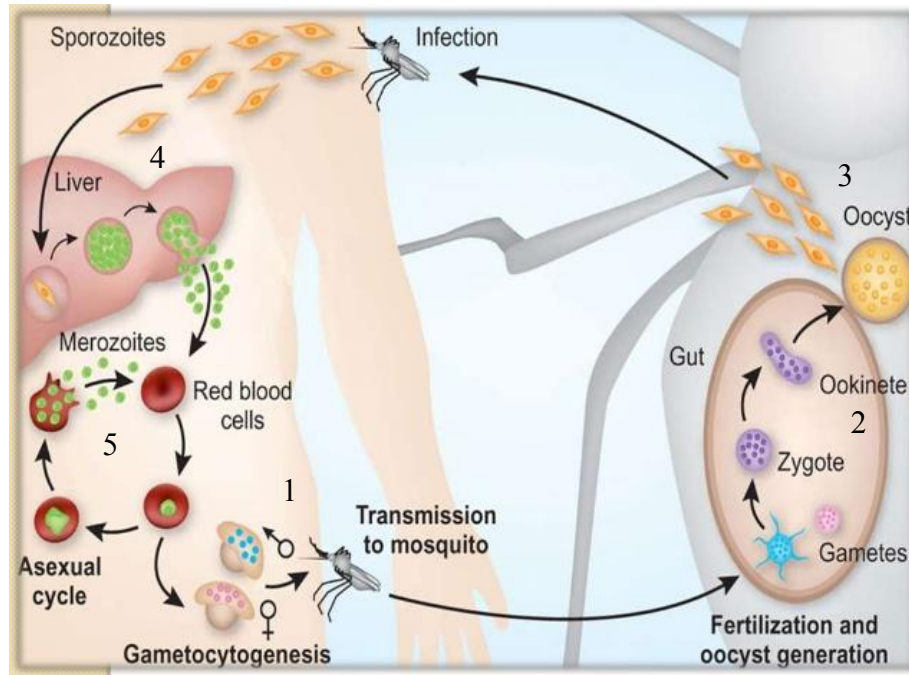
Figure 1.1. The *Plasmodium* life cycle. Adapted from Pasvol (2010).

1.3. The 'zoite' stages

Among the many developmental forms of the parasite, three life stages are motile and invade host cells: the merozoite, the ookinete and the sporozoite (Fig. 1.2). These are often referred to as the 'zoite' stages. Although these invasive stages have distinct shapes and sizes, as well as different host cell specificities, they share a structural organization which is also preserved in zoites of other apicomplexan parasites. Part of this conserved organization is the apical complex, which is composed of specialized structures and secretory organelles located at the anterior end of the zoite and functions to release different invasion factors required for interaction with and invasion of the host cell. Another conserved structure is a distinctive cortical structure known as the pellicle, which has a cytoskeletal role.

23
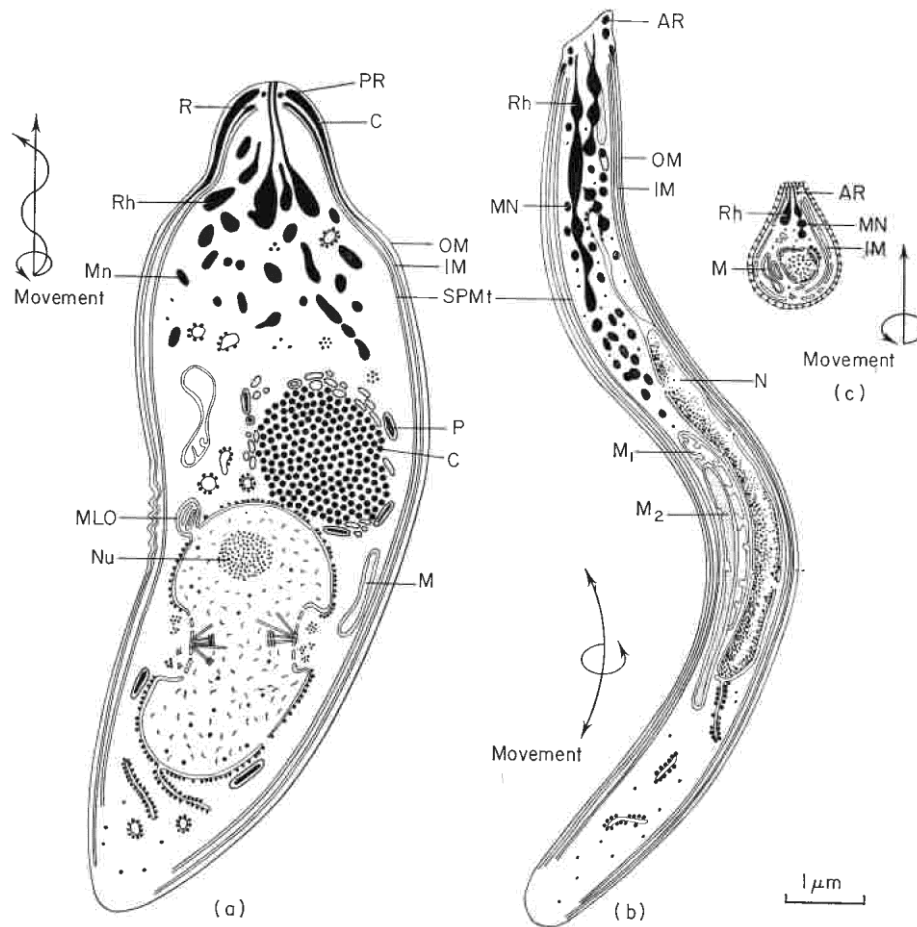
Figure 1.2. The zoite stages. (a) ookinete. (b) sporozoite. (c) merozoite. AR, apical ring; C, collar; Cr, crystalloid; IM, inner pellicle membrane; M, mitochondrion; MLO, multilamellate organelle; Mn, microneme; N, nucleus; Nu, nucleolus; OM, outer pellicle membrane; P, pigment; PR, polar ring; R, electron dense ring; Rh, rhoptry; SB, spherical body; SPMt, subpellicular microtubules. Adapted from Sinden (1978).

Apicomplexan zoites utilise a specialized form of locomotion named gliding motility, which is a substrate-dependent form of eukaryotic motility that requires neither locomotory organelles like cilia or flagella, nor major changes in cell morphology such as the pseudopod formation. Both the apical complex and pellicle are intrinsically linked to gliding motility. Gliding motility is driven by an action-myosin motor which is preserved among apicomplexan parasites (Baum *et al.*, 2006), and which is situated within the pellicle cytoplasm (Dobrowolski *et al.*, 1997; Menard, 2001; Morrissette and Sibley, 2002; Soldati and Meissner, 2004). During gliding motility transmembrane adhesion proteins such as thrombospondin-related adhesive

24

protein (TRAP) and circumsporozoite protein and TRAP-related protein (CTRP) are 'secreted' onto the parasite surface via the apical complex, connecting the molecular motor in the pellicle to the host cell receptors. The molecular motor facilitates the backward movement of the adhesion molecules and actin filaments, propelling the parasite in the other direction (Dobrowolski *et al.*, 1997; Menard, 2001; Morrissette and Sibley, 2002; Soldati and Meissner, 2004).

1.3.1. The merozoite

The merozoite is the smallest life stage of the parasite that invades the erythrocytes of the vertebrate host (Bannister and Mitchell, 2009). Initial merozoites are formed in the hepatocytes during liver stage schizogony (exoerythrocytic schizogony) and, upon release into the blood stream, they go on to replicate inside RBCs (erythrocytic schizogony). Immunologically, this stage is important as it is briefly extracellular and thus exposed to host antibodies. In contrast to the high number of merozoites (up to thousands) that are generated from a single liver schizont, fewer merozoites (up to 32) are formed by erythrocytic schizogony depending on the *Plasmodium* species. The invasion of erythrocytes is a multi-step process. After the attachment of the merozoite, it re-orientates itself with its apical end in contact with the RBC surface, establishing a tight junction between the parasite and the host cell. As the merozoite enters the RBC, a parasitophorous vacuole (PV) is formed around it, in which the parasite resides, grows and divides to form the next generation of merozoites.

The merozoite has a thick coat made up of thin filaments that are utilized for host cell capturing, but cleaved from the surface of the parasite when it enters the erythrocyte (Bannister *et al.*, 2000). The merozoite has several types of secretory organelles: micronemes, small elongated organelles which have important roles in gliding motility, host cell adhesion and invasion; rhoptries, which are larger club-shaped organelles that also have important roles in adhesion and invasion, and the establishment of the PV; dense granules, small spherical organelles with a function in PV formation (Mercier *et al.*, 2005); and exonemes, which are required for merozoite egress from the infected erythrocyte (Janse and Waters, 2007; Yeoh *et al.*, 2007).

1.3.2. The ookinete

Development of the gametocyte into the oocyst is a major population bottleneck in the parasite life cycle (Sinden and Billingsley, 2001) and for this reason is the subject of transmission blocking strategies aimed at blocking the developmental progression of the parasite within the mosquito midgut. Several molecules have been identified that play important roles in the successful invasion of the midgut epithelium by the ookinete including CTRP, protein 25 (P25), protein 28 (P28), secreted ookinete adhesive protein (SOAP), membrane attack ookinete protein (MAOP), chitinase and von Willebrand factor A domain-related protein (WARP) (Dessens *et al.*, 1999; Dessens *et al.*, 2001; Kadota *et al.*, 2004; Tomas *et al.*, 2001; Yuda *et al.*, 2001). During zygote to ookinete differentiation, several vital changes take place. Firstly, parasite surface proteins are replaced with those that the ookinete needs for its interaction with the mosquito environment, most notably P25 and P28 (Kaushal *et al.*, 1983; Sinden *et al.*, 2004). Secondly, the cortical cytoskeleton and apical complex are formed as the ookinete protrudes from the sperical zygote (Sinden *et al.*, 2004). Coinciding with ookinete differentiation, the diploid zygote undergoes DNA replication followed by meiotic division culminating in a mature ookinete containing a tetraploid nucleus with four haploid genomes. Once formed, the mature motile ookinete must escape the harsh protease-rich environment of the midgut lumen (Billingsley and Hecker, 1991). It first penetrates the peritrophic matrix, a chitinous sheath that envelops the blood meal and which serves as a defensive layer (Hegedus *et al.*, 2009). To facilitate this process the parasite secretes chitinases (Dessens *et al.*, 2001; Huber *et al.*, 1991; Shahabuddin and Kaslow, 1994). Subsequently the ookinete must cross the cells of the midgut epithelium. Invasion of the midgut cells leads to apoptosis and the production of harmful molecules like nitric oxide is induced (Han and Barillas-Mury, 2002; Han *et al.*, 2000; Luckhart *et al.*, 1998; Zieler and Dvorak, 2000). At the basal lamina, ookinete transition into oocyst takes place, usually after having crossed several epithelial cells (Sinden *et al.*, 2004; Vlachou *et al.*, 2004). Because the ookinete does not form a PV it does not contain rhoptries or dense granules.

1.3.3. The sporozoite

Oocyst rapidly grow during which they undergo multiple steps of mitosis as well as replicate of other organelles, and form a protective extracellular capsule called the oocyst wall (Sinden and Strong, 1978). Cytokinesis starts with the formation of so-called sporoblasts that are formed by invagination of the oocyst cytoplasm. Sporozoites are formed via a budding process at the surface of the limiting membrane, which is accompanied by the formation of the sporozoite pellicle. (Vanderberg and Rhodin, 1967). As the budding sporozoite elongates, a haploid nucleus is dragged into it in conjunction with a mitochondrion and an apicoplast, while the consequent development of the micronemes and rhoptries occurs in the apical region of the emerged sporozoite (Sinden and Matuschewski, 2005; Sinden and Strong, 1978). These sporozoites are usually rigid and straight until their entire formation and release from the sporoblast (Sinden and Matuschewski, 2005), where they become more flexible and motile (Sinden and Garnham, 1973; Sinden and Matuschewski, 2005). Each oocyst can produce several hundred daughter sporozoites. The rupture of the mature oocyst releases the sporozoites into the haemolymph of the mosquito. The exact process by which sporozoites egress is not well established, however, CSP (the main surface protein of the mature sporozoites), egress cysteine protease 1 (ECP1) and *Plasmodium* cysteine repeat molecular protein (PCRMP) 3 and 4 are required (Aly and Matuschewski, 2005; Douradinha *et al.*, 2011; Wang *et al.*, 2005).

After egress, the sporozoites migrate from the haemolymph to the salivary glands of the mosquito. Colonization of the glands involves attachment to and invasion of its epithelial cells. This requires active gliding motility (Kappe *et al.*, 2003). Disruption of molecules involved in gliding such as thrombospondin-related adhesive protein (TRAP) and sporozoite invasion-associated protein 1 (SIAP-1) eradicate the colonization of the mosquito salivary glands (Engelmann *et al.*, 2009; Sultan *et al.*, 1997). The parasite proteins merozoite AMA1-EBL-like protein (MAEBL) and CSP facilitate recognition of, and attachment to, the salivary glands (Kariu *et al.*, 2002; Myung *et al.*, 2004; Tewari *et al.*, 2005).

Sporozoites are deposited beneath the vertebrate host skin by mosquito bite

and then disseminate to the blood capillaries until they reach the liver (Amino *et al.*, 2006). When the sporozoites reach the liver sinusoids, they cross the endothelial layer to reach the hepatocytes. Both CSP and TRAP have vital functions in these processes due to their interaction with glycoproteins on the surface of the liver cells (Pradel *et al.*, 2002; Ying *et al.*, 1997). Sporozoites will often migrate through a number of hepatocytes (Mota *et al.*, 2001) before forming a PV and starting schizogony.

1.4. The pellicle of *Plasmodium* zoites

Zoites of apicomplexan parasites undergo considerable shape changes during migration and host-cell invasion for which they require flexibility and strength. These features are largely conferred to the parasite through a unique cortical structure called the pellicle (Fig. 1.3). The pellicle is made up of the plasma membrane and an underlying double membrane structure called the inner membrane complex (IMC). Located on the cytoplasmic side of the IMC a cytoskeletal network of intermediate filaments named the subpellicular network (SPN). Finally, subpellicular microtubules run lengthwise underneath the IMC/SPN from the apical polar ring toward the posterior end of the cell (Morrissette and Sibley, 2002; Raibaud *et al.*, 2001). A pellicle is also found in gametocytes of *P. falciparum* and various avian and reptilian *Plasmodium* species (Aikawa *et al.*, 1984a; Aikawa *et al.*, 1969; Bannister *et al.*, 2005; Dearnley *et al.*, 2012).

Electron-microscopy cross-section of a sporozoite, the figure on the right represents the boxed section
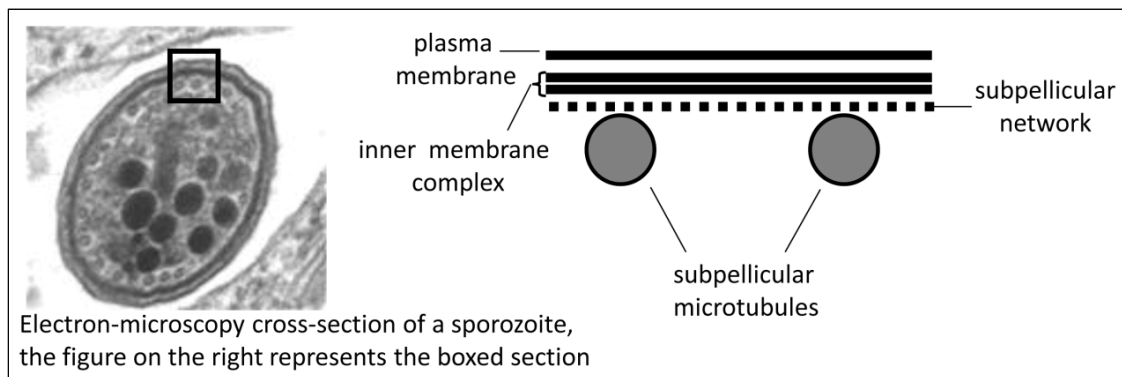
Figure 1.3. The cortical organization of the invasive stages of *Plasmodium*. Figure provided by J. Dessens.

1.4.1. The inner membrane complex

In *Plasmodium* zoites the IMC is made up of a single flattened vacuole which is sealed by a suture line that runs parallel to the subpellicular microtubules (Bannister *et al.*, 2000; Bannister and Mitchell, 1995; Dubremetz and Elsner, 1979; Raibaud *et al.*, 2001). The IMC structure is equivalent to the 'alveoli', cortical structures that are a defining morphological feature of organisms belonging to the superphylum Alveolata that comprises apicomplexans, ciliates and dinoflagellate algea. The IMC is probably derived from the endoplasmic reticulum (ER), because the IMC of *Toxoplasma gondii* stains with an ER-specific dye (de Melo and de Souza, 1997), and the fact that the IMC-resident glidesome-associated protein 50 (GAP50) localizes in the ER before its localization to the periphery of the merozoites in the mature schizont (Yeoman *et al.*, 2011). Cryofracture electron microscopy shows pores about 43 nm diameter in the ookinete IMC that were suggested to form a trafficking pathway across the membranes of the pellicle (Raibaud *et al.*, 2001). The IMC also contains intramembranous particles (IMPs) that run parallel to the subpellicular microtubules, suggesting that they link the latter to the IMC (Raibaud *et al.*, 2001). When zoites begin their transformation into the next life stage, considerable cytoskeleton remodelling takes place and the pellicle structure rapidly disappears (Aikawa *et al.*, 1984b; Bannister *et al.*, 1975; Meis *et al.*, 1985; Sinden and Strong, 1978).

1.4.2. The subpellicular microtubules

The subpellicular microtubules are unusually stable microtubules (Cyrklaff *et al.*, 2007) that originate at the apical end of the zoite and that use the apical polar ring - part of the apical complex - as their microtubule organising centre (MTOC) (Santos *et al.*, 2009). The subpellicular microtubules are thought to have roles in parasite motility and/or invasion, because microtubule destabilizing drugs interfere with merozoite invasion of the RBC (Fowler *et al.*, 1998). Consistent with cell size, ookinetes have 40-60 subpellicular microtubules (Sinden and Strong, 1978), sporozoites have 18-19 (Vanderberg and Rhodin, 1967), while *P. falciparum* merozoites have only 2-3 (Fowler *et al.*, 1998). Studies by Kudryashev and colleagues (Kudryashev *et al.*, 2010)

revealed that the microtubules of *P. berghei* sporozoites are connected to the pellicle by long tethering proteins that originate from the IMC at 32-nm intervals. Such findings suggested that these proteins could be the equivalent of the IMPs observed in ookinetes (Raibaud *et al.*, 2001). Similarly, a 32-nm periodicity was observed in the IMPs and subpellicular microtubules of *T. gondii* (Morrissette *et al.*, 1997).

1.4.3. The subpellicular network

Electron microscopy of detergent extracted *T. gondii* tachyzoites first revealed the presence of the SPN within the pelicle structure (Mann and Beckers, 2001). The SPN is a two-dimensional network of tightly interwoven intermediate filaments that is tightly connected to the IMC on its cytoplasmic side. The resistance of the SPN to detergent extraction and the fact that extracted SPN structures often maintain the shape of the cell indicated that it functions as a so-called 'membrane skeleton' that provides mechanical strength to the pellicular membranes (Mann and Beckers, 2001). The existence of a SPN in *Plasmodium* sporozoites was shown by cryogenic electron tomography (Kudryashev *et al.*, 2010). Assembly of the SPN in *T. gondii* begins early during parasite replication and a considerable variation in SPN stability between mother and daughter parasites was reported: In the immature parasites, the SPN could be solubilized by detergent, while in the mature ones it was entirely resistant to detergent extraction (Mann *et al.*, 2002). These observations point to a SPN maturation during the course of zoite morphogenesis.

1.5. The alveolins

Along with the discovery of the SPN, Mann and Beckers identified a protein component of this structure that was named *Toxoplasma gondii* inner membrane complex protein 1 (TgIMC1) (Mann and Beckers, 2001). Subsequently, an apicomplexa-specific family of structurally related proteins was identified and this protein family was given the name 'IMC1 proteins' (Khater *et al.*, 2004). In *Plasmodium* eight conserved structural homologues were identified named IMC1a to IMC1h (Khater *et al.*, 2004) (Table 1.1).

Table 1.1. Predicted *P. berghei* IMC1 proteins/alveolins and zoite expression.

Name	*P. berghei* ID (PBANKA_000000)	Zoite expression			References
		merozoite	ookinete	sporozoite	
IMC1a	040260			+	Khater et al., 2004
IMC1b	090710		+		Tremp et al., 2008
IMC1c	120200				
IMC1d	121910				
IMC1e	040270				
IMC1f	136440				
IMC1g	124060	+	+	+	Kono et al., 2012
IMC1h	143660		+	+	Tremp & Dessens, 2011

Sequence homology between the IMC proteins is confined to 1-2 conserved domains rich in valine and proline, separated by regions variable in length and amino acid composition (Fig. 1.4), indicating that the conserved domains are also the functional domains (Fukumoto *et al.*, 2003; Gubbels *et al.*, 2004; Khater *et al.*, 2004; Mann and Beckers, 2001). The *Plasmodium* IMC1 proteins have modest sequence homology with articulins, a group of membrane skeleton proteins found in several ciliates and euglenoids (Huttenlauch *et al.*, 1995; Huttenlauch *et al.*, 1998a; Huttenlauch *et al.*, 1998b; Marrs and Bouck, 1992). In a later study Gould and colleagues discovered structural homologues of the apicomplexan IMC1 proteins in ciliates and dinoflagellate algae - the other two phyla within the Alveolata superphylum - and renamed the protein family 'alveolins' which were considered distinct from articulins (Gould *et al.*, 2008). In *Toxoplasma,* 14 alveolins have been identified which, despite having distinct spatiotemporal expression patterns, all display a subcellular localization in the cortical cytoskeleton (Anderson-White *et al.*, 2011a).
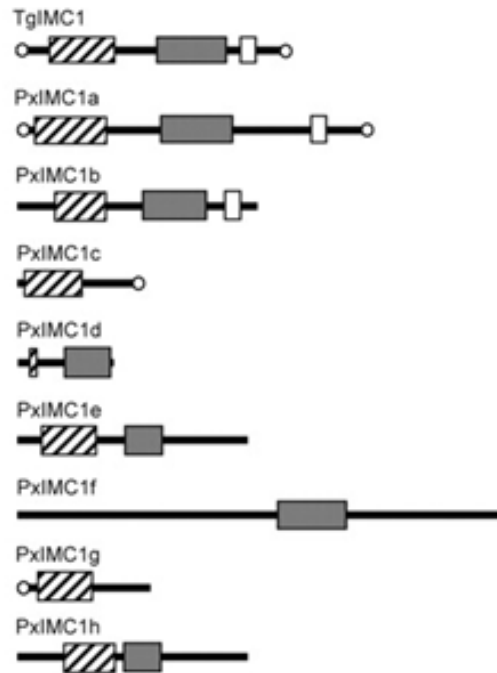
Figure 1.4. Sequence and structure of IMC1 proteins. Schematic diagram of the protein structure of TgIMC1 and its structural homologues in *Plasmodium* spp. The proteins shown are based on predicted proteins of *P. yoelii*, GenBank/EMBL/DDBJ accession nos. EAA16469 (PyIMC1a), EAA15257 (PyIMC1b),EAA16185 (PyIMC1c), EAA17029 (PyIMC1d), EAA15249 (PyIMC1e), EAA15609(PyIMC1f), EAA15402 (PyIMC1g), and EAA20426 (PyIMC1h). Boxes mark domains corresponding to the conserved amino-terminal domain (hatched), central domain (gray), and carboxy-terminal domain (open). Conserved terminal cysteine motifs are indicated with open circles. Adapted from Khater *et al.* (2004).

IMC1a was the first malaria alveolin to be characterized using targeted gene disruption in the rodent malaria species *P. berghei* (Khater *et al.*, 2004). These studies revealed that IMC1a is uniquely expressed in sporozoites where it localizes to the cortex, consistent with a localization in the pellicle. *Pb*IMC1a null mutants possessed smaller, abnormally-shaped sporozoites with a bulging, protruding area typically around the nucleus. Although IMC1a-KO sporozoites could be detected in the haemolymph, no sprorozoites succeeded in invading the salivary glands. In addition, the infection of mice with oocyst *Pb*IMC1a-KO sporozoites caused no infection (Khater *et al.*, 2004). These morphological abnormalities were accompanied by reductions in gliding motility and tensile strength of the sporozoites, which are the likely cause of the observed reduction in infectivity (Khater *et al.*, 2004). A subsequent study aimed at characterizing the expression, subcellular localization and function of IMC1b

- a closely related structural paralogue of IMC1a - showed that this alveolin was expressed uniquely in ookinetes, but had otherwise equivalent functions to IMC1a involving cell shape, motility and tensile strength (Tremp *et al.*, 2008). IMC1h, in turn, was shown to be expressed in both ookinetes and sporozoites and had loss-of-function phenotypes similar to those of IMC1b in the ookinete and IMC1a in the sporozoite, respectively (Tremp and Dessens, 2011). These combined data demonstrate that alveolins are structurally and functionally homologous and play roles in many key processes such as morphogenesis, gliding motility and the provision of tensile strength. Double knockout of both IMC1b and IMC1h in ookinetes resulted in increased reductions in motility, tensile strength and infectivity compared to the single knockouts, showing that these alveolins are functionally independent and contribute cumulatively to these properties of the zoites (Tremp and Dessens, 2011). However, ookinete cell shape did not deteriorate further upon double gene disruption, which indicates that the alveolins contribute to motility independent of their shape (Tremp and Dessens, 2011). Interestingly, disruption of the SPN-resident protein G2, which is structurally unrelated to the alveolins, also causes morphological abnormalities and reductions in motility, but did not affect tensile strenghth (Tremp *et al.*, 2013). This shows that zoite morphogenesis is also affected by disruption of other SPN proteins and is not linked to tensile strength of the cell (Tremp *et al.*, 2013). Similar observations were made when the SPN-resident protein PhIL1 was disrupted in *T. gondii* (Barkhuff *et al.*, 2011).

Beside the presence of the conserved 'alveolin' domains found in this family of proteins, a subset of alveolins possess conserved cysteine motifs at the amino- or carboxy-terminus. It is thought that these motifs may constitute sites for post-translational palmitoylation (a lipid modification, see below) aimed to strengthen the interaction of the SPN with the IMC (Mann and Beckers, 2001; Khater *et al.*, 2004; Anderson-White *et al.*, 2011).

1.6. Protein palmitoylation

A range of cellular functions are controlled by a post-translational protein

modifications. Among these are the attachment of lipid moieties like myristoyl, palmitoyl, stearoyl or farnesyl. In eukaryotes, the most common forms of protein fatty acylations are N-myristoylation and S-palmitoylation (Resh, 1999). These two fatty acylations can modify proteins both separately and concertedly with other lipid modifications.

S-palmitoylation is the addition of the 16-carbon fatty acid palmitate to cysteine residues via a thioester linkage, and is the only known reversible post-translational lipid modification (Dietrich and Ungermann, 2004; Resh, 1999). Consequently, palmitoylation is a regulatory mechanism that can facilitate the attachment of proteins to membranes as well their subcellular trafficking. In addition, S-palmitoylation has a vital roles in protein-protein interactions and protein stability. The palmitoylation reaction is catalyzed by palmitoyl-S-acyl-transferases (PATs). PATs are identifiable from having a Asp-His-His-Cys (DHHC) motif within a cysteine-rich domain, and at least 12 distinct putative PAT-encoding genes have been identified in *Plasmodium* spp. (Frenal *et al.*, 2013). Localization studies indicate that the subcellular distribution of many PATs restricted to distinct compartments including endoplasmic reticulum (e.g. DHHC7), IMC (e.g. DHHC3 and DHHC9), and rhoptries (e.g. DHHC7) (Frenal *et al.*, 2013). S-palmitoylation in *Plasmodium* affects over 400 proteins and is essential for parasite development both in the vertebrate host (Jones *et al.*, 2012) and in the mosquito vector (Santos *et al.*, 2015), underpinning the potential for developing parasite-specific PAT inhibitors for chemotherapy and/or transmission control. Generally, palmitoylation sites do not have consensus sequences making it difficult to predict whether or not a protein is palmitoylated, and the mechanisms by which substrates are recognised by PATs is a topic of intense investigation.

There are currently two recognised strategies for biochemical detection of palmitoylated proteins. The first is the acyl-biotin exchange (ABE) method (Drisdel and Green, 2004; Wan *et al.*, 2007) (Fig. 1.5). ABE is based on the exchange of the thioester-linked palmitate for a biotin group, which is then used for specific purification of biotinylated proteins using streptavidin capture. The total proteome is extracted, solubilized and then treated with N-ethylmaleimide to irreversibly block any non-

palmitoylated cysteine residues in the proteins. Thioester bonds are then cleaved with hydroxylamine, removing the palmitoyl moieties and exposing the previously linked cysteine thiol groups. These are then chemically and covalently linked to biotin. Non-hydroxylamine-treated samples are used as negative controls. The second strategy is based on the metabolic labelling of cells with a palmitic acid analogue followed by click-chemistry (MLCC) (Jones *et al.*, 2012; Roth *et al.*, 2006). Metabolic incorporation of 17-octadecynoic acid allows the specific and irreversible biotinylation of analogue-labelled proteins, which is again followed by streptavidin capture.
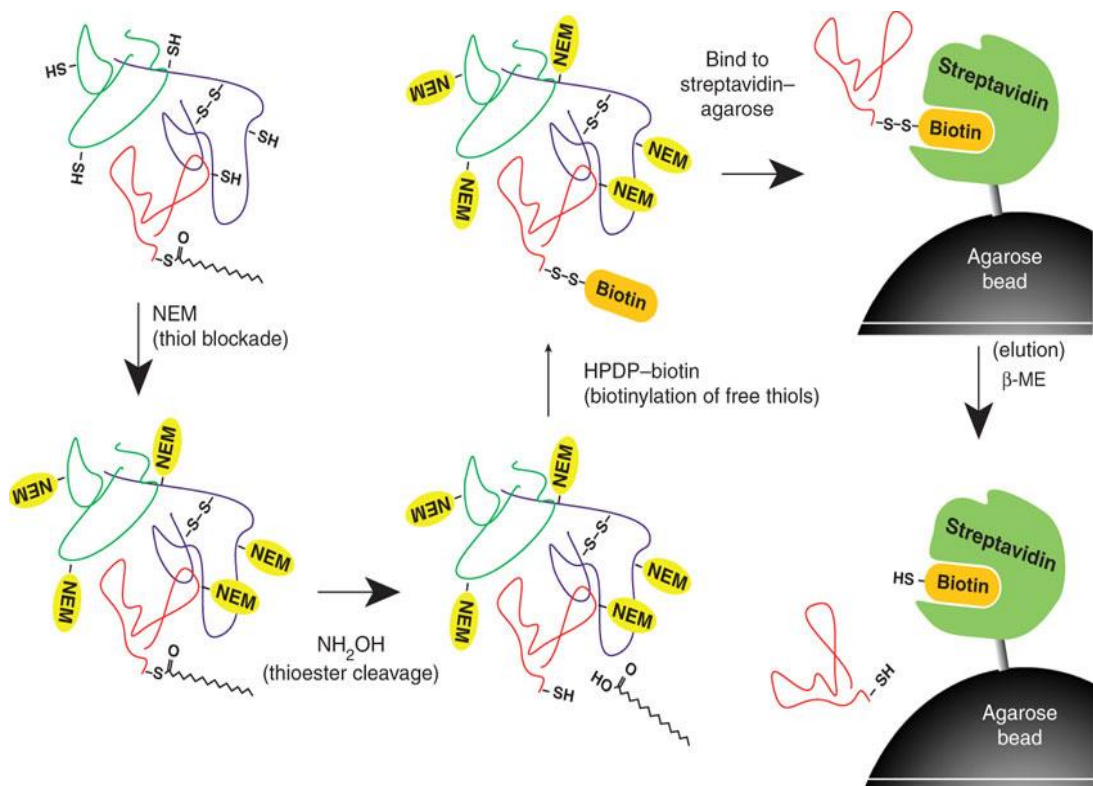
Figure 1.5. Schematic of the proteomic acyl-biotinyl exchange methodology. Adapted from Wan *et al.* (2007).

1.7. Aims and objectives

Plasmodium alveolins contribute cumulatively to the parasites' tensile strength, cell shape, motility and infectivity. The essential nature of the alveolins in malaria parasite development, their expression throughout the life cycle, and their absence in

vertebrates makes them attractive drug targets for malaria treatment, prophylaxis and transmission control. Moreover, such drugs may be active against a broad range of other apicomplexan parasites, as well as against related pathogenic protozoans. This project aims to increase our understanding of the alveolins with respect to their structure, life stage expression, subcellular localization and trafficking, as well as their contribution to parasite development and infectivity, using the mouse malaria model *P. berghei*. The specific objectives are:

(1) Carry out a comprehensive re-assessment of alveolin genes in *Plasmodium* with respect to their repertoire, interrelatedness and structural features.

(2) Generate genetically modified parasite lines that express fluorescent protein-tagged alveolins. This will enable us to follow the expression, subcellular trafficking and localization of the alveolins in live parasites using fluorescence microscopy, and to form a more complete picture of the alveolin family with regards to these properties.

(3) Generate genetically modified parasite lines that have disrupted alveolin genes. This will allow us form a better picture of the alveolin family with regards to their function, contribution to parasite development and functional redundancy.

(4) Generate genetically modified parasite lines that express mutated alveolins, in particular with respect to their terminal cysteine motifs. This will allow us to carry out structure-function analyses and to study the role of cysteine motifs and their potential role in post-translational palmitoylation.

Chapter 2

Materials and Methods

This chapter describes the general methods used in this study. Specific protocols related to particular chapters are described in each one separately. Chemicals used were purchased from Sigma Aldrich unless otherwise specified.

2.1. Construction of targeting vectors

Parasite genes were targeted by double homologous crossover recombination. To generate the targeting vectors for generating genetically modified parasite lines expressing a target protein fused at the carboxy-terminus to a fluorescent protein (gene tagging), a dual plasmid system was used. The first plasmid (pDNR) contains the coding sequence for a fluorescent protein (e.g. GFP or mCherry), followed by a generic 3' untranslated region (UTR) that is derived from the *Plasmodium berghei* dihydrofolate reductase (PbDHFR) gene. The pDNR plasmid also contains a chloramphenicol resistance gene with no bacterial promoter, in addition to two *loxP* sites flanking these combined sequences. The second plasmid (pLP) contains the sequence for a gene cassette that confers resistance to the antimalarial drug pyrimethamine (e.g. *T. gondii* DHFR, human DHFR, or human DHFR fused to yeast dihydroorotate dehydrogenase (yFCU). The selectable marker genes are driven by the promoter sequence of *pbdhfr* and have the 3' UTR of the *pbdhfr* downstream. A single *loxP* site followed by a bacterial promoter is also present.

Construction of the targeting vector for the fluorescent protein tagging of a target gene involves three steps. First, the combined coding region and 5' UTR of the target gene is amplified by PCR and introduced into the pDNR plasmid upstream of, and in-frame with, the fluorescent protein sequence. Second, the 3' UTR of the target gene of interest is PCR-amplified and inserted into the pLP plasmid downstream of the selectable marker gene cassette. Third, by *Cre-loxP* site-specific recombination, the tagged target gene sequence contained within the pDNR plasmid between the *loxP* sites is transferred to the pLP plasmid that contains the target gene-specific 3' UTR. Successful recombination places the chloramphenicol resistance gene present in the pDNR plasmid downstream of the bacterial promoter in the pLP plasmid, permitting antibiotic selection. This process is illustrated for the enhanced GFP-tagging of the

alveolin IMC1b in Fig. 2.1.
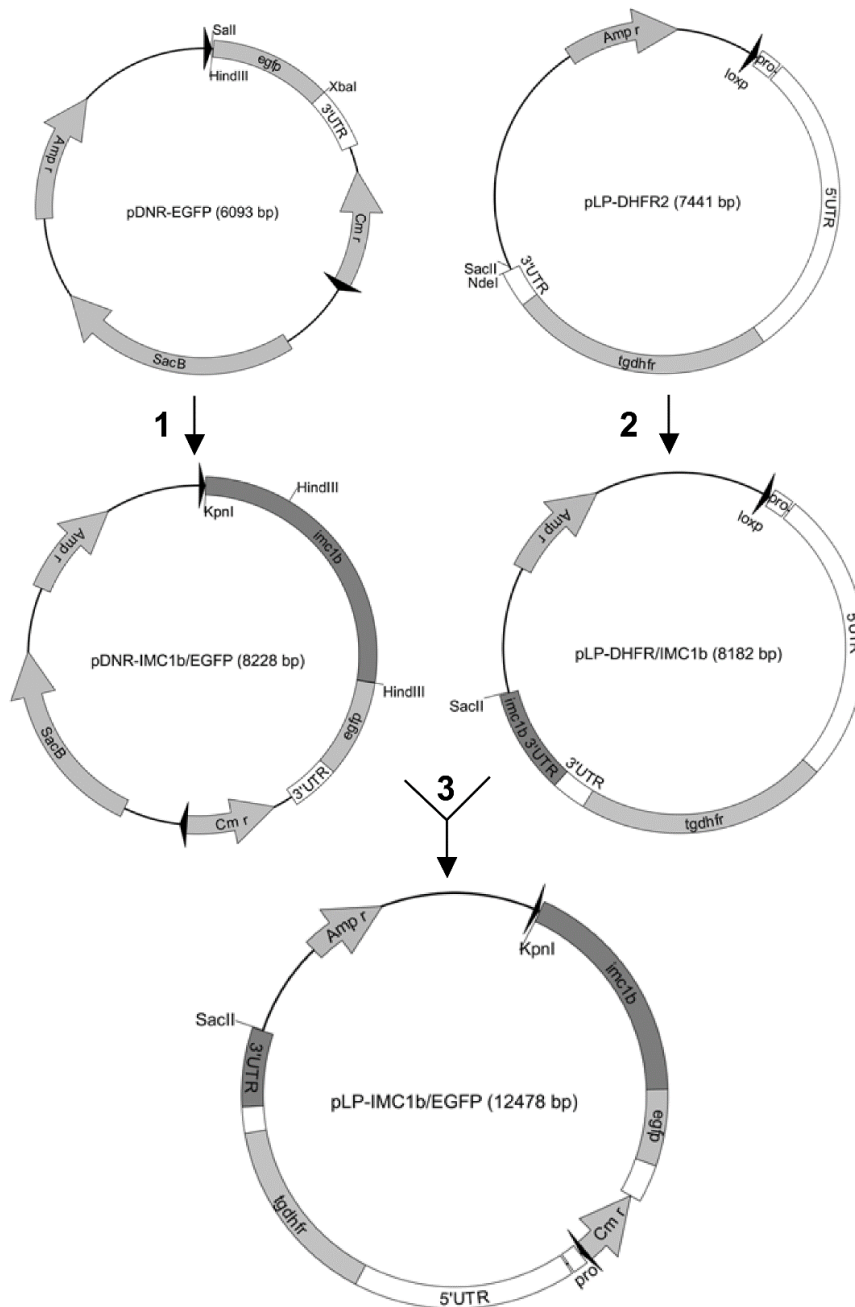
Figure 2.1. A genetic tool for generating genetically modified parasites expressing GFP-tagged IMC1b. Step 1: the imc1b coding sequence plus its 5'UTR is cloned upstream of, and in-frame with, egfp in plasmid pDNR-EGFP. Step2: 3'UTR of imc1b is cloned into plasmid pLP-DHFR2. Step 3: The imc1b-specific sequences of the above plasmids are combined with the selectable marker cassette in plasmid pLP-IMC1b/EGFP by Cre-loxP recombination. LoxP sites are indicated by black arrows; noncoding sequences are indicated in white; coding sequences are indicated in light gray; imc1b-specific sequences are indicated in dark gray; Amp r: ampicillin resistance gene; Cm r: chloramphenicol resistance gene; SacB: sucrase gene from Bacillus subtilus; egfp: enhanced green fluorescent protein; UTR: untranslated region; pro: bacterial promoter sequence. Adapted from Tremp *et al.*, 2008.

To make targeting vectors aimed at target gene disruption or mutation, the final pLP-based gene tagging constructs were subjected to site-directed mutagenesis to either remove the coding sequence (gene disruption), or to alter the coding sequence (gene mutation), in each case leaving the fluorescent protein to be expressed as a reporter gene (gene disruption) or fluorescent tag (gene mutation).

2.2. In-Fusion cloning

Rather than using traditional restriction enzyme digestion combined with T4 DNA ligase to introduce PCR fragments into plasmids, we use In-Fusion (In-Fusion Kit, Clontech/Takara Bio). To achieve in-fusion, the forward and reverse PCR primers were designed with at least 15 bases of homology with the sequences flanking the targeted insertion site in the cloning plasmid. Using these primers, amplification of the DNA was performed, and purified PCR product was introduced into a linearized cloning vector in the In-Fusion cloning reaction. The In-Fusion enzyme generates single-stranded regions of homology and then fuses the DNA insert to the vector. The added advantage of In-Fusion is that cloning is directional.

The QIAquick gel extraction kit (Qiagen) was used to purify amplified PCR product and linerized plasmids. Plasmid vectors were linearized by utilising specific restriction endonuclease enzymes and also purified. To prepare the In-Fusion cloning reaction, the linearized plasmid and insert were typically mixed together at an approximately 1:1 molar ratio in a 10μl reaction that contains 1μl In-Fusion enzyme and its appropriate buffer. Reactions were carried out at 37°C for 15min, followed by 15min at 50°C.

2.3. *Cre-loxP* recombination

Cre-loxP site-specific recombinantion was carried out with Cre recombinase (New England Biolabs). Typically, a reaction mixture of 10μl was prepared with approximately 100ng each of pDNR and pLP plasmid DNA, 1 unit of Cre recombinase, in its specific reaction buffer). After 15min of incubation at room temperature, the enzyme was immediately heat-inactivated at 70°C for 5min.

2.4. Site-directed mutagenesis

In order to create mutations or deletions at specific sites in the plasmids, a PCR-based site-directed mutagenesis method was used. The number of PCR cycles was kept low (typically 5) to minimize the undesired expansion of potential errors generated by the PCR. To compensate a higher starting amount of template plasmid DNA was used (typically 1µg). The sense and antisense primers were designed to anneal to complementary strands of the same circular template plasmid DNA and to enable the targeted deletion. Additionally, the first 16 nucleotides of each primer were each other's reverse complement to permit the re-circularization of the linear PCR product by In-Fusion. The PCR reaction was performed using Advantage HD polymerase mix (Clontech/Takara Bio) with ~1µg of DNA template, 10µM of each primer and 2.5mM of each dNTP. Following PCR, the reaction was subjected to *Dpn*I digestion overnight at 37°C to digest the methylated template DNA. The linearized PCR product was then purified and circularized by In-Fusion.

2.5. Bacterial transformation and selection

Bacterial transformation was carried out with NEB 5-alpha competent cells (New England Biolabs). Briefly, frozen competent cells were thawed on ice followed by incubation with the DNA on ice for 30min. Cells were heat-shocked for 45s at 42°C and placed on ice for 1min. To allow expression of the antibiotic resistance, cells were resuspended in 450µl super optimal broth with glucose (SOC) medium and incubated at 37°C for 1h with shaking. The cell culture was then plated onto Luria Broth (LB) agar plates supplemented with either 100µg/ml ampicillin for In-Fusion cloning, or 30µg/ml chloramphenicol plus 7% sucrose for Cre-*loxP* recombination. Colonies were picked and grown in 5ml LB culture containing 100µg/ml ampicillin and incubated at 37°C overnight. Plasmid DNA was extracted and purified from the overnight culture using the Wizard Plus SV Minipreps DNA purification system (Promega) and analysed by diagnostic restriction enzyme digestion.

2.6. Parasite maintenance

P. berghei ANKA clone 234 parasites were maintained as cryopreserved stabilates or by mechanical blood passage and mosquito transmission. For cryopreservation parasitized blood was mixed with an equal volume of cryopreservation solution (20% dimethyl sulfoxide (DMSO), 10% fetal bovine serum (FBS), 70% RPMI 1640) and slowly frozen to -80°C before transfer to liquid nitrogen for long-term storage. As rodent hosts, CD1 mice (typically 20-25g, female) were used. Animals were infected by intraperitoneal injection of fresh or cryopreserved parasitized blood. The levels of infection were monitored observed by light microscopic examination of Giemsa-stained blood films.

2.7. Mosquito maintenance and infection

A. stephensi SD500 mosquitoes were maintained in cages at ~27°C, high relative humidity, under a 12h light/dark cycle and fed on 10% glucose solution. Adult insects were fed on horse blood in membrane feeders (kept at 37°C) twice a week to induce egg laying.

Naive mosquitoes were infected with *P. berghei* by feeding on anaesthetized, gametocytemic mice or by membrane feeding with cultured ookinetes. For optimal development of the parasite, experimental mosquitoes were kept at 19-21°C at high relative humidity and with 10% glucose for feeding. Transmission of sporozoites was carried out with sporozoite-infected mosquitoes (about three weeks post-infection) and naive mice.

2.8. Purification of gametocytes

Purification of gametocytes was performed according to Raabe and colleagues (Raabe *et al.*, 2009). In order to obtain high gametocytaemia, mice were treated with phenylhydrazine (~10µl/g body weight of a 6mg/ml solution in phosphate buffered saline (PBS)) to induce reticulocytosis (and therefore promote *P. berghei* proliferation), and 10^7-10^8 parasites were injected three days later. After three days, infected animals were injected i.p. with chloroquine (200µl of 2mg/ml in PBS) in order to kill asexual blood stages. The following day, gametocytaemic blood was harvested and directly mixed with gametocyte maintenance buffer (GMB: RPMI 1640 containing 25mM Hepes

and L-glutamine (Invitrogen) plus 0.1% BSA). Cells were collected by spinning for 15min at 800$\times g$ at room temperature, loaded onto a 48% Nycodenz cushion in GMB (100% Nycodenz contains 27.6% [w/v] Nycodenz powder in 5mM Tris-HCl pH 7.2, 3mM KCl, 0.3mM EDTA), and centrifuged at 450$\times g$ at room temperature for 20min (gametocytes collect at the interphase). After harvest, the purity of the gametocytes was assessed by examination of Giemsa-stained blood films.

2.9. Culture and purification of ookinetes

To induce reticulocytosis, mice were treated with phenylhydrazine (~10µl/g body weight of a 6mg/ml solution in PBS) followed by injection of 10^7–10^8 parasites three days later. Three days following infection, parasitized blood was harvested and mixed with 10 volumes of ookinete medium (RPMI 1640 containing 25mM Hepes and L-glutamine, 2g/L sodium bicarbonate, 1/100 volume of 10,000u/ml penicillin/10mg/ml streptomycin solution (Gibco), 50mg/L hypoxanthine, 100mM xanthurenic acid and 20% FBS, pH 7.4). Cultures were incubated at 19-21°C for 18-24h to allow ookinete development.

For ookinete purification, cells were collected by centrifugation at 800xg for 5min at 4°C, the pellet resuspended in ice-cold 0.17M ammonium chloride and incubated on ice for 30min to lyse the unparasitized RBCs. Parasites were collected by centrifugation at 800xg for 10min at 4°c with low deceleration and washed twice in PBS (500xg centrifugation). The number of ookinetes was estimated by haemocytometer count.

2.10. Generation of genetically modified parasite lines

For the generation of transgenic *P. berghei* parasite lines, purified schizonts were transfected followed by drug selection and limiting dilution cloning, according to described methods (Janse *et al.*, 2006). To achieve double homologous crossover recombination, targeting vectors were digested with specific enzymes to remove the backbone of the vector and column purified.

Blood was harvested from *P berghei*-infected mice with parasitaemia between

1% and 4%, and added to 100ml filter-sterilized schizont culture medium [RPMI 1640 containing 20mM Hepes and L-glutamine (Sigma R73880), 0.8g/L sodium bicarbonate, 1/200 volume of neomycin solution (Sigma N1142) and 20% FBS, pH 7.2]. The culture was equilibrated with a 5% CO_2, 10% O_2, 85% N_2 gas mixture (BOC) and the flask sealed airtight, followed by incubation at 36°C with gentle shaking (60–80 revolutions per minute) for 20h. Schizonts were purified by centrifugation for 30min at 500xg at room temperature (no brake) on a 50% Nycodenz (in PBS) cushion (100% Nycodenz contains 27.6% [w/v] Nycodenz powder in 5mM Tris-HCl pH 7.2, 3mM KCl, 0.3mM EDTA). The interface layer containing the schizonts was harvested and centrifuged for 8min at 450$xg.$ The schizont pellet was gently resuspended in complete nucleofector solution (Human T Cell Nucleofector kit, Amaxa VPA-1002), and for each transfection 100µl was mixed with DNA (1-5µg in 10-12µl dH_2O or TE buffer). Electroporation was carried out with programme U-033 of the Nucleofector^{TM} II Device (Amaxa). Directly post electroporation, approximately 250µl of naïve blood (previously incubated at 37°C) was added to the parasites, and the mixture was kept at 37°C for 30min to permit merozoite invasion of naive RBCs. Finally, the parasite/RBC mixture was injected i.p. into one or two naive mice.

One day after transfection, pyrimethamine selection was started (supplied in drinking water at a dose equal to 10mg/kg/day) until patent parasitaemia was observed (usually 7-10 days post-inoculation). When parasitaemia reached around 1%, limiting dilution cloning was carried out. Parasites were diluted in RPMI to an estimated 0.3 parasites/inoculum, and typically 10 naive animals were inoculated by i.p. injection. Mice were monitored for parasitaemia after a week.

2.11. Western blot analysis

Protein samples were run through pre-cast NuPAGE Bis-Tris SDS gels (Invitrogen) using an XCell SureLock Mini-Cell system (Invitrogen). Before loading, samples were heated at 70°C for 10min in the presence or absence of 1% reducing agent (Invitrogen). The fractionated protein was then transferred onto a polyvinylidene fluoride (PVDF)

membrane by electroblotting in an XCell II Blot Module (Invitrogen). Membranes were blocked for 1h at room temperature in PBS supplemented with 0.1% Tween 20 and 5% skimmed milk. Membranes were incubated either overnight at 4°C or for 1h at room temperature with specific antibody at the appropriate dilution. Typically horse radish peroxidase (HRP) conjugated antibodies were used to visualise the signal by chemiluminescence, using ECL Western Blotting Substrate (Pierce) and X-ray film (CL-XPosure™ Film, Pierce).

2.12. Light microscopy

Standard light microscopic analysis of parasite and mosquito samples, Giemsa-stained blood films and haemocytometer counts were undertaken using an Olympus CX41 microscope. An Olympus SZ microscope was used for mosquito dissections. For assessment of fluorescence, live or fixed parasite samples were assessed, and images captured, on a Zeiss LSM510 inverted confocal microscope, or on a Zeiss Axioplan-2 fluorescent microscope with Retiga 2000R CCD camera system and Volocity software.

Chapter 3

Distinct temporal recruitment of *Plasmodium* alveolins

to the subpellicular network

Research Paper Cover Sheet

SECTION A – Student Details

Student	Fatimah Al-Khattaf
Principal Supervisor	Johannes Dessens
Thesis Title	Functional characterization of the alveolins, a family of cytoskeleton proteins of malaria parasites

SECTION B – Paper already published

Where was the work published?	Parasitology Research		
When was the work published?	2014		
If the work was published prior to registration for your research degree, give a brief rationale for its inclusion			
Have you retained the copyright for the work?*	**Yes**	Was the work subject to academic peer review?	**Yes**

SECTION D – Multi-authored work

For multi-authored work, give full details of your role in the research included in the paper and in the preparation of the paper. (Attach a further sheet if necessary)	Student generated the mCherry-tagged IMC1c parasite line and carried out the attempted disruption of IMC1c and IMC1e expression. Student performed and analyszed genotyping and phenotyping experiments, in particular with regards to the temporal recruitment and genetic crosses. Student contributed to preparation of the paper (text and figures).

Student Signature: _____   **Date:** _____

Supervisor Signature: _____   _____   **Date:** _____

ORIGINAL PAPER

Distinct temporal recruitment of *Plasmodium* alveolins to the subpellicular network

Annie Z. Tremp · Fatimah S. Al-Khattaf · Johannes T. Dessens

Abstract The zoite stages of malaria parasites (merozoite, ookinete and sporozoite) possess a distinctive cortical structure termed the pellicle, which is defined by a double membrane layer named the inner membrane complex (IMC). The IMC is supported by a cytoskeleton of intermediate filaments, termed the subpellicular network (SPN). *Plasmodium* IMC1 proteins, or alveolins, make up a conserved family of structurally related proteins that comprise building blocks of the SPN. Here, using green fluorescent protein (GFP) tagging in *P. berghei*, we show that the alveolins *Pb*IMC1c and *Pb*IMC1e are expressed in all three zoite stages. Our data reveal that *Pb*IMC1e is assembled into the SPN concurrent with pellicle development, while *Pb*IMC1c is assembled after pellicle formation. In the sexual stages, these processes are accompanied by different gene expressions from maternal and paternal alleles: *Pb*IMC1e is expressed uniquely from the maternal allele, while *Pb*IMC1c is expressed from the maternal allele in gametocytes, but from both parental alleles during ookinete development. These findings establish biogenesis of the cortical cytoskeleton in *Plasmodium* to be a complex and dynamic process, involving distinct parental gene expression and chronological recruitment of its protein constituents. While allelic replacement of the *pbimc1c* and *pbimc1e* genes with GFP-tagged versions was readily achieved using double crossover homologous recombination, attempts to disrupt these genes by this strategy only resulted in the integration of the selectable marker and GFP

reporter into non-specific genomic locations. The recurrent inability to disrupt these genes provides the first genetic evidence that alveolins are necessary for asexual blood-stage parasite development in *Plasmodium*.

Introduction

Malaria parasite transmission is initiated by the ingestion of gametocytemic blood by a vector mosquito, which initiates gametogenesis followed by fertilization. Zygotes transform into motile ookinetes that traverse the gut wall of the insect and transform into oocysts (Meis & Ponnudurai, 1987; Meis et al., 1989). An approximately 2-week period of growth and replication culminates in hundreds of motile sporozoites being released from each oocyst. These invade the salivary glands and are transmitted to new hosts, again by blood feeding of the insect. Once in the host, sporozoites rapidly infect liver cells and replicate each to produce thousands of merozoites. The motile merozoites are released into the bloodstream, where they infect red blood cells and either replicate to form more merozoites or differentiate into sexual-stage male and female gametocytes to complete the life cycle.

The three motile and invasive stages (zoites) of *Plasmodium* species (i.e. ookinetes, sporozoites and merozoites), as well as zoites of other apicomplexan parasites, possess a similar cortical structure termed the pellicle. The pellicle is essentially made up of the plasma membrane and an underlying double membrane structure termed the inner membrane complex (IMC) (Bannister et al., 2000; Morrissette & Sibley, 2002; Santos et al., 2009). Closely associated with the IMC on its cytoplasmic side is a network of intermediate filaments

The authors Annie Z. Tremp and Fatimah S. Al-Khattaf contributed equally to this work.

A. Z. Tremp · F. S. Al-Khattaf · J. T. Dessens (✉)
Pathogen Molecular Biology Department, Faculty of Infectious and Tropical Diseases, London School of Hygiene and Tropical Medicine, Keppel Street, London WC1E 7HT, UK
e-mail: johannes.dessens@lshtm.ac.uk

F. S. Al-Khattaf
Department of Infection Control, College of Medicine, King Saud University, Riyadh, Saudi Arabia

termed the subpellicular network (SPN), which supports the pellicular membranes and provides mechanical strength to the cell (Mann & Beckers, 2001). The pellicular membranes are further supported by subpellicular microtubules that run lengthwise from the anterior towards the posterior end, completing the cortical cytoskeleton (Bannister et al., 2000; Morrissette & Sibley, 2002; Santos et al., 2009).

Several members of an Apicomplexa-specific family of proteins termed IMC1 proteins have been identified as components of the SPN (Khater et al., 2004; Mann & Beckers, 2001). Structurally related proteins from ciliates and dinoflagellate algae have since been added to this protein family renamed 'alveolins', which now defines the Alveolata infrakingdom (Gould et al., 2008). In the genus *Plasmodium*, the number of members of the alveolin family has risen to 12 (Kono et al., 2012), which are encoded by conserved and syntenic genes. The alveolin family members display differential expression between the three zoite stages of the parasite, with the largest repertoires present in the ookinete and sporozoite according to proteomic studies (Florens et al., 2002; Hall et al., 2005; Lasonder et al., 2002; Lindner et al., 2013; Treeck et al., 2011). It has been shown in the rodent malaria species *Plasmodium berghei* that the disruption of individual alveolin family members expressed in sporozoites (*Pb*IMC1a), in ookinetes (*Pb*IMC1b) or in both these zoites (*Pb*IMC1h) results in morphological abnormalities that are accompanied by reduced tensile strength of the zoite stages in which they are expressed (Khater et al., 2004; Tremp & Dessens, 2011; Tremp et al., 2008; Volkmann et al., 2012). Besides roles in morphogenesis and mechanical strength, the *Plasmodium* alveolins are also involved in gliding motility in both ookinetes and sporozoites, most likely through interactions with components of the glideosome that are situated within the pellicular cytoplasm (Khater et al., 2004; Tremp & Dessens, 2011; Tremp et al., 2008; Volkmann et al., 2012).

In this study, we investigate the expression, subcellular distribution and function of two further members of the alveolin/IMC1 protein family, *Pb*IMC1c and *Pb*IMC1e, revealing fundamental differences in the manner they are expressed and participate in zoite morphogenesis. In addition, we provide the first evidence that both *Pb*IMC1c and *Pb*IMC1e are essential for the development of the asexual blood stages of the parasite in the host, underpinning the alveolins as potential target molecules for chemotherapy-based intervention.

Materials and methods

Animal use

All laboratory animal work undergoes regular ethical review by the London School of Hygiene and Tropical Medicine and has been approved by the United Kingdom Home Office. Work was carried out in accordance with the United Kingdom Animals (Scientific Procedures) Act 1986 implementing European Directive 2010/63 for the protection of animals used for experimental purposes. Experiments were conducted in 6–8-week-old female CD1 mice, specific pathogen free and maintained in filter cages. Animal welfare was assessed daily, and animals were humanely killed upon reaching experimental or humane endpoints. Mice were infected with parasites suspended in RPMI or PBS by intraperitoneal injection or by infected mosquito bite on anaesthetized animals. Parasitemia was monitored regularly by collecting a small drop of blood from a superficial tail vein. Drugs were administered by intraperitoneal injection or, where possible, supplied in drinking water. Parasitized blood was harvested by cardiac bleed under general anaesthesia without recovery.

Parasite maintenance, transmission, culture and purification

P. berghei ANKA clone 234 parasites were maintained as cryopreserved stabilates or by mechanical blood passage and regular mosquito transmission. Ookinete cultures were set up overnight from gametocytemic blood as previously described (Arai et al., 2001). After 18–20 h, ookinetes were purified via ice-cold 0.17M ammonium chloride lysis and centrifugation at 800×*g* for 10 min, followed by PBS washes. Mosquito infection and transmission assays were previously described using *Anopheles stephensi* (Dessens et al., 1999; Khater et al., 2004), and infected insects were maintained at 20 °C at approximately 70 % relative humidity.

Gene-targeting constructs

The entire *pbimc1c* coding sequence plus ca. 0.55 kb of upstream sequence was PCR amplified from *P. berghei* genomic DNA with primers pDNR-IMC1c-F (ACGAAGTTATCA GTCGACGGTACCAAGTGCATTTAGTATGTTGTGGC) and pDNR-IMC1c-R (ATGAGGGCCCCTAAGCTTCTGC ATGTACCTGTACAGCAT) and cloned into *Sal*I/*Hin*dIII-digested pDNR-EGFP (Tremp et al., 2008) by in-fusion cloning to give plasmid pDNR-IMC1c/GFP. The 3′UTR of *pbimc1c* was amplified with primers pLP-IMC1c-F (ATAT GCTAGAGCGGCCTTTCGTGAAAAATGCAGTTAACA) and pLP-IMC1c-R (CACCGCGGTGGCGGCCGAAAGA AGACAATAAATAAAATAGAAAGTATGG) and the resulting ca. 0.6 kb fragment cloned into *Not*I-digested pLP-hDHFR by in-fusion cloning to give plasmid pLP-hDHFR/ IMC1c. The *pbimc1c/gfp*-specific sequence from pDNR-IMC1c/GFP was transferred to pLP-hDHFR/IMC1c by Cre/ *lox*P recombination to give the final construct pLP-IMC1c/ GFP. This plasmid served as template in a PCR-based site-directed mutagenesis using primers IMC1c-KO-F (CAACCG TCATGAGTAAAGGAGAAGAACTTTTCAC) and IMC1c-

KO-R (TTACTCATGACGGTTGATGTCTCTTTAGTGT). The resulting PCR product was circularized using in-fusion to give plasmid pLP-IMC1c-KO. In this plasmid, the *pbimc1c* coding sequence except for the first amino acids has been removed.

The entire *pbimc1e* coding sequence plus ca. 0.58 kb of upstream sequence was PCR amplified from genomic DNA with primers pDNR-IMC1e-F (ACGAAGTTATCAGTCG ACGGTACCGCATAAATTAACTTAGTTTCATTGAACT TC) and pDNR-IMC1e-R (ATGAGGGCCCCTAAGCTTTC GTTTAAGACGGGTGGTAC) and cloned into *Sal*I/*Hin*dIII-digested pDNR-EGFP by in-fusion cloning to give plasmid pDNR-IMC1e/GFP. The 3′UTR of *pbimc1e* was amplified with primers pLP-IMC1e-F (ATATGCTAGAGCGGCCTT TGGCTTCGATTTTTGTG) and pLP-IMC1e-R (CACCGC GGTGGCGGCCTAACAGCATTATGAAAGATTGGC) and the resulting ca. 0.87 kb fragment cloned into *Not*I-digested pLP-hDHFR by in-fusion cloning to give plasmid pLP-hDHFR/IMC1e. The *pbimc1e*/*gfp*-specific sequence from pDNR-IMC1e/GFP was transferred to pLP-hDHFR/IMC1e by Cre/*lox*P recombination to give the final construct pLP-IMC1e/GFP. This plasmid served as template in a PCR-based site-directed mutagenesis using primers IMC1e-KO-F (AATA TGTGATGAGTAAAGGAGAAGAACTTTTCAC) and IMC1e-KO-R (TTACTCATCACATATTTAGTGCCACAAT TGC). The resulting PCR product was circularized using in-fusion to give plasmid pLP-IMC1e-KO. In this plasmid, the *pbimc1e* coding sequence except for the first amino acids has been removed.

To generate a mCherry-tagged version in *Pb*IMC1c, the mCherry coding sequence was amplified from pDNR-mCherry/PbSR/EGFP (Carter et al., 2008) with primers pDNR-mCherry-F (CAGTCGACTTAAGCTTAGGGGCCC TCATGGTGAGCAAGGGCG) and pDNR-mCherry-R (AACGGGATCTTCTAGTTACTTGTACAGCTCGTCCAT GC) and introduced into *Hin*dIII/*Xba*I-digested pDNR-EGFP by in-fusion to give plasmid pDNR-mCherry. A 3.8-kb fragment corresponding to the entire *pbimc1c* gene plus upstream intergenic region was PCR amplified from *P. berghei* gDNA using primers IMC1c-mCherry-F (ACGAAGTTATCAGT CGAGGTACCTTCTCATTGTCAATGGCTCC) and pDNR-imc1c-R and introduced into *Sal*I/*Hin*dIII-digested pDNR-mCherry by in-fusion to give plasmid pDNR-IMC1c/mCherry. The *Pb*IMC1c/mCherry-specific sequence from pDNR-IMC1c/mCherry was introduced into plasmid pLP-hDHFR/IMC1c by Cre/lox recombination to give plasmid pLP-IMC1c/mCherry/hDHFR.

Generation and genomic analysis of genetically modified parasites

Parasite transfection, pyrimethamine selection and dilution cloning were performed as previously described (Waters et al., 1997). Prior to performing transfections, plasmid DNA was digested with *Kpn*I and *Sac*II to remove the plasmid backbone. Genomic DNA extraction was performed as previously described (Dessens et al., 1999). For the FP-tagged lines, confirmation of correct targeting and integration into the *pbimc1c* and *pbimc1e* loci was carried out with diagnostic PCR across the integration sites using primer pair hDHFR/ERI-F (ACAAAGAATTCATGGTTG GTTCGCTAAACT) and IMC1c-3′R (TTAGAGCCGATT TTATCTTGTTACAC) for parasite lines IMC1c/GFP and IMC1c/mCherry; and hDHFR/ERI-F and IMC1e-3′R (AAGGTATAAAGTTTATGCATTTTAGCTATC) for parasite line IMC1e/GFP. Confirmation of the absence of the WT allele in the transgenic lines was carried out with primer pairs pDNR-IMC1c-F and IMC1c-3′R (for IMC1c/ GFP); IMC1c-5′F (CTATACCACGCAGCAACAATG) and IMC1c-3′R (for IMC1c/mCherry); and pDNR-IMC1e-F and IMC1e-3′R (for IMC1e/GFP).

Western blot analysis

Parasite samples were heated directly in SDS-PAGE loading buffer at 70 °C for 10 min. Proteins were fractionated by electrophoresis through NuPage 4–12 % Bis-Tris precast gels (Invitrogen) and transferred to PVDF membrane (Invitrogen) according to the manufacturer's instructions. Membranes were blocked for non-specific binding in PBS supplemented with 0.1 % Tween 20 and 5 % skimmed milk for 1 h at room temperature. Goat polyclonal antibody to green fluorescent protein (GFP) conjugated to horse radish peroxidase (Abcam ab6663) diluted 1:5,000 was applied to the membrane for 1 h at room temperature. After washing, signal was detected by chemiluminescence (Pierce ECL western blotting substrate) according to the manufacturer's instructions.

Microscopy

For assessment of fluorescence, live parasite samples were assessed, and images captured, on a Zeiss LSM510 inverted confocal microscope or on a Zeiss Axioplan-2 fluorescent microscope with Retiga 2000R CCD camera system and Volocity software.

Results

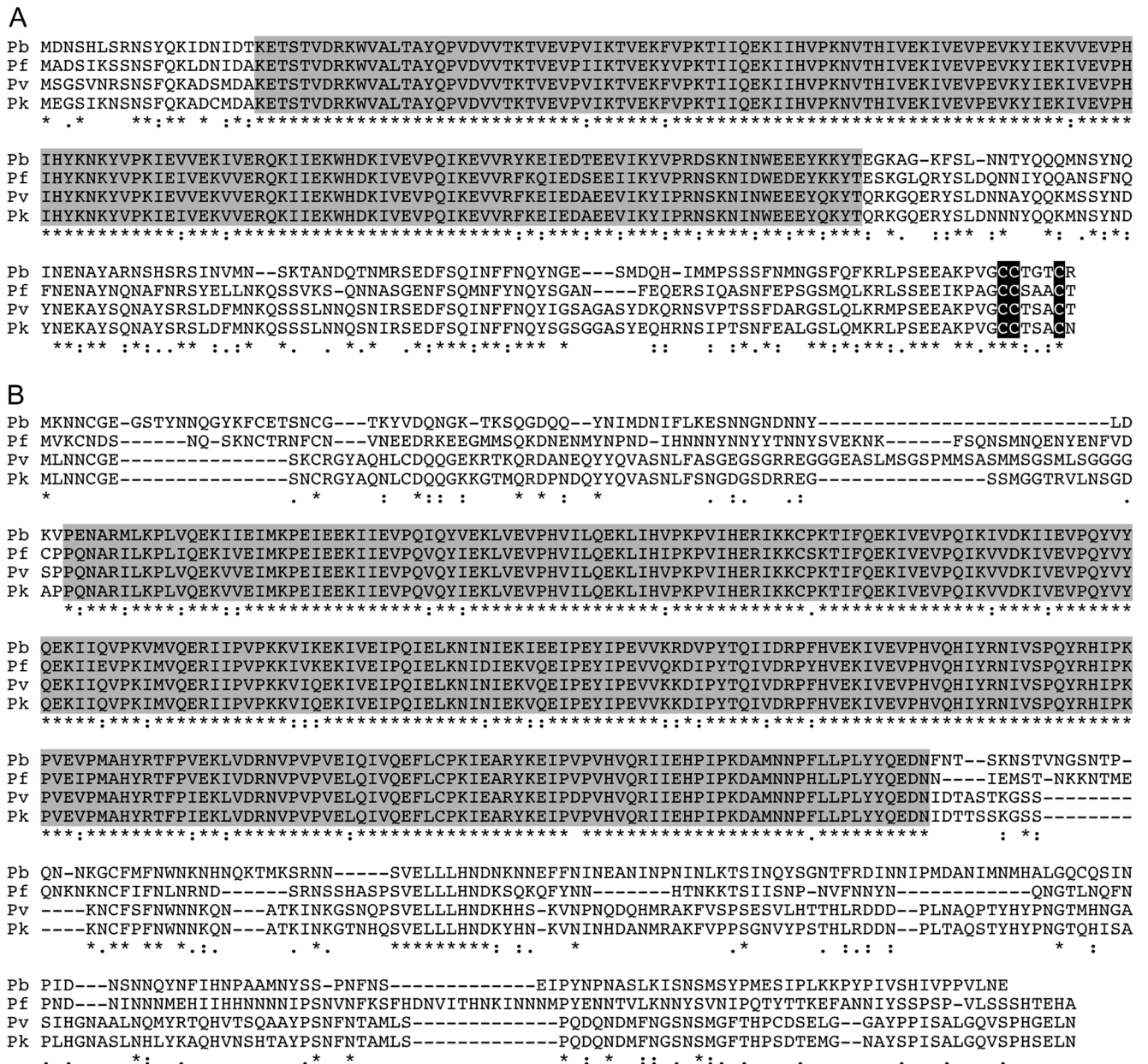Structure of the ***Plasmodium*** alveolins IMC1c and IMC1e

The *Plasmodium* IMC1 protein family was first published in 2004 using gene models of *P. yoelii* (Khater et al., 2004). *Pb*IMC1c (PBANKA_120200) is composed of 278 amino acids encoded by a single exon. *Pb*IMC1c and its orthologous

proteins share a highly conserved amino-terminal domain related to the IMCp domain superfamily (Pfam12314) that defines the IMC1 proteins/alveolins (Fig. 1a). The proteins also possess a conserved cysteine motif at the carboxy-terminus similar to the cysteine motifs described in *Pb*IMC1a and *Tg*IMC1 (Fig. 1a) that is believed to act as a palmitoylation signal (Khater et al., 2004; Mann & Beckers, 2001). *Pb*IMC1e (PBANKA_040270) is composed of 512 amino acids encoded by a single exon. Sequence conservation is limited to an IMCp domain in their central portions

(Fig. 1b). Interestingly, the *Plasmodium imc1e* locus is located directly downstream of its family member *imc1a* in the opposite orientation, suggesting that these two genes could be sharing promoter elements.

Fluorescent protein tagging of PbIMC1c and PbIMC1e

To achieve GFP tagging of *Pb*IMC1c and *Pb*IMC1e, we adopted a strategy of double crossover homologous recombination in which the wild-type alleles were replaced with

A

```
Pb  MDNSHLSRNSYQKIDNIDTKETSTVDRKWVALTAYQPVDVVTKTVEVPVIKTVEKFVPKTIIQEKIIHVPKNVTHIVEKIVEVPEVKYIEKVVEVPH
Pf  MADSIKSSNSFQKLDNIDAKETSTVDRKWVALTAYQPVDVVTKTVEVPIIKTVEKYVPKTIIQEKIIHVPKNVTHIVEKIVEVPEVKYIEKIVEVPH
Pv  MSGSVNRSNSFQKADSMDAKETSTVDRKWVALTAYQPVDVVTKTVEVPVIKTVEKFVPKTIIQEKIIHVPKNVTHIVEKIVEVPEVKYIEKIVEVPH
Pk  MEGSIKNSNSFQKADCMDAKETSTVDRKWVALTAYQPVDVVTKTVEVPVIKTVEKFVPKTIIQEKIIHVPKNVTHIVEKIVEVPEVKYIEKIVEVPH
    * .*      **:**  * :*:***********************:*******:****:*************:********************:*****

Pb  IHYKNKYVPKIEVVEKIVERQKIIEKWHDKIVEVPQIKEVVRYKEIEDTEEVIKYVPRDSKNINWEEEYKKYTEGKAG-KFSL-NNTYQQQMNSYNQ
Pf  IHYKNKYVPKIEIVEKVVERQKIIEKWHDKIVEVPQIKEVVRFKQIEDSEEIIKYVPRNSKNIDWEDEYKKYTESKGLQRYSLDQNNIYQQANSFNQ
Pv  IHYKNKYVPKIEVVEKVVERQKIIEKWHDKIVEVPQIKEVVRFKEIEDAEEVIKYIPRNSKNINWEEEYQKYTQRKGQERYSLDNNAYQQKMSSYND
Pk  IHYKNKYVPKIEIVEKVVERQKIIEKWHDKIVEVPQIKEVVRFKEIEDAEEVIKYIPRNSKNINWEEEYQKYTQRKGQERYSLDNNNYQQKMNSYND
    ***********:**:**********************:*****::*****:.***:**:***:**:****:**:**:***: *. :.:** :*   *:.*:*:

Pb  INENAYARNSHSRSINVMN--SKTANDQTNMRSEDFSQINFFNQYNGE---SMDQH-IMMPSSSFNMNGSFQFKRLPSEEAKPVGCCTGTCR
Pf  FNENAYNQNAFNRSYELLNKQSSVKS-QNNASGENFSQMNFYNQYSGAN----FEQERSIQASNFEPSGSMQLKRLSSEEIKPAGCCSAACT
Pv  YNEKAYSQNAYSRSLDFMNKQSSSLNNQSNIRSEDFSQINFFNQYIGSAGASYDKQRNSVPTSSFDARGSLQLKRMPSEEAKPVGCCTSACT
Pk  YNEKAYSQNAYSRSLDFMNKQSSSLNNQSNIRSEDFSQINFFNQYSGSGGASYEQHRNSIPTSNFEALGSLQMKRLPSEEAKPVGCCTSACN
    **:** :*:..** ::.:*  *.  .  *.*  .*:***:**:*** *      ::    :  :*.*:  **:*:**:.*** **.***..:*
```

B

```
Pb  MKNNCGE-GSTYNNQGYKFCETSNCG---TKYVDQNGK-TKSQGDQQ--YNIMDNIFLKESNNGNDNNY-------------------------LD
Pf  MVKCNDS------NQ-SKNCTRNFCN---VNEEDRKEEGMMSQKDNENMYNPND-IHNNNYNNYYTNNYSVEKNK------FSQNSMNQENYENFVD
Pv  MLNNCGE--------------SKCRGYAQHLCDQQGEKRTKQRDANEQYYQVASNLFASGEGSGRREGGGEASLMSGSPMMSASMMSGSMLSGGGG
Pk  MLNNCGE--------------SNCRGYAQNLCDQQGKKGTMQRDPNDQYYQVASNLFSNGDGSDRREG--------------SSMGGTRVLNSGD
    *            . *   :  *:: :    * * : *         . :.   .:

Pb  KVPENARMLKPLVQEKIIEIMKPEIEEKIIEVPQIQYVEKLVEVPHVILQEKLIHVPKPVIHERIKKCPKTIFQEKIVEVPQIKIVDKIIEVPQYV
Pf  CPPQNARILKPLIQEKIVEIMKPEIEEKIIEVPQVQYIEKLVEVPHVILQEKLIHIPKPVIHERIKKCSKTIFQEKIVEVPQIKVVDKIVEVPQYV
Pv  SPPQNARILKPLVQEKVVEIMKPEIEEKIIEVPQVQYIEKLVEVPHVILQEKLIHVPKPVIHERIKKCPKTIFQEKIVEVPQIKVVDKIVEVPQYV
Pk  APPQNARILKPLVQEKVVEIMKPEIEEKIIEVPQVQYIEKLVEVPHVILQEKLIHVPKPVIHERIKKCPKTIFQEKIVEVPQIKVVDKIVEVPQYV
    *:***:*****:***::*******************:**:************************:***.***:************:***:*******

Pb  QEKIIQVPKVMVQERIIPVPKKVIKEKIVEIPQIELKNINIEKIEEIPEYIPEVVKRDVPYTQIIDRPFHVEKIVEVPHVQHIYRNIVSPQYRHIPK
Pf  QEKIIEVPKIMVQERIIPVPKKIVKEKIVEIPQIELKNIDIEKVQEIPEYIPEVVQKDIPYTQIVDRPYHVEKIVEVPHVQHIYRNIVSPQYRHIPK
Pv  QEKIIQVPKIMVQERIIPVPKKVIQEKIVEIPQIELKNINIEKVQEIPEYIPEVVKDIPYTQIVDRPFHVEKIVEVPHVQHIYRNIVSPQYRHIPK
Pk  QEKIIQVPKIMVQERIIPVPKKVIQEKIVEIPQIELKNINIEKVQEIPEYIPEVVKKDIPYTQIVDRPFHVEKIVEVPHVQHIYRNIVSPQYRHIPK
    *****:***:************::::*********************:**:*********::*:*****:***:***:*************************

Pb  PVEVPMAHYRTFPVEKLVDRNVPVPVEIQIVQEFLCPKIEARYKEIPVPVHVQRIIEHPIPKDAMNNPFLLPLYYQEDNFNT--SKNSTVNGSNTP-
Pf  PVEIPMAHYRTFPVEKIVDRNVPVPVELQIVQEFLCPKIEARYKEIPVPVHVQRIIEHPIPKDAMNNPHLLPLYYQEDNN----IEMST-NKKNTME
Pv  PVEVPMAHYRTFPIEKLVDRNVPVPVELQIVQEFLCPKIEARYKEIPDPVHVQRIIEHPIPKDAMNNPFLLPLYYQEDNIDTASTKGSS-------
Pk  PVEVPMAHYRTFPIEKLVDRNVPVPVELQIVQEFLCPKIEARYKEIPVPVHVQRIIEHPIPKDAMNNPFLLPLYYQEDNIDTTSSKGSS-------
    ***:*********:**:**********:******************** ***********************.********** : *:

Pb  QN-NKGCFMFNWNKNHNQKTMKSRNN-----SVELLLHNDNKNNEFFNINEANINPNINLKTSINQYSGNTFRDINNIPMDANIMNMHALGQCQSIN
Pf  QNKNKNCFIFNLNRRND------SRNSSHASPSVELLLHNDKSQKQFYNN-------HTNKKTSIISNP-NVFNNYN-----------QNGTLNQFN
Pv  ----KNCFSFNWNNKQN---ATKINKGSNQPSVELLLHNDKHHS-KVNPNQDQHMRAKFVSPSESVLHTTHLRDDD--PLNAQPTYHYPNGTMHNGA
Pk  ----KNCFPFNWNNKQN---ATKINKGTNHQSVELLLHNDKYHN-KVNINHDANMRAKFVPPSGNVYPSTHLRDDN--PLTAQSTYHYPNGTQHISA
    *.** ** *.::.      .*.       *********: :.   *          .*       . :.:: :          * :

Pb  PID---NSNNQYNFIHNPAAMNYSS-PNFNS-------------EIPYNPNASLKISNSMSYPMESIPLKKPYPIVSHIVPPVLNE
Pf  PND---NINNNMEHIIHHNNNNIPSNVNFKSFHDNVITHNKINNNMPYENNTVLKNNYSVNIPQTYTTKEFANNIYSSPSP-VLSSSHTEHA
Pv  SIHGNAALNQMYRTQHVTSQAAYPSNFNTAMLS-------------PQDQNDMFNGSNSMGFTHPCDSELG--GAYPPISALGQVSPHGELN
Pk  PLHGNASLNHLYKAQHVNSHTAYPSNFNTAMLS-------------PQDQNDMFNGSNSMGFTHPSDTEMG--NAYSPISALGQVSPHSELN
    . .     *:  .       .* *    * : *   ::. *::.  .          * : *  :: .*:. .
```

Fig. 1 Sequence and structure of *Pb*IMC1 proteins. Multiple amino acid sequence alignment of the predicted IMC1c (**a**) and IMC1e (**b**) proteins from *P. berghei* (Pb), *P. knowlesi* (Pk), *P. vivax* (Pv) and *P. falciparum* (Pf). Indicated are conserved alveolin domains (*shaded*) and gaps introduced to allow optimal alignment (*hyphens*). Conserved amino acid identities (*asterisks*) and similarities (*colons* and *points*) are indicated underneath. Also shown is a conserved cysteine motif at the carboxy-terminus of IMC1c (*black shading*). The alignment was made with ClustalW

recombinant full-length wild-type alleles fused to GFP at their carboxy-terminus (Fig. 2a). After the transfection of purified schizonts, pyrimethamine-resistant parasites were selected and cloned by limiting dilution as described (Tremp & Dessens, 2011; Tremp et al., 2008) to give parasite lines IMC1c/GFP and IMC1e/GFP, respectively. PCR diagnostic for integration into the *pbimc1c* locus produced a specific band of 1.8 kb in the IMC1c/GFP clones, while PCR diagnostic for the presence of the wild-type *imc1c* allele gave a specific band of 2.1 kb only in wild-type parasites (Fig. 2b). Likewise, PCR diagnostic for integration into the *pbimc1e* locus produced a specific band of 2.0 kb in the IMC1e/GFP clones, while PCR diagnostic for the presence of the wild-type *pbimc1e* allele gave a specific band of 3.0 kb only in wild-type parasites (Fig. 2b). Both genetically modified parasite lines generated displayed normal parasite development in mouse and mosquito and were readily transmitted by sporozoite-infected mosquito bites, indicating that the carboxy-terminal GFP fusions had not adversely affected the function of *Pb*IMC1c and *Pb*IMC1e. Both parasite lines displayed GFP fluorescence in ookinetes (see below), and immuno blot analysis of purified, cultured ookinetes with anti-GFP antibodies detected specific bands corresponding to the *Pb*IMC1c and *Pb*IMC1e fusion proteins with GFP, respectively (Fig. 2c).

Life-stage expression of PbIMC1c and PbIMC1e

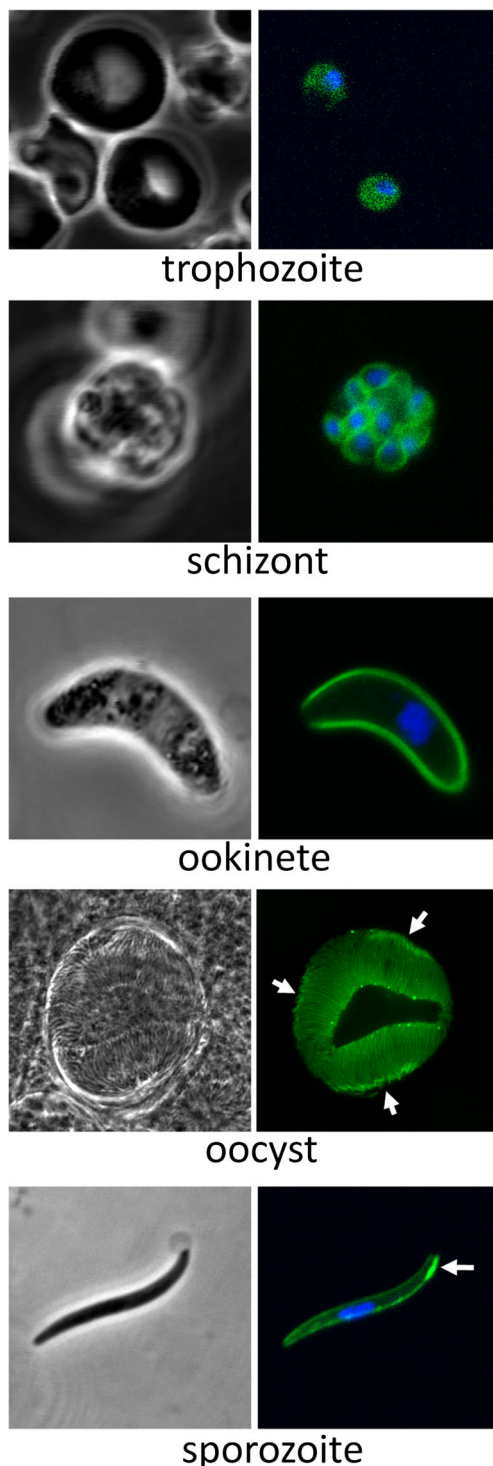The expression and subcellular distribution of *Pb*IMC1c and *Pb*IMC1e were assessed by UV and laser scanning microscopy of live parasites. IMC1c/GFP parasites displayed strong fluorescence throughout asexual blood-stage development that appeared cytoplasmic, except in mature schizonts where it showed clear peripheral localization in individual merozoites (Fig. 3). To assess *Pb*IMC1c expression in the mosquito stages, we set up ookinete cultures and infected *A. stephensi* vector mosquitoes. Cultured ookinetes displayed very strong fluorescence with a cortical distribution (Fig. 3). Sporulated oocysts and sporozoites also displayed strong fluorescence, which was concentrated at the cortex of the sporozoites (Fig. 3). These combined observations are fully consistent with a pellicular localization of *Pb*IMC1c and are in agreement with it being a predicted SPN resident. Besides the peripheral distribution of *Pb*IMC1c in sporozoites, a thickened area was present near one extremity of the cell (Fig. 3). In *P. berghei* sporozoites, the nucleus is consistently positioned closer to the posterior end of the cell (Kudryashev et al., 2010). Accordingly, based on its position relative to the sporozoite nucleus, as well as its localization away from the sporoblast in sporulated oocysts (Fig. 3), the discrete area of fluorescence appears to be located at the anterior end.

In contrast to IMC1c/GFP parasites, IMC1e/GFP parasites exhibited very weak GFP-based fluorescence in blood stages that required recording with a CCD digital microscope camera (Fig. 4). Because of these low fluorescence levels, it was difficult to discern a specific subcellular distribution. In contrast to the blood stages, mature ookinetes displayed much stronger GFP fluorescence that was distributed predominantly in the cell cortex (Fig. 4), consistent with a pellicular
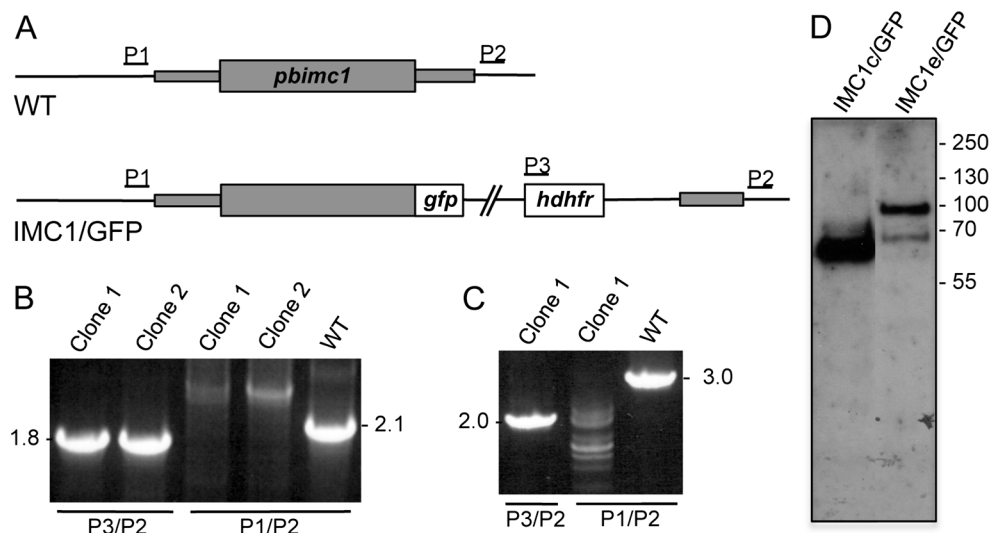
Fig. 2 Generation and molecular analyses of genetically modified parasite lines. **a** General targeting strategy for the GFP tagging of *pbimc1c* and *pbimc1e* via double crossover homologous recombination. Both the wild-type (WT) and modified, GFP-tagged (IMC1/GFP) alleles are shown. The *pbimc1* gene is indicated with coding sequence (*wide bars*) and non-coding sequence (*narrow bars*). Also indicated are the enhanced GFP module (*gfp*), the hDHFR selectable marker gene cassette (*hdhfr*) and primers used for diagnostic PCR amplification (P1-P3). **b** PCR diagnostic for the presence of the GFP-tagged *pbimc1* alleles using primers P2 and P3 (P3/P2) and the absence of the wild-type *pbimc1* alleles using primers P1 and P2 (P1/P2) from clonal parasite populations of IMC1c/GFP (*left panel*) and IMC1e/GFP (*right panel*). WT parasites are included as positive controls for the unmodified alleles. **c** Western blot analysis of purified, cultured ookinete samples of parasite lines IMC1c/GFP and IMC1e/GFP using anti-GFP antibodies, showing corresponding *Pb*-IMC1::GFP fusion proteins

Fig. 3 Expression and subcellular localization of *Pb*IMC1c. Confocal bright-field and GFP fluorescence images of trophozoite, schizont, ookinete, mature oocyst and sporozoite life stages. Hoechst DNA staining (*blue*) indicates position of nuclei. *Arrows* point to anterior structures in sporozoites

Fig. 4 Expression and subcellular localization of *Pb*IMC1e. Bright-field and GFP fluorescence images of schizont, ookinete, mature oocyst and sporozoite life stages. The schizont image was captured using a CCD camera due to the low levels of fluorescence, while the other images were captured by confocal microscopy. Hoechst DNA staining (*blue*) indicates the position of nuclei. *Arrows* point to posterior structures in ookinetes and sporozoites

localization of the protein and its predicted function in the SPN. *Pb*IMC1e was also present in an unknown structure situated at one extremity of the ookinete (Fig. 4). A genetic cross with parasite line G2/GFP, which labels the collar (i.e. an

apical cap-like structure of the ookinete) (Tremp et al., 2013), gave rise to heterokaryotic ookinetes that simultaneously displayed both the *Pb*G2-labelled collar and *Pb*IMC1e-labelled structure (data not shown), indicating that the latter is positioned at the posterior end of the ookinete. Sporulated oocysts and sporozoites also displayed GFP florescence, which localized to the periphery of the sporozoites (Fig. 4). Sporozoites possessed a small fluorescent spot at one extremity which, based on its position relative to the sporozoites nucleus, as well as its localization in sporulated oocysts lining

the sporoblast (Fig. 4), appears to correspond to the sporozoite posterior end.

PbIMC1c and PbIMC1e display distinct temporal recruitment to the SPN

To further study the recruitment of *Pb*IMC1c and *Pb*IMC1e to the pellicle, we examined retorts (i.e. immature ookinetes), which contain an elongated 'ookinete' portion that contains pellicle and a spherical 'zygote' part that does not. This revealed a marked difference between the two alveolins: whereas *Pb*IMC1e was clearly localized to the periphery of the elongated 'ookinete' portion of the retort, *Pb*IMC1c was not (Fig. 5a). In fact, *Pb*IMC1e was detected in the pellicle of very young retorts, indicating that it is assembled into the ookinete SPN from the start of pellicle/SPN formation (Fig. 5b). Interestingly, this process was accompanied by the formation of several fluorescent spots in the spherical 'zygote' section (Fig. 5c).

When examining oocysts on IMC1c/GFP parasite-infected *A. stephensi* midguts at 2 weeks post-infection, we observed fully sporulated oocysts with very strong GFP fluorescence that clearly was localized at the sporozoites' cortex (Fig. 5d). However, on the same midguts, we found sporozoite-containing oocysts that exhibited very low, baseline GFP fluorescence levels similar to not yet sporulated oocysts (Fig. 5d). These observations indicate that *Pb*IMC1c is predominantly expressed after sporozoite budding and—similar to the situation in the ookinete—is recruited to the SPN after pellicle formation. By contrast, IMC1e/GFP parasite-infected midguts had sporulated oocysts that exhibited strong fluorescence without exception.

PbIMC1c and PbIMC1e are differentially expressed from maternal and paternal alleles in the sexual stages
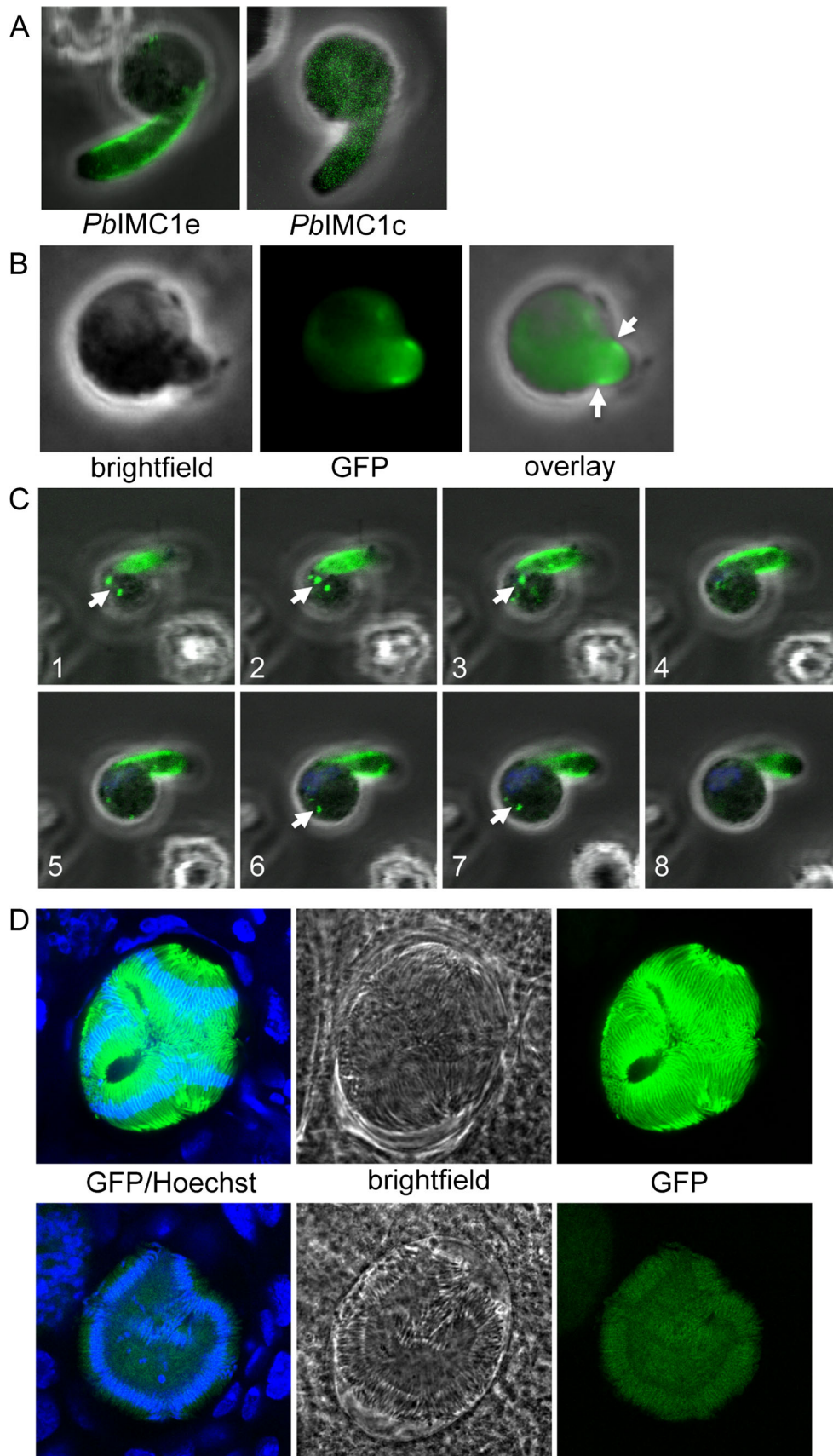
Interestingly, we found a weak cytoplasmic *Pb*IMC1c::GFP expression in gametocytes, but only in females (possessing the smaller nucleus) (Fig. 6a). We did not see a discernible increase in fluorescence until some 7–8 h post-gametogenesis, resulting in mature ookinetes at 24-h ookinetes with very strong fluorescence levels (Fig. 3). To test IMC1c expression from the paternal allele, parasite line IMC1c/mCherry was generated to express a red fluorescent protein-tagged version of *Pb*IMC1c, which was then crossed with the equivalent GFP-tagged parasite line. The strategy used to generate IMC1/mCherry was the same as for IMC1c/GFP (Fig. 2). Accordingly, PCR diagnostic for the integration of the selectable marker into the *pbimc1c* locus amplified a 1.8-kb fragment from different clones of this parasite line and not from wild-type parasites, as expected (Fig. 6b). Additionally, PCR diagnostic for the wild-type *pbimc1c* allele amplified a 2.3-kb product from wild-type parasites, but not from the transgenic

lines, as expected (Fig. 6b). The resulting *Pb*IMC1c::mCherry fusion protein displayed similar life-stage expression and subcellular distribution as its GFP-tagged counterpart (data not shown and Fig. 6c). After a genetic cross with parasite line IMC1c/GFP, heterozygous ookinetes (derived from cross fertilization) were produced that dually expressed red and green fluorescent proteins (Fig. 6c). This demonstrates that *Pb*IMC1c is expressed from both the maternal- and paternal-inherited alleles in the mature ookinete. In a time course, dual expression of GFP and mCherry was first detected at approximately 7 h post-gametogenesis, indicating this is the point when protein expression from the paternal *pbimc1c* allele commences.

Parasite line IMC1e/GFP exhibited very weak GFP fluorescence in gametocytes (data not shown). In this parasite, fluorescence levels increased around 4 h post-gametogenesis prior to the start of pellicle formation. To test *Pb*IMC1e expression from the paternal allele, we crossed parasite line IMC1e/GFP with parasite line PbSR/EGFP (Carter et al., 2008). The latter expresses a GFP-tagged version of *Pb*LAP1, which is maternally inherited (Raine et al., 2007). In mature ookinetes, *Pb*LAP1 is almost exclusively present in the crystalloids, which appear as one or two distinctive fluorescent spots in ookinetes of parasite line *Pb*SR/EGFP (Carter et al., 2008). In the crossed ookinete culture, we could not detect any mature heterokaryotic ookinetes that displayed, at the same time, fluorescent crystalloids and a fluorescent cortex (64 % only peripheral GFP, 36 % only crystalloid GFP; $n=$ 100). A similar result (59 % only peripheral GFP, 41 % only crystalloid GFP; $n=100$) was obtained when we crossed IMC1e/GFP with parasite line *Pb*LAP3/GFP, which expresses a GFP-tagged family member of *Pb*LAP1 that is also maternally expressed (Saeed et al., 2010, 2012). These observations show that, in contrast to *Pb*IMC1c, *Pb*IMC1e is only expressed from the maternal allele in the sexual stages.

PbIMC1c and PbIMC1e are essential for blood-stage asexual parasite development

To achieve knockout of *Pb*IMC1c and *Pb*IMC1e expression, we again adopted a strategy of double crossover homologous recombination identical to the GFP-tagging approach. The coding sequences of *pbimc1c* and *pbimc1e* were removed leaving GFP under control of the native *pbimc1* gene promoters to act as a reporter (Fig. 7a). In contrast to the transfections aimed at GFP tagging, which readily resulted in a specific integration into the *pbimc1c* and *pbimc1e* loci (Fig. 2), our attempts to disrupt *pbimc1c* and *pbimc1e* repeatedly failed to give integration of the selectable marker into the target loci (based on five independent transfections for each gene knockout). This indicated that these genes are important for the development of asexual blood stages and cannot be disrupted, which is consistent with the observed expression of

A

*Pb*IMC1e   *Pb*IMC1c

B

brightfield   GFP   overlay

C

D

GFP/Hoechst   brightfield   GFP

these genes in asexual blood-stage parasites (Figs. 3 and 4). This notion was corroborated by the fact that the 'knockout' transfections produced drug-resistant parasites that displayed green fluorescence resulting from the expression of the GFP reporter gene. However, in both cases, the GFP fluorescence was only observed in gametocytes, with fluorescence levels being markedly stronger after targeting *pbimc1e* than after targeting *pbimc1c* (Fig. 7b). The lack of integration of the selectable marker and GFP reporter into the target loci, combined with the clear disparity between the expression profiles of GFP in these transfections compared to those that generated GFP-tagged *Pb*IMC1c and *Pb*IMC1e (Figs. 3 and 4), strongly points to integration into non-specific genomic locations. Such events are likely to be selected only when homologous recombination is detrimental to parasite development. Hence, these observations strongly support a critical role for *Pb*IMC1c and *Pb*IMC1e in asexual blood-stage development of the parasite.

Discussion

This study shows that a further two members of the *Plasmodium* alveolin/IMC1 protein family are recruited to the SPN in the zoite stages where they are expressed as protein. This faithful localization to the pellicle further supports the notion that alveolins have a predominantly cytoskeletal function and, hence, that the structural similarities (i.e. the IMCp domains) reflect functional properties. We show that *Pb*IMC1c and *Pb*IMC1e are expressed in all three zoite stages of the malaria parasite including merozoites. Recent studies based on cryo-electron tomography failed to detect an apparent subpellicular structure in merozoites, suggesting that a SPN may not be present in this zoite stage (Kudryashev et al., 2012). However, the clear peripheral distribution of *Pb*IMC1c in merozoites shown here (Fig. 3) supports the presence of a SPN within the merozoite pellicle. The IMC1 protein expression profiles thus far established by us and others in *P. berghei* (Khater et al., 2004; Kono et al., 2012;
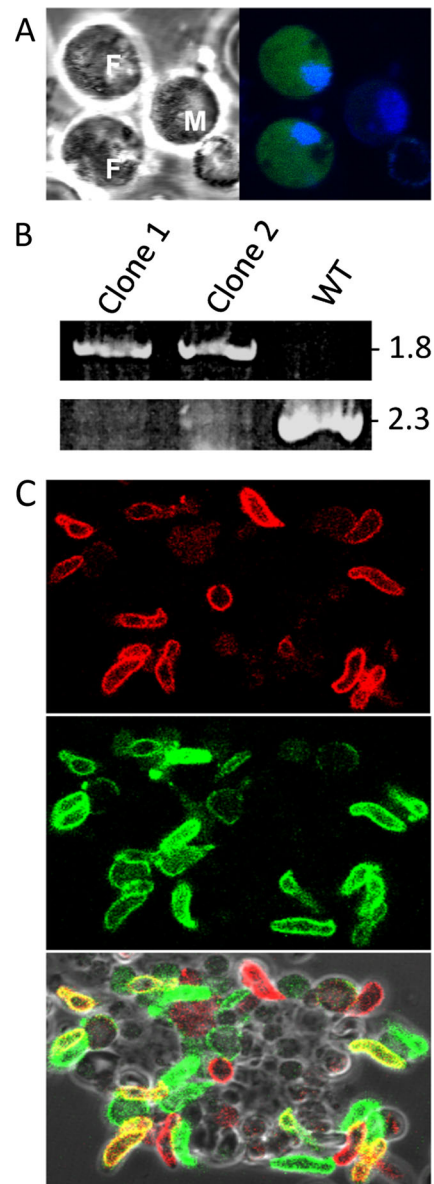
Fig. 6 Expression of *Pb*IMC1c from parental alleles in the sexual stages. **a** Confocal bright-field and GFP fluorescence images of female (*F*) and male (*M*) gametocytes of parasite line IMC1c/GFP. Hoechst staining (*blue*) labels nuclei. **b** PCR diagnostic for the integration of the selectable marker into the *pbimc1c* locus in two different clones of parasite line IMC1c/mCherry, amplying a 1.8-kb fragment (*top panel*). PCR diagnostic for the unmodified *pbimc1c* allele amplified a 2.3-kb product only from WT parasites (*bottom panel*). **c** Confocal images of ookinetes derived from a genetic cross between parasite lines IMC1c/GFP and IMC1c/mCherry, showing mCherry (*top*) and GFP fluorescence (*middle*). *Bottom panel* shows overlay with bright field and identifies dual-labelled ookinetes (*yellow*) pointing to expression from both parental alleles

Tremp & Dessens, 2011; Tremp et al., 2008; Volkmann et al., 2012) fit very well with available *Plasmodium falciparum* protein expression data (Florens et al., 2002; Hall et al., 2005; Lasonder et al., 2002; Lindner et al., 2013; Treeck et al., 2011), indicating that *Plasmodium* alveolin orthologues

A

B
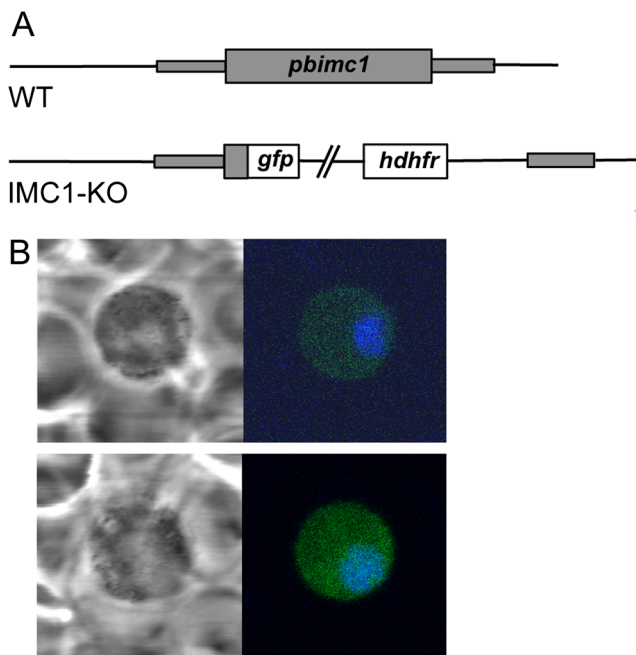
Fig. 7 Targeted disruption of *Pb*IMC1c and *Pb*IMC1e. **a** Gene structure of *pbimc1* alleles in WT and *Pb*IMC1-KO *parasite lines*. The *pbimc1* gene is indicated with coding sequence (*wide bars*) and non-coding sequence (*narrow bars*). Also indicated are the enhanced GFP module (*gfp*) and the hDHFR selectable marker gene cassette (*hdhfr*). **b** Confocal bright-field and GFP fluorescence images of gametocytes after attempted disruption of *pbimc1c* (*top panel*) and *pbimc1e* (*bottom panel*). Hoechst DNA staining (*blue*) labels nuclei

have conserved stage-specific expression profiles. The new alveolin expression data reported here are therefore likely to apply also to *P. falciparum* and other human malaria species. An exception to this may be the gametocyte, which possesses a pellicle structure in *P. falciparum*, but not in *P. berghei* (Dearnley et al., 2012). Moreover, antibodies to a generic alveolin epitope label the periphery of *P. falciparum* gametocytes (Gould et al., 2008), indicating that alveolins are indeed present in the gametocyte SPN.

Our data show for the first time that clear differences exist between *Plasmodium* alveolins with respect to their assembly into the SPN of ookinetes and sporozoites (Fig. 5). Whereas *Pb*IMC1e appears to be assembled concurrent with pellicle formation, *Pb*IMC1c joins the SPN only after pellicle formation. Accordingly, we anticipate that *Pb*IMC1c is not required for normal ookinete and sporozoite morphogenesis, in contrast to its family members *Pb*IMC1a, *Pb*IMC1b and *Pb*IMC1h (Khater et al., 2004; Tremp & Dessens, 2011; Tremp et al., 2008). Our observations provide a clear demonstration that the SPN continues to develop after zoite formation. This could, for instance, explain why cryo-electron tomography points to midgut sporozoites having a less prominent SPN than salivary gland sporozoites (Kudryashev et al., 2012). Our observations are also consistent with studies of *Toxoplasma* showing that the SPN of older parasites becomes detergent insoluble, reflecting a change in rigidity and

mechanical strength of the structure (Mann et al., 2002). These observations all point to a process of maturation of the SPN after its initial biogenesis.

There are clear parallels between the *Plasmodium* alveolins described here and some of those characterized in *Toxoplasma gondii* (Anderson-White et al., 2011). For example, *T. gondii* IMC1, IMC3, IMC6 and IMC10 localize to the cortical cytoskeleton during tachyzoite daughter cell budding, whereas IMC7, IMC12 and IMC14 are only found in the mature pellicles and not in those of the emerging daughter cells (Anderson-White et al., 2011). Even though the alveolin repertoires differ between *Plasmodium* and *Toxoplasma* (Anderson-White et al., 2011; Kono et al., 2012), the distinct chronological assembly of certain family members into the SPN appears to be a common feature that is likely to reflect a biological requirement for different physical properties of the SPN at different phases of zoite development. Another similarity with *Toxoplasma* alveolins is that, although their main site of action is the cortical cytoskeleton, some are also found in additional subcellular structures such as the basal body and centrosome (Anderson-White et al., 2011). *Pb*IMC1c and *Pb*IMC1e, too, localize to additional structures (Figs. 3 and 4). For the ookinete, defined basal structures that could correspond to the posterior structure containing *Pb*IMC1e have not been described. It is notable that the posterior structure associated with the ookinete appears almost exterior of the cell, indicating that it could constitute residual 'zygote' material left over from the transformation of the spherical zygote into the elongated ookinete. Notably, assembly of *Pb*IMC1e into the pellicle is accompanied by the formation of multiple discrete *Pb*IMC1e-containing 'spots' that lie mainly within the cytoplasm of the spherical zygote portion, which may become trapped within the residual zygote membrane at the posterior end of the cell. Similar spots were not apparent during the formation of ookinetes that express GFP-tagged *Pb*IMC1b or *Pb*IMC1h (Tremp & Dessens, 2011; Tremp et al., 2008). In sporozoites, the posterior structure that is labelled with *Pb*IMC1e could correspond to, or co-localize with, the posterior polar ring (Kudryashev et al., 2010). It is also not clear what the apical structure in sporozoites labelled with *Pb*IMC1c corresponds to. It is notable that the area is present only on one side of the anterior sporozoite, and one possibility is that it could co-localize with the apical ring complex that sits at a sharp angle towards the ventral side of the sporozoite tip (Kudryashev et al., 2012).

Although *Pb*IMC1c is present in asexual, sexual and sporogonic life stages, it is not constitutively expressed as the protein was not detected in male gametocytes or in oocysts before sporulation. The apparent lack of GFP fluorescence in male gametocytes indicates that *Pb*IMC1c is not carried over from the preceding trophozoite stage; if this was the case, both male and female gametocytes would be expected to express GFP. Rather, the restricted expression in female gametocytes

points to an early commitment to sexual stage development that occurs before trophozoite development. Female gametocytes in *P. berghei* are spherical cells that do not possess a discernible pellicle, so it is not clear why the protein is expressed here. One possibility is that *Pb*IMC1c could have a function in the gametocyte that is not linked to the SPN. It should be noted that a study by Mair and colleagues (Mair et al., 2006) shows significantly reduced transcript levels of both *pbimc1c* and *pb1mc1e* in gametocytes of the helicase DOZI (development of zygote inhibited) null mutant parasites. This suggests that these genes are subject to translational repression, a female gametocyte-specific mechanism of translational silencing involved in the development of the parasite post-fertilization (Mair et al., 2006). Translational repression of *pbimc1c* and *pbimc1e* is consistent with the failure to detect significant amounts of the respective gene products in gametocytes using high-accuracy mass spectrometry-based proteomics (Hall et al., 2005; Khan et al., 2005). In *P. falciparum*, too, *pfimc1c* and *pfimc1e* mRNAs are abundant in mature blood-stage gametocytes (Lopez-Barragan et al., 2011), while the corresponding gene products have not been detected in this life stage by mass spectrometry (Silvestrini et al., 2010), again supporting a scenario of translational repression. The low expression of *Pb*IMC1c observed in female gametocytes could be the result of 'leaky' translational repression, where only a fraction of the *pbimc1c* mRNA is silenced.

The failure to achieve a structural disruption of the *pbimc1c* and *pbimc1e* genes indicates that these genes are refractory to genetic depletion. This, in turn, indicates that these genes are essential for the completion of the cycle of blood-stage schizogony or for infectivity of the merozoites. Besides repeated failure of the transfections aimed at gene 'knockout' in contrast to those aimed at gene 'tagging', we obtained additional evidence which strongly supports a vital role of *Pb*IMC1c and *Pb*IMC1e in blood-stage parasite development: In both cases the transfections aimed at gene disruption resulted in a non-specific integration of the GFP reporter and the accompanying drug selection marker, giving rise to green fluorescent gametocytes (Fig. 7b). We presume that these events must have occurred via non-homologous recombination-based integration into a 'random' gene, leaving its respective promoter to drive GFP reporter expression. Because homologous recombination is much more efficient than non-homologous recombination, the latter is likely to be selected only when homologous recombination is detrimental to parasite development. Interestingly, we obtained similar GFP expression after replicate transfections, suggesting that the integration site may not be entirely indiscriminate and perhaps could constitute the 'next best' site with regards to sequence homology with the target DNA. We propose that this phenomenon can be a useful marker for the identification of genes that are vital for asexual development.

References

Anderson-White BR, Ivey FD, Cheng K, Szatanek T, Lorestani A, Beckers CJ, Ferguson DJ, Sahoo N, Gubbels MJ (2011) A family of intermediate filament-like proteins is sequentially assembled into the cytoskeleton of *Toxoplasma gondii*. Cell Microbiol 13(1):18–31

Arai M, Billker O, Morris HR, Panico M, Delcroix M, Dixon D, Ley SV, Sinden RE (2001) Both mosquito-derived xanthurenic acid and a host blood-derived factor regulate gametogenesis of *Plasmodium* in the midgut of the mosquito. Mol Biochem Parasitol 116(1):17–24

Bannister LH, Hopkins JM, Fowler RE, Krishna S, Mitchell GH (2000) A brief illustrated guide to the ultrastructure of *Plasmodium falciparum* asexual blood stages. Parasitol Today 16(10):427–433

Carter V, Shimizu S, Arai M, Dessens JT (2008) PbSR is synthesized in macrogametocytes and involved in formation of the malaria crystalloids. Mol Microbiol 68(6):1560–1569

Dearnley MK, Yeoman JA, Hanssen E, Kenny S, Turnbull L, Whitchurch CB, Tilley L, Dixon MW (2012) Origin, composition, organization and function of the inner membrane complex of *Plasmodium falciparum* gametocytes. J Cell Sci 125(8):2053–2063

Dessens JT, Beetsma AL, Dimopoulos G, Wengelnik K, Crisanti A, Kafatos FC, Sinden RE (1999) CTRP is essential for mosquito infection by malaria ookinetes. EMBO J 18(22):6221–6227

Florens L, Washburn MP, Raine JD, Anthony RM, Grainger M, Haynes JD, Moch JK, Muster N, Sacci JB, Tabb DL, Witney AA, Wolters D, Wu Y, Gardner MJ, Holder AA, Sinden RE, Yates JR, Carucci DJ (2002) A proteomic view of the *Plasmodium falciparum* life cycle. Nature 419(6906):520–526

Gould SB, Tham WH, Cowman AF, McFadden GI, Waller RF (2008) Alveolins, a new family of cortical proteins that define the protist infrakingdom Alveolata. Mol Biol Evol 25(6):1219–1230

Hall N, Karras M, Raine JD, Carlton JM, Kooij TW, Berriman M, Florens L, Janssen CS, Pain A, Christophides GK, James K, Rutherford K, Harris B, Harris D, Churcher C, Quail MA, Ormond D, Doggett J, Trueman HE, Mendoza J, Bidwell SL, Rajandream MA, Carucci DJ, Yates JR 3rd, Kafatos FC, Janse CJ, Barrell B, Turner CM, Waters AP, Sinden RE (2005) A comprehensive survey of the *Plasmodium* life cycle by genomic, transcriptomic, and proteomic analyses. Science 307(5706):82–86

Khan SM, Franke-Fayard B, Mair GR, Lasonder E, Janse CJ, Mann M, Waters AP (2005) Proteome analysis of separated male and female gametocytes reveals novel sex-specific *Plasmodium* biology. Cell 121(5):675–687

Khater EI, Sinden RE, Dessens JT (2004) A malaria membrane skeletal protein is essential for normal morphogenesis, motility, and infectivity of sporozoites. J Cell Biol 167(3):425–432

Kono M, Herrmann S, Loughran NB, Cabrera A, Engelberg K, Lehmann C, Sinha D, Prinz B, Ruch U, Heussler V, Spielmann T, Parkinson J, Gilberger TW (2012) Evolution and architecture of the inner

membrane complex in asexual and sexual stages of the malaria parasite. Mol Biol Evol 29(9):2113–2132

Kudryashev M, Lepper S, Stanway R, Bohn S, Baumeister W, Cyrklaff M, Frischknecht F (2010) Positioning of large organelles by a membrane- associated cytoskeleton in *Plasmodium* sporozoites. Cell Microbiol 12(3):362–371

Kudryashev M, Munter S, Lemgruber L, Montagna G, Stahlberg H, Matuschewski K, Meissner M, Cyrklaff M, Frischknecht F (2012) Structural basis for chirality and directional motility of *Plasmodium* sporozoites. Cell Microbiol 14(11):1757–1768

Lasonder E, Ishihama Y, Andersen JS, Vermunt AM, Pain A, Sauerwein RW, Eling WM, Hall N, Waters AP, Stunnenberg HG, Mann M (2002) Analysis of the *Plasmodium falciparum* proteome by high-accuracy mass spectrometry. Nature 419(6906):537–542

Lindner SE, Swearingen KE, Harupa A, Vaughan AM, Sinnis P, Moritz RL, Kappe SH (2013) Total and putative surface proteomics of malaria parasite salivary gland sporozoites. Mol Cell Proteomics 12(5):1127–1143

Lopez-Barragan MJ, Lemieux J, Quinones M, Williamson KC, Molina-Cruz A, Cui K, Barillas-Mury C, Zhao K, Su XZ (2011) Directional gene expression and antisense transcripts in sexual and asexual stages of *Plasmodium falciparum*. BMC Genomics 12:587

Mair GR, Braks JA, Garver LS, Wiegant JC, Hall N, Dirks RW, Khan SM, Dimopoulos G, Janse CJ, Waters AP (2006) Regulation of sexual development of *Plasmodium* by translational repression. Science 313(5787):667–669

Mann T, Beckers C (2001) Characterization of the subpellicular network, a filamentous membrane skeletal component in the parasite *Toxoplasma gondii*. Mol Biochem Parasitol 115(2):257–268

Mann T, Gaskins E, Beckers C (2002) Proteolytic processing of TgIMC1 during maturation of the membrane skeleton of *Toxoplasma gondii*. J Biol Chem 277(43):41240–41246

Meis JF, Ponnudurai T (1987) Ultrastructural studies on the interaction of *Plasmodium falciparum* ookinetes with the midgut epithelium of *Anopheles stephensi* mosquitoes. Parasitol Res 73(6):500–506

Meis JF, Pool G, van Gemert GJ, Lensen AH, Ponnudurai T, Meuwissen JH (1989) *Plasmodium falciparum* ookinetes migrate intercellularly through *Anopheles stephensi* midgut epithelium. Parasitol Res 76(1):13–19

Morrissette NS, Sibley LD (2002) Cytoskeleton of apicomplexan parasites. Microbiol Mol Biol Rev 66(1):21–38

Raine JD, Ecker A, Mendoza J, Tewari R, Stanway RR, Sinden RE (2007) Female inheritance of malarial lap genes is essential for mosquito transmission. PLoS Pathog 3(3):e30

Saeed S, Carter V, Tremp AZ, Dessens JT (2010) *Plasmodium berghei* crystalloids contain multiple LCCL proteins. Mol Biochem Parasitol 170(1):49–53

Saeed S, Tremp AZ, Dessens JT (2012) Conformational co-dependence between *Plasmodium berghei* LCCL proteins promotes complex formation and stability. Mol Biochem Parasitol 185(2):170–173

Santos JM, Lebrun M, Daher W, Soldati D, Dubremetz JF (2009) Apicomplexan cytoskeleton and motors: key regulators in morphogenesis, cell division, transport and motility. Int J Parasitol 39(2):153–162

Silvestrini F, Lasonder E, Olivieri A, Camarda G, van Schaijk B, Sanchez M, Younis Younis S, Sauerwein R, Alano P (2010) Protein export marks the early phase of gametocytogenesis of the human malaria parasite *Plasmodium falciparum*. Mol Cell Proteomics 9(7):1437–1448

Treeck M, Sanders JL, Elias JE, Boothroyd JC (2011) The phosphoproteomes of *Plasmodium falciparum* and *Toxoplasma gondii* reveal unusual adaptations within and beyond the parasites' boundaries. Cell Host Microbe 10(4):410–419

Tremp AZ, Dessens JT (2011) Malaria IMC1 membrane skeleton proteins operate autonomously and participate in motility independently of cell shape. J Biol Chem 286(7):5383–5391

Tremp AZ, Khater EI, Dessens JT (2008) IMC1b is a putative membrane skeleton protein involved in cell shape, mechanical strength, motility, and infectivity of malaria ookinetes. J Biol Chem 283(41):27604–27611

Tremp AZ, Carter V, Saeed S, Dessens JT (2013) Morphogenesis of *Plasmodium* zoites is uncoupled from tensile strength. Mol Microbiol 89(3):552–564

Volkmann K, Pfander C, Burstroem C, Ahras M, Goulding D, Rayner JC, Frischknecht F, Billker O, Brochet M (2012) The alveolin IMC1h is required for normal ookinete and sporozoite motility behaviour and host colonisation in *Plasmodium berghei*. PLoS One 7(7):e41409

Waters AP, Thomas AW, van Dijk MR, Janse CJ (1997) Transfection of malaria parasites. Methods 13(2):134–147

Chapter 4

Plasmodium alveolins possess distinct

but structurally and functionally related

multi-repeat domains

Research Paper Cover Sheet

SECTION A – Student Details

Student	Fatimah Al-Khattaf
Principal Supervisor	Johannes Dessens
Thesis Title	Functional characterization of the alveolins, a family of cytoskeleton proteins of malaria parasites

SECTION B – Paper already published

Where was the work published?	Parasitology Research		
When was the work published?	2015		
If the work was published prior to registration for your research degree, give a brief rationale for its inclusion			
Have you retained the copyright for the work?*	**Yes**	Was the work subject to academic peer review?	**Yes**

SECTION D – Multi-authored work

For multi-authored work, give full details of your role in the research included in the paper and in the preparation of the paper. (Attach a further sheet if necessary)	Student generated the IMC1d knockout parasite line and performed and analysed genotyping and phenotyping experiments. Student contributed to preparation of the paper (text and figures).

Student Signature: _____   **Date:** _____

Supervisor Signature: _____ **Date:** _____

Plasmodium alveolins possess distinct but structurally and functionally related multi-repeat domains

Fatimah S. Al-Khattaf · Annie Z. Tremp · Johannes T. Dessens

Abstract The invasive and motile life stages of malaria parasites (merozoite, ookinete and sporozoite) possess a distinctive cortical structure termed the pellicle. The pellicle is characterised by a double-layered 'inner membrane complex' (IMC) located underneath the plasma membrane, which is supported by a cytoskeletal structure termed the subpellicular network (SPN). The SPN consists of intermediate filaments, whose major constituents include a family of proteins called alveolins. Here, we re-appraise the alveolins in the genus *Plasmodium* with respect to their repertoire, structure and interrelatedness. Amongst 13 family members identified, we distinguish two domain types that, albeit distinct at the primary structure level, are structurally related and contain tandem repeats with a consensus 12-amino acid periodicity. Analysis in *Plasmodium berghei* of the most divergent alveolin, *Pb*IMC1d, reveals a zoite-specific expression in ookinetes and a subcellular localisation in the pellicle, consistent with its predicted role as a SPN component. Knockout of *Pb*IMC1d gives rise to a wild-type phenotype with respect to ookinete morphogenesis, tensile strength, gliding motility and infectivity, presenting the first example of apparent functional redundancy amongst alveolin family members.

Keywords Cytoskeleton · Intermediate filament · Articulin · Tandem repeats

Fatimah S. Al-Khattaf and Annie Z. Tremp contributed equally to this work.

F. S. Al-Khattaf · A. Z. Tremp · J. T. Dessens (✉)
Pathogen Molecular Biology Department, Faculty of Infectious and Tropical Diseases, London School of Hygiene & Tropical Medicine, Keppel Street, London WC1E 7HT, UK
e-mail: johannes.dessens@lshtm.ac.uk

F. S. Al-Khattaf
Department of Infection Control, College of Medicine, King Saud University, Riyadh, Saudi Arabia

Introduction

Malaria parasite transmission begins when gametocytaemic blood is ingested by a vector mosquito. This initiates rapid gametogenesis followed by fertilisation. Zygotes transform into motile ookinetes that cross the midgut wall of the insect and transform into oocysts (Meis and Ponnudurai 1987; Meis et al. 1989). An approximately 2-week period of growth and replication concludes in hundreds of motile sporozoites being released from each oocyst and invading the salivary glands. Blood feeding of the insect transmits the sporozoites to the vertebrate host, where they replicate to each produce thousands of merozoites. The motile merozoites are released into the bloodstream, where they infect red blood cells and either replicate to form more merozoites or differentiate into sexual stage male and female gametocytes to complete the life cycle.

The three zoite stages of *Plasmodium* species (i.e. ookinetes, sporozoites and merozoites) possess a characteristic peripheral cytoskeletal structure known as the pellicle. The pellicle is defined by a double-membrane structure termed the inner membrane complex (IMC) (Bannister et al. 2000; Morrissette and Sibley 2002; Santos et al. 2009). The IMC is equivalent to a system of flattened membranous sacs that underlie the plasma membrane, the so-called 'alveoli', which are a defining feature of unicellular microorganisms belonging to the phyla Apicomplexa, Ciliophora (ciliates) and Dinoflagellata (dinoflagellates) within the protist Alveolata superphylum. Tightly associated with the IMC on its cytoplasmic side lies a network of intermediate filaments termed the subpellicular network (SPN), which supports the pellicular membranes and provides mechanical strength to the cell (Mann and Beckers 2001). Members of an Apicomplexa-specific family of proteins, termed IMC1 proteins, were identified as building blocks of the SPN (Khater et al. 2004; Mann and Beckers 2001). Subsequently, structurally related proteins from ciliates and dinoflagellates were identified and added to

🙢 Springer

this protein family renamed 'alveolins' (Gould et al. 2008). In the genus *Plasmodium*, the alveolin family members display differential expression between different zoite stages of the parasite. In the rodent malaria species *Plasmodium berghei*, it was shown that disruption of individual alveolin family members expressed in sporozoites (*Pb*IMC1a), in ookinetes (*Pb*IMC1b) or in both these zoites (*Pb*IMC1h) results in morphological abnormalities that are accompanied by reduced tensile strength of the zoite stages in which they are expressed (Khater et al. 2004; Tremp and Dessens 2011; Tremp et al. 2008; Volkmann et al. 2012). Besides their roles in morphogenesis and tensile strength, the *Plasmodium* alveolins are also involved in gliding motility, most likely through interactions with components of the glideosome that are situated within the pellicular cytoplasm (Khater et al. 2004; Tremp and Dessens 2011; Tremp et al. 2008; Volkmann et al. 2012). Apart from their expression throughout the *Plasmodium* life cycle, alveolins are essential for parasite development both in the vertebrate and insect hosts (Khater et al. 2004; Tremp et al. 2014; Tremp and Dessens 2011), which makes them potentially attractive targets for malaria treatment, prophylaxis and transmission control. For this reason, it is important to better understand their core architecture, as well as the underlying mechanisms for their assembly into the supramolecular structures that make up the cortical cytoskeleton of the zoite stages.

In this study, we carried out a critical re-evaluation of the *Plasmodium* alveolins with respect to their repertoire, structure and interrelatedness. Our analyses identify two distinct domain types that are structurally and functionally related without possessing significant homology at the primary structure level.

Materials and methods

Animal use

All laboratory animal work undergoes regular ethical review by the London School of Hygiene & Tropical Medicine and has been approved by the UK Home Office. Work was carried out in accordance with the UK Animals (Scientific Procedures) Act 1986 implementing European Directive 2010/63 for the protection of animals used for experimental purposes. Experiments were conducted in 6–8-week-old female CD1 mice, specific pathogen free and maintained in filter cages. Animal welfare was assessed daily, and animals were humanely killed upon reaching experimental or humane endpoints. Mice were infected with parasites suspended in RPMI or phosphate-buffered saline (PBS) by intraperitoneal injection or by infected mosquito bite on anaesthetised animals. Parasitaemia was monitored regularly by collecting of a small drop of blood from a superficial tail vein. Drugs were administered by intraperitoneal injection or where possible

were supplied in drinking water. Parasitised blood was harvested by cardiac bleed under general anaesthesia without recovery.

Parasite maintenance, transmission, culture and purification

P. berghei ANKA clone 234 parasites were maintained as cryopreserved stabilates or by mechanical blood passage and regular mosquito transmission. Ookinete cultures were set up overnight from gametocytaemic blood as previously described (Arai et al. 2001). After 20–24 h, ookinetes were purified via ice-cold 0.17 M ammonium chloride lysis and centrifugation at 800×*g* for 10 min, followed by PBS washes. Mosquito infection and transmission assays were as previously described using *Anopheles stephensi* (Dessens et al. 1999; Khater et al. 2004), and infected insects were maintained at 20 °C at approximately 70 % relative humidity.

Gene targeting constructs

The entire *pbimc1d* coding sequence plus ca. 0.55 kb of upstream sequence was PCR amplified from genomic DNA with primers pDNR-IMC1d-F (ACGAAGTTATCAGTCGAGGT ACCAGCCAAAATCACCGAAAAG) and pDNR-IMC1d-R (ATGAGGGCCCCTAAGCTTTCAGATATTAAAGGAGCA TTATCAATG) and cloned into *Sal*I/*Hin*dIII-digested pDNR-EGFP by in-fusion cloning to give plasmid pDNR-IMC1d/ GFP. The 3′ untranslated region of *pbimc1d* was amplified with primers pLP-IMC1d-F (ATATGCTAGAGCGGCCTAGTAA GTCTTTTGCATTTTATCAATGC) and pLP-IMC1d-R (CACCGCGGTGGCGGCCAAAATATGAAGAAATGAC AAAACAGAAG) and the resulting ca. 0.62-kb fragment cloned into *Not*I-digested pLP-hDHFR by in-fusion cloning to give plasmid pLP-hDHFR/IMC1d. The *pbimc1d/gfp*-specific sequence from pDNR-IMC1d/GFP was transferred to pLP-hDHFR/IMC1d by Cre/*lox*P recombination to give the final construct pLP-IMC1d/GFP. This plasmid served as template in PCR-based site-directed mutagenesis using primers IMC1d-KO-F (AGCCAGTGATGAGTAAAGGAGAAGAACTTT TCAC) and IMC1d-KO-R (TTACTCATCACTGGCTTATA AAATGCATTTATT). The resulting PCR product was circularised using in-fusion to give plasmid pLP-IMC1d-KO.

Generation and genotyping of genetically modified parasites

Parasite transfection, pyrimethamine selection and dilution cloning were performed as previously described (Waters et al. 1997). Prior to performing transfections, plasmid DNA was digested with *Kpn*I and *Sac*II to remove the vector backbone. Genomic DNA extraction was performed as previously described (Dessens et al. 1999). Integration into the *pbimc1d* locus was confirmed with primers IMC1d-5′F (TACCCGCA TATTTATCATTG) and LAP-GFP-R (GTGCCCATTAACAT

CACC), and the absence of the wild-type allele was confirmed using primers IMC1d-5′F and IMC1d-3′R (GGTTACATGTATTTTTATTTCCGC).

RT-PCR analysis

Reverse transcription PCR (RT-PCR) analysis was carried out as described (Claudianos et al. 2002) using primers IMC1d-ORF-F (TTGAAAATGGAGATGCTATTACAAG) and pDNR-IMC1d-R (for *pbimc1d*) and primers tub1-F (GAAG TAATAAGTATACATGTAGG) and tub1-R (ACACATCA ATGACTTCTTTACC) (for *pbtubulin1*).

Western blot analysis

Parasite samples were heated directly in SDS-PAGE loading buffer at 70 °C for 10 min. Proteins were fractionated by electrophoresis through NuPage 4–12 % Bis-Tris precast gels (Invitrogen) and transferred to PVDF membrane (Invitrogen) according to the manufacturer's instructions. Membranes were blocked for non-specific binding in PBS supplemented with 0.1 % Tween 20 and 5 % skimmed milk for 1 h at room temperature. Goat polyclonal antibody to GFP conjugated to horseradish peroxidase (Abcam ab6663) diluted 1:5000 was applied to the membrane for 1 h at room temperature. After washing, signal was detected by chemiluminescence (Pierce ECL western blotting substrate) according to the manufacturer's instructions.

Tensile strength and viability assays

Unpurified ookinetes present in ookinete cultures were subjected to hypo-osmotic shock of 0.5× normal osmotic strength by adding an equal volume of water. After 5 min, normal osmotic conditions were restored by adding an appropriate amount of 10× PBS. Cell viability was scored by fluorescence microscopy in the presence of 5 mL/L propidium iodide and 1 % Hoechst 33258. Ookinetes whose nucleus stained positive for both propidium iodide and Hoechst were scored as non-viable, whereas ookinetes whose nucleus only stained positive for Hoechst were scored as viable.

Assessment of ookinete shape and motility

Images of Giemsa-stained ookinetes were captured by microscopy and their length and width measured. The ookinete motility assay was performed as previously described (Moon et al. 2009). Ookinete cultures were added to an equal volume of Matrigel (BD Biosciences) on ice, mixed thoroughly, spotted onto a microscope slide and covered with a Vaseline-rimmed cover slip. The Matrigel was allowed to set at room temperature for at 30 min.

Time-lapse videos (one frame every 10 s for 10 min) were taken on a Zeiss Axioplan II microscope. Movies were analysed with ImageJ using the Manual Tracking plugin (http://fiji.sc/wiki/index.php/Manual_Tracking).

Microscopy

For assessment of fluorescence, live parasite samples were assessed and images captured on a Zeiss LSM510 inverted laser scanning confocal microscope.

Bioinformatics

Conserved domains were identified by multiple alignments of orthologous proteins from *P. berghei*, *P. falciparum*, *P. vivax* and *P. knowlesi*. Multiple alignments were obtained using Clustal Omega, and phylogenetic analyses were carried out using ClustalW2 Phylogeny, accessed through the EMBL-EBI website. Amino acid sequence similarity searches were carried out by protein BLAST, accessed through the National Centre for Biotechnology Information (NCBI), PlasmoDB or ToxoDB. Trees were drawn using TreeDraw. The program HHrepID was accessed through the Bioinformatics Toolkit, Max-Planck Institute for Developmental Biology.

Results

Repertoire and interrelatedness of *Plasmodium* alveolins

The existence of an alveolin protein family in *Plasmodium* was first reported in 2004, identifying eight putative members named IMC1a through to IMC1h (Khater et al. 2004). More recent studies identified several additional alveolins (Gould et al. 2008; Kono et al. 2012; Tremp et al. 2013), here named IMC1i to IMC1l in keeping with original nomenclature (Table 1). To evaluate the structural interrelatedness of these alveolins, we carried out a systematic analysis of the *Plasmodium* genome using BLAST similarity searches with each of the family members. In the process, we identified a 13th family member, named IMC1m (Table 1). Alveolin hits from each of the BLAST searches were given an arbitrary integer score (relating to the scores of the BLAST hits, lowest score receives 1) to generate a similarity matrix (Table 2). For each alveolin, a total score was then calculated to reflect its structural similarity to the *Plasmodium* alveolin family as a whole. This, in turn, allowed a ranking of the 13 alveolins with respect to their interrelatedness. Accordingly, IMC1e (ranked 1) was identified as being structurally most similar to the alveolin population: it both detects and is detected by the highest number of family members (Table 2). In contrast, IMC1d (ranked 13) has the most divergent structure (Table 2). This suggests that

Table 1 Predicted *Plasmodium* IMC1 proteins/alveolins and zoite stage expression

Name	*P. berghei* gene ID (PBANKA_000000)	*P. falciparum* gene ID (PF3D7_0000000)	Alternative name(s)	Zoite expression			References
				Merozoite	Ookinete	Sporozoite	
IMC1a	040260	0304000	Alv1			+	Khater et al. 2004
IMC1b	090710	1141900			+		Tremp et al. 2008
IMC1c	120200	1003600	Alv5	+	+	+	Tremp et al. 2014
IMC1d	121910	0708600	hsp90, hsp86, o2		+		this paper
IMC1e	040270	0304100	Alv2	+	+	+	Tremp et al. 2014
IMC1f	136440	1351700	Alv6				
IMC1g	124060	0525800	Alv4	+	+	+	Kono et al. 2012
IMC1h	143660	1221400	Alv3		+	+	Tremp and Dessens 2011
IMC1i	070710	0823500					
IMC1j	112040	0621400	Alv7, Pfs77				
IMC1k	135490	1341800					
IMC1l	102570	1417000					
IMC1m	051300	1028900					

IMC1e represents the most recent common ancestor. Indeed, *Pb*IMC1e was much more successful than *Pb*IMC1d at detecting alveolins in other genera within the Apicomplexa phylum. For example, in *Toxoplasma gondii*, which encodes 14 alveolins (named *Tg*IMC1 and *Tg*IMC3–*Tg*IMC15) (Anderson-White et al. 2011), *Pb*IMC1e detected 13 family members in protein BLAST, whilst *Pb*IMC1d detected five.

Domain structure of *Plasmodium* alveolins

Plasmodium alveolins are typified by possessing, within their primary amino acid sequences, highly conserved regions that are flanked by sequences more variable in length and amino acid composition (Khater et al. 2004; Tremp et al. 2008, 2014; Tremp and Dessens 2011). The functional properties of the alveolins are likely to be defined by these conserved domains. Closer examination showed that the sequence similarities between the alveolins identified from the BLAST searches (Table 2) were largely confined to two conserved domains, here named type 1 and type 2, which by phylogenetic analysis split into distinct clades and which are variably distributed amongst the family members (Fig. 1). The alveolins *Pb*IMC1a and *Pb*IMC1b are the only family members that possess interspersed type 1 and type 2 domains (Fig. 1b) (Khater et al. 2004; Tremp et al. 2008). Whilst these different domain types share little sequence homology, both have a strong compositional bias for the amino acids P, I, V, D, E and K (e.g. 66 % for *Pb*IMC1a type 1, 62 % for *Pb*IMC1a type 2, 64 % for *Pb*IMC1b type 1, 66 % for *Pb*IMC1b type 2). These observations suggested that the type 1 and type 2 domains could be structurally related, despite a lack of discernible primary amino acid sequence homology.

*Pb*IMC1d is expressed in ookinetes and localises to the pellicle/SPN

*Pb*IMC1d is not only the most divergent alveolin family member (Table 2) but is the only alveolin that possesses only a type 2 domain (Fig. 1). We used *Pb*IMC1d to assess the functional relationship between the type 1 and type 2 domains by determining its life stage expression, subcellular distribution and contribution to parasite development. *Pb*IMC1d is encoded by a two-exon gene, separated by a 170-bp intron. The gene is annotated as a putative heat shock protein 90 (hsp90) in *P. berghei* (hsp86 in *P. falciparum*), but it has no actual sequence similarity to heat shock proteins. The full-length protein is composed of 249 amino acids with a calculated M_r of 29,361. The type 2 domain in *Pb*IMC1d is highly conserved and has a 68 % amino acid content composed of P, I, V, D, E and K.

*Pb*IMC1d expression and localisation was studied by tagging the gene with enhanced green fluorescent protein (GFP) in genetically modified parasites. To achieve this, we used a strategy of double crossover homologous recombination in which the wild-type allele was replaced with a recombinant full-length wild-type allele fused to enhanced GFP at its carboxy terminus (Fig. 2a), giving rise to stably transfected parasites. To study the function of *Pb*IMC1d, we generated a null mutant using a similar gene targeting strategy, but removing most of the *pbimc1d* coding sequence whilst leaving the *gfp* gene under control of the native *pbimc1d* promoter to act as a reporter (Fig. 2a). After transfection of purified schizonts, pyrimethamine-resistant parasites were selected and cloned by limiting dilution as described (Tremp and Dessens 2011; Tremp et al. 2008) to give parasite lines

Table 2 Similarity matrix and ranking of *Plasmodium berghei* alveolins

*Pb*IMC1	Hit[a]	a	b	c	d	e	f	g	h	i	j	k	l	m	
Query															
a			9	8	7	5	6	2	0	1	3	4	0	0	45
b		5		2	4	0	3	0	0	0	1	0	0	0	15
c		11	5		0	9	10	8	7	6	2	4	1	3	66
d		3	2	0		0	1	0	0	0	0	0	0	0	6
e		5	1	9	0		7	11	8	10	3	4	2	6	66
f		3	1	4	0	5		0	2	0	0	0	0	0	15
g		1	0	8	0	10	5		7	9	2	6	3	4	55
h		0	0	5	0	7	4	6		1	0	2	0	3	28
i		0	0	3	0	4	2	5	0		0	0	1	0	15
j		1	8	3	0	7	2	6	0	4		9	0	5	45
k		7	0	5	0	6	3	4	1	2	8		0	0	36
l		0	0	0	0	2	3	4	0	1	0	0		0	10
m		1	0	7	0	9	8	5	6	2	4	0	3		45
		37	26	54	11	64	54	51	31	36	23	29	10	21	Total[c]
Ranking[b]		4	11	2	13	1	5	3	9	10	6	8	12	7	

[a] Each 'Query' alveolin was run with protein-protein BLAST against the *P. berghei* genome in PlasmoDB. The lowest scoring 'Hit' alveolin was given an arbitrary similarity score of 1, the second lowest a score of 2, and so forth. A 0 value meant the alveolin was not detected

[b] Ranking was done by combining the bottom and right-hand side 'Total' scores for each alveolin. The highest scoring alveolin was ranked 1

[c] Total scores reflect the ability of each alveolin to detect (right-hand side), or to be detected by (bottom), other alveolins in the BLAST similarity search

IMC1d/GFP and IMC1d-KO, respectively. PCR diagnostic for integration into the *pbimc1d* locus produced a specific band of approximately 1.1 kb in the IMC1d-KO parasite, whilst this product was approximately 1.7 kb in parasite line IMC1d/GFP (Fig. 2b). The size difference between these PCR products reflects the removal of the *pbimc1d* coding sequence in the null mutant. PCR diagnostic for the presence of the wild-type *pbimc1d* allele gave a specific band of approximately 2.4 kb only in wild-type parasites (Fig. 2b). Parasite line IMC1d/GFP

Fig. 1 Repertoire and domain structure of *Plasmodium* alveolins. **a** Phylogeny of conserved domains within the alveolin family members *Pb*IMC1a to *Pb*IMC1m (*a–m*). *Numbers* give amino acid coordinates of the conserved domains in the corresponding *Pb*IMC1 protein. Type 1 (*red*) and type 2 (*green*) domains separate into distinct clades. **b** Schematic diagram depicting the 13 alveolin family members (*a–m*), showing relative positions of the type 1 (*red*) and type 2 (*green*) domains
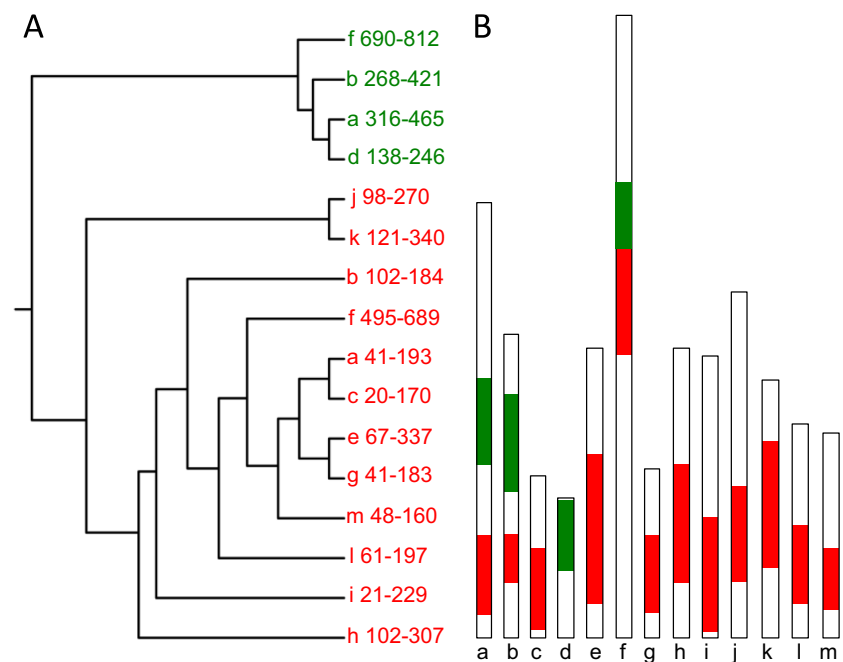
developed normally in mouse and mosquito. GFP fluorescence was only observed in zygotes and ookinetes and in the latter was predominantly distributed at the cell cortex (Fig. 2c). Immunoblot analysis of purified, cultured ookinetes with anti-GFP antibodies detected a specific band corresponding to the *Pb*IMC1d::GFP fusion protein (Fig. 2d). These data show that *Pb*IMC1d is specifically expressed in only one of the zoite stages, the ookinete, and is targeted to the pellicle structure/SPN. In *T. gondii*, the 'alveolin domain' was shown to be the main determinant in targeting the protein to the cell cortex (Anderson-White et al. 2011). Thus, the pellicular localisation of *Pb*IMC1d in ookinetes suggests that the type 2 domain in its own right is able to target proteins to this cellular compartment,

as does the type 1 domain in other *Plasmodium* alveolins (Tremp et al. 2014; Tremp and Dessens 2011).

Expression profiling of *pbimc1d* messenger RNA by RT-PCR with *pbimc1d*-specific primers flanking its intron amplified an approximately 0.75-kb messenger RNA (mRNA)-specific product in both gametocytes and ookinetes, but in asexual blood stages only amplified an approximately 0.9-kb product from genomic DNA (this product is larger in size due to the intron) (Fig. 2e). By contrast, mRNA of the control gene tubulin1 was present in all parasite samples (Fig. 2e). The discrepancy between *pbimc1d* mRNA and *Pb*IMC1d protein expression in gametocytes strongly points to translational repression of the *pbimc1d* gene, as is predicted for the majority of alveolins in *P. berghei* (Mair et al. 2006). Translational
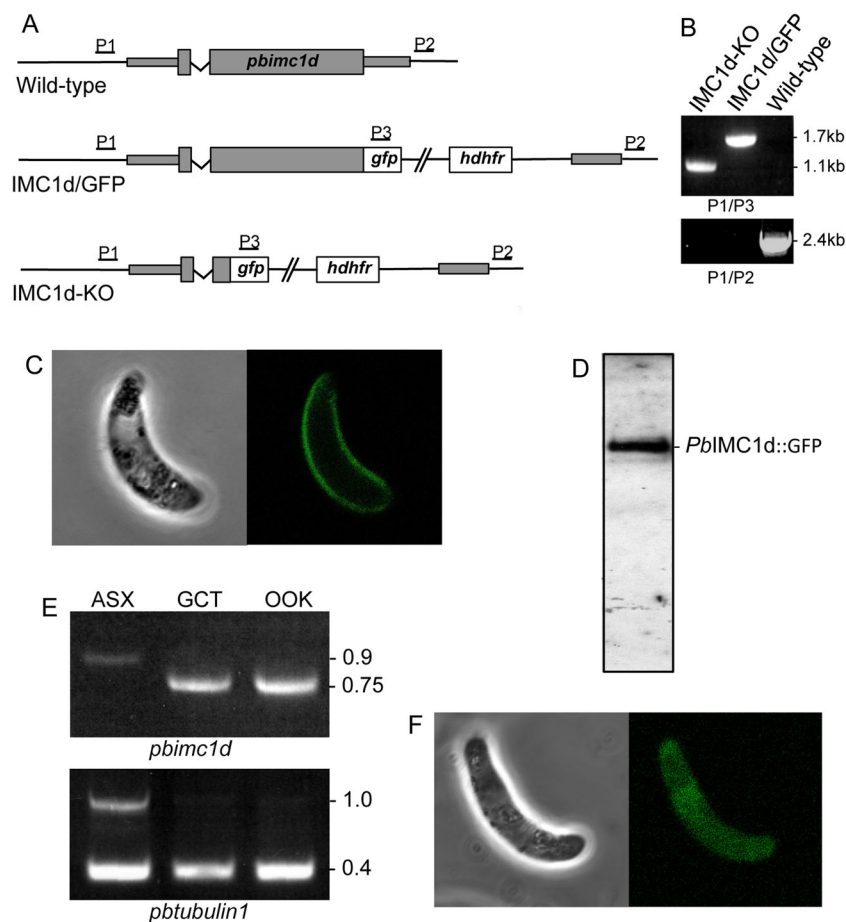
Fig. 2 Generation and molecular analyses of genetically modified parasite lines. **a** General targeting strategy for the GFP tagging and gene disruption of *pbimc1d* via double crossover homologous recombination. Both wild-type (WT) GFP-tagged (IMC1d/GFP) and disrupted (IMC1d-KO) alleles are shown. The *pbimc1d* gene is indicated with coding sequence (*wide bars*) and non-coding sequence (*narrow bars*). Also indicated are the enhanced GFP module (*gfp*), the hDHFR selectable marker gene cassette (*hdhfr*) and primers used for diagnostic PCR amplification (*P1–P3*). **b** PCR diagnostic for the presence of the modified GFP-tagged *pbimc1d* alleles using primers P2 and P3 and the absence of the wild-type *pbimc1d* allele using primers P1 and P2, from clonal parasite populations of IMC1d/GFP and IMC1d-KO.

WT parasites are included as positive controls for the wild-type alleles. **c** Confocal brightfield and GFP fluorescence image of a cultured, mature ookinete of parasite line IMC1d/GFP, showing cortical fluorescence. **d** Western blot analysis of purified, cultured ookinetes of parasite lines IMC1d/GFP using anti-GFP antibodies, showing the *Pb*IMC1d::GFP fusion protein. **e** RT-PCR analysis of wild-type parasite samples enriched for asexual stages (*ASX*), gametocytes (*GCT*) and ookinetes (*OOK*) using primers specific for *pbimc1d* and *pbtubulin1*. Due to the primers flanking introns, for each gene, the larger PCR products are amplified from gDNA and the smaller from cDNA. **f** Confocal brightfield and GFP fluorescence image of a cultured, mature ookinete of parasite line IMC1d-KO, showing cytoplasmic fluorescence

repression is a female gametocyte-specific mechanism of translational silencing involved in the development of the parasite post-fertilisation (Mair et al. 2006).

*Pb*IMC1d is functionally redundant

Ookinetes of the *Pb*IMC1d-null mutant displayed cytoplasmic GFP fluorescence resulting from expression of the GFP reporter from the *pbimc1d* promoter (Fig. 2f), which is consistent with the expression pattern of *Pb*IMC1d as determined by GFP tagging. The cell shape of *Pb*IMC1d-null mutant ookinetes was not significantly different from that of control IMC1d/GFP ookinetes (length 11.49±0.10 μm for IMC1d/GFP, 11.26± 0.12 μm for IMC1d-KO; width 2.15±0.036 μm for IMC1d/ GFP, 2.23±0.034 μm for IMC1d-KO; n=100), and the ookinetes were equally effective in producing oocysts in mosquitoes (140±39 oocysts per mosquito for IMC1d/GFP, 140± 28 for IMC1d-KO; n=20), indicating that they possess normal tensile strength and motility. Indeed, ookinetes of both parasite lines displayed similar resistance to hypo-osmotic shock (78 and 76 % survival for IMC1d/GFP and IMC1d-KO, respectively; n=100), indicating that the knockout did not adversely affect tensile strength. Furthermore, ookinete motility through Matrigel was comparable between the two parasite lines (42.6± 1.7 μm per 10 min for IMC1d/GFP; 41.3±2.6 μm for IMC1d-KO; n=15). Finally, sporozoites of both parasite lines were readily transmitted by mosquito bite. Thus, *Pb*IMC1d appears to be functionally redundant under our experimental conditions.

Alveolins possess tandem repeat sequences with a 12-amino acid periodicity

Alveolins have been reported to possess a core of repeated sequence motifs (Gould et al. 2008). We tested each of the family members for the presence of tandem repeat sequences using the program HHrepID. This method predicts structural repeats in protein sequences based on Hidden Markov Model (HMM)-HMM comparison, exploiting evolutionary information derived from multiple sequence alignment of homologues (Biegert and Soding 2008). These analyses revealed that all 13 *Plasmodium* alveolins possess predicted multi-repeat sequences within their conserved type 1 and type 2 domains, supporting the notion that they constitute genuine alveolins. Repeats within the large majority of type 1 domains revealed a clear minimum periodicity of 12 residues (e.g. *Pb*IMC1e, Fig. 3a). Tandem 12-amino acid repeats were also identified in type 2 domains (e.g. *Pb*IMC1b, Fig. 3b), albeit typically with lower probability scores. Articulins and plateins, cortical cytoskeleton proteins from *Euglena* and *Euplotes* spp., respectively, have also been reported to have 12-amino acid repetitive motifs rich in valine and proline residues and, in this respect, are similar to alveolins (Huttenlauch et al. 1995;

Huttenlauch and Stick 2003; Kloetzel et al. 2003a, b; Marrs and Bouck 1992). This was confirmed by HHrepID analysis, which readily detected 12-amino acid tandem repeat structures in these proteins (Fig. 3c, d).

Discussion

This study brings the number of *Plasmodium* alveolin family members that have been identified to 13. Of these, seven have now experimentally been shown to localise to the pellicle
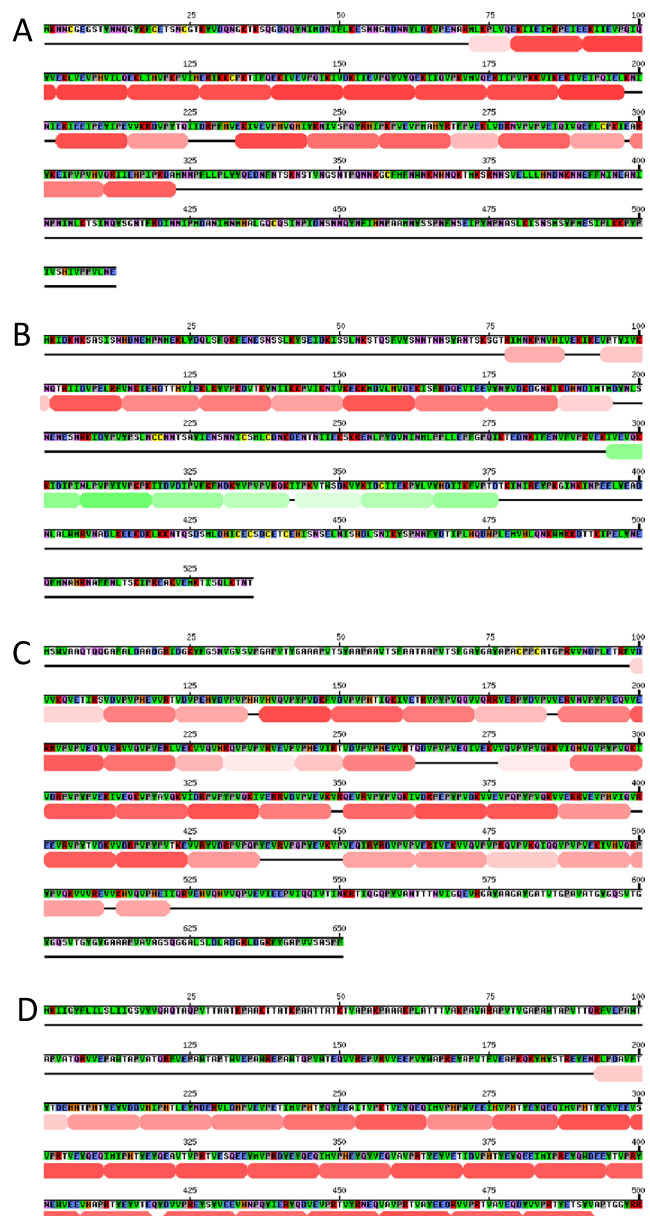
Fig. 3 Tandem repeat identification in alveolins, articulins and plateins by the program HHrepID. **a** *P. berghei* IMC1e. **b** *P. berghei* IMC1b. **c** *Euglena gracilis* articulin (AAB23241.1). **d** *Euplotes aediculatus* alpha-2 platein precursor (AAM94463.1)

structure. This includes the most divergent family member, IMC1d, characterised here, which gives strong support to the concept that all *Plasmodium* alveolins are fundamentally involved with the cortical cytoskeleton in malaria parasites. This is supported by several alveolin knockout studies that reveal key roles in morphogenesis, tensile strength and gliding motility. Studies involving double knockout of *Pb*IMC1b and *Pb*IMC1h showed that the functional contribution of these alveolins to tensile strength and motility is both cumulative and mutually independent (Tremp and Dessens 2011). In contrast, the apparent no-phenotype knockout of *Pb*IMC1d reported here points to a functional redundancy amongst the alveolin family members. The highly conserved type 2 domain of IMC1d indicates that the gene is under selective pressure, and we cannot rule out that the phenotype of the *Pb*IMC1d-null mutant is very subtle, or might only become apparent under conditions that are different from our experimental set-up. However, another possible explanation for the seemingly redundant role of *Pb*IMC1d is that the formation and function of the SPN entail a system of co-operating proteins that are able to bypass, or substitute for, each other's functions. This attractive hypothesis, if true, would add robustness to a complex biological system that serves roles in many key processes such as morphogenesis, motility and invasion.

The creation of internal repetitions forms an important mechanism for proteins to adapt their structure and function under evolutionary pressure (Marcotte et al. 1999). However, after fixation of duplications, sequence similarities amongst repeats can quickly erode whilst structure and function are preserved (Andrade et al. 2001). Although such mismatch or 'fuzzy' repeats are widespread, they are difficult to detect due to their low similarity, polymorphism and vast diversity. This is further confounded by the potential for non-canonical repeats, degenerate repeats and discontinuities (i.e. short insertions between repeats) to arise, which for example are known to frequently occur in coiled-coil domains, a well-known type of tandem repeat structure with a consensus 7-amino acid periodicity (Brown et al. 1996). The type 1 and type 2 domains identified here in the *Plasmodium* alveolins are likely to be the result of similar evolutionary forces. These alveolin domains lack discernible homology at the primary structure level and fall into distinct clades, but are clearly related with regard to their amino acid composition, tandem repeat structure and functional localisation. There is further indication that the type 2 repeats arose from type 1 repeats (or vice versa). First, in IMC1f, the type 1 and type 2 domains are located tandemly within a single uninterrupted block of conserved sequence (Fig. 1b). Second, four *T. gondii* alveolins share sequence similarity in protein BLAST with both *Pb*IMC1e and *Pb*IMC1d. In three of these (*Tg*IMC6, *Tg*IMC14 and *Tg*IMC15), the regions of sequence similarity with *Pb*IMC1e and *Pb*IMC1d overlap, pointing to the presence of domains with 'intermediate' homology between type 1 and type 2.

These combined observations suggest that the primary amino acid sequences of the type 1 and type 2 repeats have evolved in a way that has preserved their overall structure and function. This phenomenon of 'constrained evolution' has also been observed in other protist cytoskeletal proteins with repeat motifs (Gould et al. 2011).

Many bioinformatics programs for internal repeat detection in proteins utilise algorithms based on local alignment and substitution matrices (Andrade et al. 2000; Heger and Holm 2000). These approaches have been modestly successful in predicting tandem repeats within the alveolins. By contrast, HHrepID is based on building and matching Hidden Markov Models to identify repeat sequences (Biegert and Soding 2008). Our findings demonstrate that HHrepID successfully predicts tandem repeats in the *Plasmodium* alveolins and show for the first time that these repeats have a consensus 12-amino acid length. Accordingly, the multi-repeat structures of alveolins are very similar, both in periodicity and amino acid composition, to those of cytoskeletal proteins in other protists: the articulins and plateins. Whilst *Euplotes* plateins possess canonical ER signal peptides and form plate-like structures inside alveoli (Kloetzel et al. 2003b), *Euglena* articulins form intermediate filaments with a more classic membrane skeleton role (Huttenlauch et al. 1995). Our findings give support to the concept that articulins, plateins and alveolins have a common structural scaffold and thus should be grouped within the same protein superfamily. Structural studies are being carried out to test this hypothesis. Interestingly, prokaryotic articulin homologues have been discovered in *Caulobacter crescentus*, the first bacterium described to rely on an intermediate filament-based cytoskeleton for its cell shape (Ausmees et al. 2003). Thus, articulin-like proteins like alveolins could be far more widespread than originally assumed.

References

Anderson-White BR, Ivey FD, Cheng K, Szatanek T, Lorestani A, Beckers CJ, Ferguson DJ, Sahoo N, Gubbels MJ (2011) A family of intermediate filament-like proteins is sequentially assembled into the cytoskeleton of *Toxoplasma gondii*. Cell Microbiol 13(1):18–31

Andrade MA, Ponting CP, Gibson TJ, Bork P (2000) Homology-based method for identification of protein repeats using statistical significance estimates. J Mol Biol 298(3):521–537

Andrade MA, Perez-Iratxeta C, Ponting CP (2001) Protein repeats: structures, functions, and evolution. J Struc Biol 134(2–3):117–131

Arai M, Billker O, Morris HR, Panico M, Delcroix M, Dixon D, Ley SV, Sinden RE (2001) Both mosquito-derived xanthurenic acid and a host blood-derived factor regulate gametogenesis of *Plasmodium* in the midgut of the mosquito. Mol Biochem Parasitol 116(1):17–24

Ausmees N, Kuhn JR, Jacobs-Wagner C (2003) The bacterial cytoskeleton: an intermediate filament-like function in cell shape. Cell 115(6):705–713

Bannister LH, Hopkins JM, Fowler RE, Krishna S, Mitchell GH (2000) A brief illustrated guide to the ultrastructure of *Plasmodium falciparum* asexual blood stages. Parasitol Today 16(10):427–433

Biegert A, Soding J (2008) De novo identification of highly diverged protein repeats by probabilistic consistency. Bioinformatics 24(6):807–814

Brown JH, Cohen C, Parry DA (1996) Heptad breaks in alpha-helical coiled coils: stutters and stammers. Proteins 26(2):134–145

Claudianos C, Dessens JT, Trueman HE, Arai M, Mendoza J, Butcher GA, Crompton T, Sinden RE (2002) A malaria scavenger receptor-like protein essential for parasite development. Mol Microbiol 45(6):1473–1484

Dessens JT, Beetsma AL, Dimopoulos G, Wengelnik K, Crisanti A, Kafatos FC, Sinden RE (1999) CTRP is essential for mosquito infection by malaria ookinetes. EMBO J 18(22):6221–6227

Gould SB, Tham WH, Cowman AF, McFadden GI, Waller RF (2008) Alveolins, a new family of cortical proteins that define the protist infrakingdom Alveolata. Mol Biol Evol 25(6):1219–1230

Gould SB, Kraft LG, van Dooren GG, Goodman CD, Ford KL, Cassin AM, Bacic A, McFadden GI, Waller RF (2011) Ciliate pellicular proteome identifies novel protein families with characteristic repeat motifs that are common to alveolates. Mol Biol Evol 28(3):1319–1331

Heger A, Holm L (2000) Rapid automatic detection and alignment of repeats in protein sequences. Proteins 41(2):224–237

Huttenlauch I, Stick R (2003) Occurrence of articulins and epiplasmins in protists. J Eukaryot Microbiol 50(1):15–18

Huttenlauch I, Geisler N, Plessmann U, Peck RK, Weber K, Stick R (1995) Major epiplasmic proteins of ciliates are articulins: cloning, recombinant expression, and structural characterization. J Cell Biol 130(6):1401–1412

Khater EI, Sinden RE, Dessens JT (2004) A malaria membrane skeletal protein is essential for normal morphogenesis, motility, and infectivity of sporozoites. J Cell Biol 167(3):425–432

Kloetzel JA, Baroin-Tourancheau A, Miceli C, Barchetta S, Farmar J, Banerjee D, Fleury-Aubusson A (2003a) Cytoskeletal proteins with N-terminal signal peptides: plateins in the ciliate Euplotes define a new family of articulins. J Cell Sci 116(7):1291–1303

Kloetzel JA, Baroin-Tourancheau A, Miceli C, Barchetta S, Farmar J, Banerjee D, Fleury-Aubusson A (2003b) Plateins: a novel family of signal peptide-containing articulins in euplotid ciliates. J Eukaryot Microbiol 50(1):19–33

Kono M, Herrmann S, Loughran NB, Cabrera A, Engelberg K, Lehmann C, Sinha D, Prinz B, Ruch U, Heussler V, Spielmann T, Parkinson J,

Gilberger TW (2012) Evolution and architecture of the inner membrane complex in asexual and sexual stages of the malaria parasite. Mol Biol Evol 29(9):2113–2132

Mair GR, Braks JA, Garver LS, Wiegant JC, Hall N, Dirks RW, Khan SM, Dimopoulos G, Janse CJ, Waters AP (2006) Regulation of sexual development of plasmodium by translational repression. Science 313(5787):667–669

Mann T, Beckers C (2001) Characterization of the subpellicular network, a filamentous membrane skeletal component in the parasite *Toxoplasma gondii*. Mol Biochem Parasitol 115(2):257–268

Marcotte EM, Pellegrini M, Yeates TO, Eisenberg D (1999) A census of protein repeats. J Mol Biol 293(1):151–160

Marrs JA, Bouck GB (1992) The two major membrane skeletal proteins (articulins) of *Euglena gracilis* define a novel class of cytoskeletal proteins. J Cell Biol 118(6):1465–1475

Meis JF, Ponnudurai T (1987) Ultrastructural studies on the interaction of *Plasmodium falciparum* ookinetes with the midgut epithelium of *Anopheles stephensi* mosquitoes. Parasitol Res 73(6):500–506

Meis JF, Pool G, van Gemert GJ, Lensen AH, Ponnudurai T, Meuwissen JH (1989) *Plasmodium falciparum* ookinetes migrate intercellularly through *Anopheles stephensi* midgut epithelium. Parasitol Res 76(1):13–19

Moon RW, Taylor CJ, Bex C, Schepers R, Goulding D, Janse CJ, Waters AP, Baker DA, Billker O (2009) A cyclic GMP signalling module that regulates gliding motility in a malaria parasite. PLoS Pathog 5(9):e1000599

Morrissette NS, Sibley LD (2002) Cytoskeleton of apicomplexan parasites. Microbiol Mol Biol Rev 66(1):21–38

Santos JM, Lebrun M, Daher W, Soldati D, Dubremetz JF (2009) Apicomplexan cytoskeleton and motors: key regulators in morphogenesis, cell division, transport and motility. Int J Parasitol 39(2):153–162

Tremp AZ, Dessens JT (2011) Malaria IMC1 membrane skeleton proteins operate autonomously and participate in motility independently of cell shape. J Biol Chem 286(7):5383–5391

Tremp AZ, Khater EI, Dessens JT (2008) IMC1b is a putative membrane skeleton protein involved in cell shape, mechanical strength, motility, and infectivity of malaria ookinetes. J Biol Chem 283(41):27604–27611

Tremp AZ, Carter V, Saeed S, Dessens JT (2013) Morphogenesis of *Plasmodium* zoites is uncoupled from tensile strength. Mol Microbiol 89(3):552–564

Tremp AZ, Al-Khattaf FS, Dessens JT (2014) Distinct temporal recruitment of *Plasmodium* alveolins to the subpellicular network. Parasitol Res 113(11):4177–4188

Volkmann K, Pfander C, Burstroem C, Ahras M, Goulding D, Rayner JC, Frischknecht F, Billker O, Brochet M (2012) The alveolin IMC1h is required for normal ookinete and sporozoite motility behaviour and host colonisation in *Plasmodium berghei*. PLoS One 7(7):e41409

Waters AP, Thomas AW, van Dijk MR, Janse CJ (1997) Transfection of malaria parasites. Methods 13(2):134–147

Chapter 5

The *Plasmodium* alveolin IMC1a is stabilised

by its terminal cysteine motifs

and facilitates sporozoite morphogenesis and

infectivity

in a dose-dependent manner

Research Paper Cover Sheet

SECTION A – Student Details

Student	Fatimah Al-Khattaf
Principal Supervisor	Johannes Dessens
Thesis Title	Functional characterization of the alveolins, a family of cytoskeleton proteins of malaria parasites

SECTION C – Prepared for publication, but not yet published

Where is the work intended to be published?	Journal of Biological Chemistry
Please list the paper's authors in the intended authorship order:	Al-Khattaf F, Tremp AZ, El-Houderi A, Dessens JT
Stage of publication	Undergoing revision

SECTION D – Multi-authored work

For multi-authored work, give full details of your role in the research included in the paper and in the preparation of the paper. (Attach a further sheet if necessary)	Student generated the mCherry-tagged IMC1a mutant parasite lines and performed and analysed genotyping and phenotyping experiments. Student contributed to preparation of the paper (text and figures).

Student Signature: _____   **Date:** _____

Supervisor Signature: _____   **Date:** _____

The *Plasmodium* Alveolin IMC1a

is Stabilised by its Terminal Cysteine Motifs

and Facilitates Sporozoite Morphogenesis and Infectivity

in a Dose-Dependent Manner

Fatimah S. Al-Khattaf, Annie Z. Tremp, Amira El-Houderi, and Johannes T. Dessens

From the Department of Pathogen Molecular Biology, London School of Hygiene & Tropical Medicine, Keppel street, London WC1E 7HT, United Kingdom

Running title: *Role of cysteine motifs of the alveolin IMC1a*

To whom correspondence should be addressed: Johannes T. Dessens, London School of Hygiene & Tropical Medicine, Keppel street, London WC1E 7HT, United Kingdom, Telephone: (44) 2079272865; FAX: (44) 2076374314; E-mail: Johannes.Dessens@lshtm.ac.uk

74

Abstract

Apicomplexan parasites possess a unique cortical cytoskeleton structure composed of intermediate filaments. Its building blocks are provided by a conserved family of proteins named alveolins. The core alveolin structure is made up of tandem repeat sequences, thought to be responsible for the filamentous properties of these proteins. A subset of alveolins also possess conserved motifs composed of three closely spaced cysteine residues situated near the ends of the polypeptides. The roles of these cysteine motifs in alveolin function is unknown. The sporozoite-expressed IMC1a is unique within the *Plasmodium* alveolin family in having cysteine motifs at both termini. Using transgenic *Plasmodium berghei* parasites, we show in this structure-function study that mutagenesis of the amino- or carboxy-terminal cysteine motif causes marked reductions in IMC1a protein levels in the parasite. These phenotypes are accompanied by partial losses of sporozoite shape and infectivity. Our results show furthermore that within the carboxy-terminal motif a double cysteine contributes chiefly to these properties. Our findings give important new insight into alveolin function, identifying a dose-dependent effect of alveolin depletion on parasite morphogenesis and infectivity, and vital roles of the terminal cysteine motifs in promoting alveolin expression and stability in the parasite.

Introduction

Plasmodium species, the causative agents of malaria, have a complex life cycle in vertebrate host and mosquito vector. Among the many different developmental forms of the parasite feature three motile and invasive stages (also known as 'zoites'): the ookinete, sporozoite and merozoite. The zoites of *Plasmodium,* as well as those of related apicomplexan parasites, possess an unusual cortical structure termed the pellicle. The pellicle is defined by a double membrane structure termed the inner membrane complex (IMC) situated directly underneath the plasma membrane, which is equivalent to a system of flattened sacs or alveoli (Bannister *et al.*, 2000; Morrissette and Sibley, 2002; Santos *et al.*, 2009). On the cytoplasmic face of the IMC is anchored a network of intermediate filaments termed the subpellicular network (SPN), the function of which is to support the pellicle membranes and give the cell mechanical strength (Mann and Beckers, 2001).

A family of proteins now termed alveolins have been identified as components of the SPN (Khater *et al.*, 2004; Mann and Beckers, 2001). The alveolin superfamily includes structurally related proteins from apicomplexan parasites, ciliates and dinoflagellate algae, the three phyla comprising the Alveolata superphylum (Gould *et al.*, 2008). In the genus *Plasmodium*, 13 conserved and syntenic alveolin family members have been identified that are differentially expressed among the three different zoites stages of malaria parasites (Al-Khattaf *et al.*, 2015; Kaneko *et al.*, 2015). It has been shown in the rodent malaria species *P. berghei* that disruption of alveolins gives rise to morphological aberrations that are accompanied by reduced tensile strength of the zoite stages in which they are found (Kaneko *et al.*, 2015; Khater *et al.*, 2004; Tremp and Dessens, 2011; Tremp *et al.*, 2008; Volkmann *et al.*, 2012). *Plasmodium* alveolins also have roles in parasite gliding motility (Khater *et al.*, 2004; Tremp and Dessens, 2011; Tremp *et al.*, 2008; Volkmann *et al.*, 2012) most likely by tethering components of the glideosome that reside in the IMC.

The 13 alveolins identified in *Plasmodium* are characterised by having one or more highly conserved domains separated by regions of variable length and amino acid composition. We have recently shown that these conserved 'alveolin' domains

are composed of tandem repeat sequences of 12 amino acid residues (Al-Khattaf *et al.*, 2015). This has revealed an interesting parallel with metazoan intermediate filament proteins such as lamins and keratins, whose underlying architectures include a helical rod domain that can form coiled-coils by virtue of a seven amino acid tandem repeat structure (Herrmann and Aebi, 2004). These coiled-coil domains are thought to be fundamental for the filament-forming properties of these molecules. Apart from the conserved alveolin domains, a subset of the alveolins also possess conserved cysteine motifs close to their amino- or carboxy-terminus (Fig. 5.1). These motifs are made up of a single cysteine and a double cysteine that are separated by a small number of other amino acids (Fig. 5.1). With the exception of IMC1i, The N- and C-terminal motifs are inverted, with the single cysteine located nearest the end of the polypeptide (Fig. 5.1). The function of these cysteine motifs is unknown. IMC1a is the only alveolin with such motifs at both ends, and in this study we employ site-directed mutagenesis and gene targeting to investigate the contribution of these motifs to the function of the protein and the SPN as a whole, in transgenic *P. berghei* parasite lines.

```
IMC1a (4X)C(5X)CC.........CC(3X)C(4x)
IMC1c ....................CC(3X)C(1X)
IMC1g (1X)C(7X)CC....................
IMC1i ...................C(5X)CC(3X)
IMC1j (5X)C(6X)CC...................
```

Figure 5.1. Conserved cysteine motifs at the amino and carboxy-terminal ends of Plasmodium alveolins IMC1a, IMC1c, MC1g, IMC1i and IMC1j. The number of non-cysteine residues (X) adjacent to the conserved cysteines (C) are indicated.

Experimental procedures

Animal use

All laboratory animal work is subject to regular ethical review by the London School of Hygiene and Tropical Medicine, and has approval from the United Kingdom Home Office. Work was carried out in accordance with the United Kingdom Animals (Scientific Procedures) Act 1986 implementing European Directive 2010/63 for the protection of animals used for experimental purposes. Experiments were conducted in 6-8 weeks old female CD1 mice, specific pathogen free and maintained in filter cages. Animal welfare was assessed daily and animals were humanely killed upon reaching experimental or humane endpoints. Mice were infected with parasites by intraperitoneal injection, or by infected mosquito bite on anaesthetized animals. Parasitemia was monitored regularly by collecting of a small drop of blood from a superficial tail vein. Drugs were administered by intraperitoneal injection or where possible were supplied in drinking water. Parasitized blood was harvested by cardiac bleed under general anaesthesia without recovery.

Parasite maintenance, transmission, culture and purification

P. berghei ANKA clone 2.34 parasites were maintained as cryopreserved stabilates or by mechanical blood passage and regular mosquito transmission. Mosquito infection and transmission assays were as previously described using *Anopheles stephensi* (Dessens *et al.*, 1999; Khater *et al.*, 2004) and infected insects were maintained at 20°C at approximately 70% relative humidity.

Gene targeting vectors

An approximately 3.5kb fragment corresponding to the entire *imc1a* gene (introns included) plus 5'-UTR was PCR amplified from *P. berghei* gDNA using primers pDNR-imc1a-F (ACGAAGTTATCAGTCGAGGTACCTTTCATGATTCTATCTATTGTTAATTTTAATTG) and pDNR-imc1a-R

(ATGAGGGCCCCTAAGCTTTTATCTTGATTACAAAAATAATTACAACATTTG) and introduced into SalI/HindIII-digested pDNR-mCherry (Tremp *et al.*, 2014) by in-fusion to give plasmid pDNR-IMC1a/mCherry.

Mutations of the terminal cysteine motifs in IMC1a were made in such a way that the desired cysteines were substituted whilst making minimal changes to the original sequence, and at the same time introducing unique diagnostic restriction sites in order to screen targeting vectors and transgenic parasites for the presence of the desired mutation. To substitute the N-terminal cysteine motif of IMC1a (Mutant 1) primers IMC1a-Mut1-F (GAAAATAAATAGTAATCTCGAGCATGATGAGTTGGGAGAAGACA) and IMC1a-Mut1-R (ATTACTATTTATTTTCCATGCATCAAACATTTTAATTAAATG) were used to PCR amplify pDNR-IMC1a/mCherry. Template plasmid was removed after the PCR by *Dpn*I digestion, and the PCR product was circularized by in-fusion, to give plasmid pDNR-IMC1a-Mutant 1. This mutation introduces a diagnostic *Xho*I restriction site, changing the double cysteine (CC) in the amino-terminal motif to leucine-glutamate (LE) (Fig. 5.2B).

To substitute the C-terminal cysteine motif of IMC1a (Mutant 2) primers IMC1a-Mut2-F (CTCGAGAATTATTTTTGGAATCAAGATAAAAGCTTAGGGGC) and IMC1a-Mut2-R (CCAAAAATAATTCTCGAGTTTGTCTTCAGAATTATCACTTTTTTTT) were used to PCR amplify pDNR-IMC1a/mCherry. Template plasmid was removed after the PCR by *Dpn*I digestion, and the PCR product was circularized by in-fusion, to give plasmid pDNR-IMC1a-Mutant 2. This mutation introduces a diagnostic *Xho*I restriction site, changing the double cysteine (CC) in the carboxy-terminal motif to leucine-glutamate (LE) (Fig. 5.2B).

To substitute the double cysteine from the C-terminal cysteine motif of IMC1a (Mutant 3) primers IMC1a-Mut3-F (CTCGAGAATTATTTTTGTAATCAAGATAAAAGCTTAGGGGC) and IMC1a-Mut3-R (ACAAAAATAATTCTCGAGTTTGTCTTCAGAATTATCACTTTTTTTT) were used to PCR amplify pDNR-IMC1a/mCherry. Template plasmid was removed after the PCR by *Dpn*I digestion, and the PCR product was circularized by in-fusion, to give plasmid pDNR-IMC1a-Mutant 3. This mutation introduces a diagnostic *Xho*I restriction site,
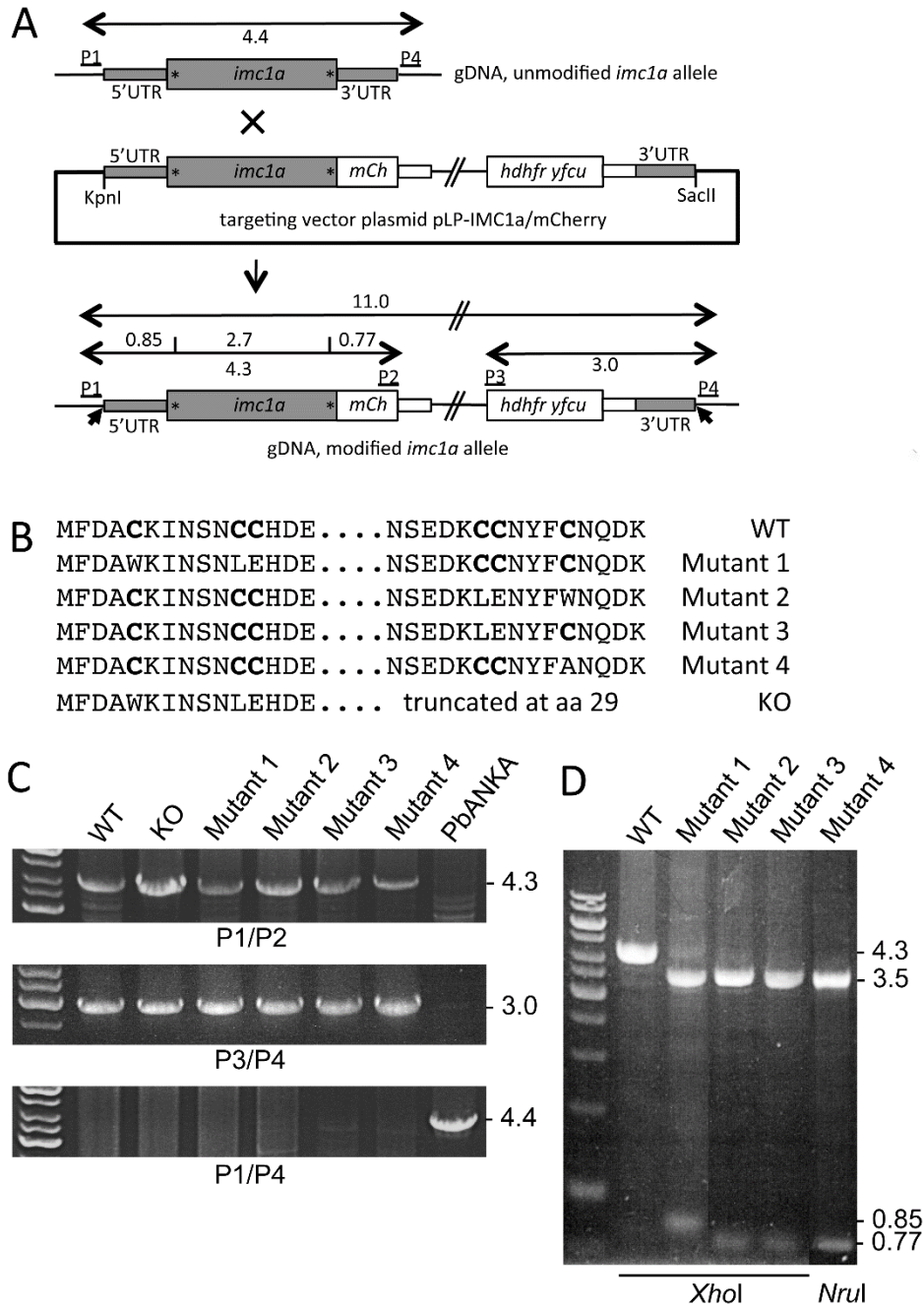
changing the double cysteine (CC) in the carboxy-terminal motif to leucine-glutamate (LE) (Fig. 5.2B).

To substitute the single cysteine from the C-terminal cysteine motif of IMC1a (Mutant 4) primers IMC1a-Mut4-F (TTATTTCGCGAATCAAGATAAAAGCTTAGGGGC) and IMC1a-Mut4-R (TTGATTCGCGAAATAATTACAACATTTGTCTTCAGAATTATCACT) were used to PCR amplify pDNR-IMC1a/mCherry. Template plasmid was removed after the PCR by *Dpn*I digestion, and the PCR product was circularized by in-fusion, to give plasmid pDNR-IMC1a-Mutant 4. This mutation introduces a diagnostic *Nru*I restriction site, changing the single cysteine (C) in the carboxy-terminal motif to alanine (A) (Fig. 5.2B).

Primers hDHFR/ERI-F (ACAAAGAATTCATGGTTGGTTCGCTAAACT) and hDHFR/ERI-R (ACCATGAATTCTTTGTAACATTTAGGTGTGTATTTATATATATAAGC) were used to PCR amplify plasmid pLP-hDHFR (Saeed *et al.*, 2010). Template plasmid DNA was removed after the PCR by DpnI digestion, and the PCR product was circularized by in-fusion, to give plasmid pLP-hDHFR/EcoRI. In this plasmid the BamHI restriction site site at beginning of the hDHFR gene is replaced with an EcoRI. A 1.7 kb fragment corresponding to the *hdhfryfcu* gene was PCR amplified from plasmid pL0035 with primers hDHFRyFCU-F (ATGTTACAAAGAATTCATGGTTGGTTCGCTAAACTG) and hDHFRyFCU-R (AAGAAAAACGGGATCCTTAAACACAGTAGTATCTGTCACCAAAG) and introduced into *Eco*RI/*Bam*HI-digested pLP-hDHFR/EcoRI by in-fusion to give pLP-hDHFRyFCU. A 0.75 kb fragment corresponding to the 3'UTR of the *imc1a* gene was amplified from *P. berghei* gDNA with primers pLP-imc1a-F (ATATGCTAGAGCGGCCAAAATATGGTATTTTAAAACTATTGAATTGG) and pLP-imc1a-R (CACCGCGGTGGCGGCCAGCGACACTTAAGAGATAGCATAAGA) and introduced into *Not*I-digested pLP-hDHFRyFCU by in-fusion to give plasmid pLP-hDHFRyFCU/IMC1a. Cre-*lox*p recombination of pDNR-IMC1a/mCherry, pDNR-IMC1a-Mutant 1, pDNR-IMC1a-Mutant 2, pDNR-IMC1a-Mutant 3 and pDNR-IMC1a-Mutant 4 was carried out with pLP-hDHFRyFCU/IMC1a to give final plasmids pLP-IMC1a/mCherry-WT, pLP-IMC1a/mCherry-Mutant 1, pLP-IMC1a/mCherry-Mutant 2,

and pLP-IMC1a/mCherry-Mutant 3 and pLP-IMC1a/mCherry-Mutant 4, respectively. All gene targeting vectors were sequenced across the IMC1a::mCherry-encoding region to verify the absence of undesired mutations. This identified one plasmid that had obtained an undesired frameshift close to the 5'-end of the *imc1a* coding sequence. This plasmid was used to generate an independent IMC1a knockout parasite, following the same targeting strategy as the other parasite lines.

A

B
```
MFDACKINSNCCHDE....NSEDKCCNYFCNQDK          WT
MFDAWKINSNLEHDE....NSEDKCCNYFCNQDK          Mutant 1
MFDACKINSNCCHDE....NSEDKLENYFWNQDK          Mutant 2
MFDACKINSNCCHDE....NSEDKLENYFCNQDK          Mutant 3
MFDACKINSNCCHDE....NSEDKCCNYFANQDK          Mutant 4
MFDAWKINSNLEHDE.... truncated at aa 29         KO
```

C

D

Figure 5.2. Generation and genetic analyses of IMC1a mutant parasite lines. A: Targeting strategy for the mCherry tagging of IMC1a via double crossover homologous recombination, showing unmodified (top) and modified (bottom) imc1a alleles, a well as the targeting vector pLP-IMC1a/mCherry (middle). The pbimc1a gene is indicated with coding sequence (wide grey bars, introns not shown) and 5' and 3' untranslated regions (UTRs) (narrow grey bars). Also indicated are the relative positions of the terminal cysteine motifs (asterisks), the mCherry module (mCh); the hDHFRyFCU selectable marker gene cassette (hdhfr yfcu); the generic 3'UTR from pbdhfr (narrow white bars); and primers used for diagnostic PCR amplification (P1-P4). Primer P1 and P4 sequences are not present within the targeting vector. Arrowheads mark 5' and 3' integration sites. Also shown are the relative positions of KpnI and SacII restriction sites used to remove the plasmid backbone from the targeting vector. **B**: Amino acid sequences of the amino- and carboxy-terminal ends of IMC1a in parasite lines IMC1a/mCherry-WT (wildtype IMC1a sequence, but with mCherry tag), IMC1a/mCherry-Mutant 1, IMC1a/mCherry-Mutant 2, IMC1a/mCherry-Mutant 3, IMC1a/mCherry-Mutant 4, and IMC1a/mCherry-KO (null mutant). The conserved cysteines are marked in bold. **C**: PCR with primer pair P1/P2 across the 5' integration site diagnostic for the presence of the mCherry-tagged pbimc1a alleles (top); PCR with primer pair P3/P4 across the 3' integration site diagnostic for the presence of the hdhfr yfcu selectable marker allele (middle); and PCR with primer pair P1/P4 diagnostic for the presence of the unmodified imc1a allele (bottom), carried out on genomic DNA from clonal transgenic parasite and parental (PbANKA) parasite populations. **D**: Restriction enzyme digestion (XhoI or NruI) of PCR amplicons from **C**, diagnostic for the presence of the desired cysteine motif mutations. Cleavage products of 3.5kb and either 0.85kb (Mutant 1), or 0.77kb (Mutants 2-4) are visible except for the non-mutated version of imc1a::mcherry in parasite line IMC1a/mCherry-WT.

Generation and genomic analysis of genetically modified parasites

Parasite transfection, pyrimethamine selection and dilution cloning were performed as previously described (Waters *et al.*, 1997). Prior to performing transfections, plasmid DNA was digested with *Kpn*I and *Sac*II to remove the plasmid backbone. Genomic DNA extraction was performed as previously described (Dessens *et al.*, 1999). After each transfection, drug resistant parasites were subjected to limiting dilution cloning. Following this, integration of the selectable marker gene into the *imc1a* locus was confirmed by diagnostic PCR across the 3' integration site using primers P3 (ACAAAGAATTCATGGTTGGTTCGCTAAAC) and P4 (TGCACACCCACCTGATTG) (Fig 5.2A). Integration of the mCherry-encoding sequence into the *imc1a* locus was confirmed by diagnostic PCR across the 5' integration site with primers P1 (GCACATTAATGCATTTGGG) and P2 (AACGGGATCTTCTAGTTACTTGTACAGCTCGTCCATGC) (Fig. 5.2A). The absence of the

unmodified *imc1a* allele in the clonal parasite lines was confirmed by diagnostic PCR with primers P1 and P4 (Fig. 5.2A).

Sporozoite footprint measurements

Sporozoite-infected tissues were dissected from parasite-infected mosquitoes and the sporozoites gently released in a Dounce homogenizer. Sporozoites were spotted onto glass microscope slides, allowed to adhere and then air dried. After methanol fixation, Giemsa-stained images of individual cells were captured by microscopy on Zeiss LSM510 inverted laser scanning confocal microscope. Using Zeiss LSM image browser software the circumference was measured, and the surface area occupied (*i.e.* the footprint) calculated. Statistical analysis was carried out using two-tailed t-test.

Western blot analysis

Parasite samples were heated directly in SDS-PAGE loading buffer at 70ºC for 10 min. Proteins were fractionated by electrophoresis through NuPage 4-12% Bis-Tris precast gels (Invitrogen) and transferred to PVDF membrane (Invitrogen) according to the manufacturer's instructions. Membranes were blocked for non-specific binding in PBS supplemented with 0.1% Tween 20 and 5% skimmed milk for 1h at room temperature. Rabbit polyclonal antibody against RFP (Abcam) diluted 1 in 5,000 was applied to the membrane for 1h at room temperature. After washing, membranes were incubated with goat anti rabbit IgG conjugated to horse radish peroxidase (HRP) (Abcam) diluted 1 in 5,000 for 1h at room temperature. After further washing, signal was detected by chemiluminescence (ECL western blotting substrate, Pierce) according to manufacturer's instructions. For reprobing, the blot was incubated in 30% hydrogen peroxide solution for 30min at 37 degrees to inactivate residual HRP (Sennepin *et al.*, 2009). The membrane was reblocked and then incubated with monoclonal antibody 3D11 against circumzoite protein (CSP) diluted 1 in 1000 for 1h at room temperature. After washing secondary goat-anti-mouse polyclonal antibody conjugated to HRP (Invitrogen 81-6520) diluted 1 in

5000 was added and incubated for 1h at room temperature prior to washing and chemilluminescence detection.

RT-PCR analysis

Twenty midguts were harvested from parasite-infected mosquitoes at two weeks post-infection, pooled, and total RNA was extracted using a Qiagen RNeasy mini kit according to manufacturer's instructions. First strand cDNA was synthesized with M-MLV reverse transcriptase, (RNase H minus point mutation; Promega) using oligo(dT)$_{25}$ as primer, for 1h at 50°C. Excess primer was removed by column purification (Qiaquick gel extraction kit; Qiagen) and the eluted cDNA was subjected to PCR amplification with primers A30 (ATATAGTCCATTTAGTTAGAGTTTGTG) and pDNR-imc1a-R

(ATGAGGGCCCCTAAGCTTTTATCTTGATTACAAAAATAATTACAACATTTG) for *imc1a*, and primers tub1-F (GAAGTAATAAGTATACATGTAGG) and tub1-R (ACACATCAATGACTTCTTTACC) for *tubulin 1*.

Microscopy

For assessment of fluorescence, live parasite samples were assessed, and images captured, on a Zeiss LSM510 inverted confocal microscope and Zeiss LSM image browser software. To allow comparison of samples, images were captured with the same settings using the 'reuse' function.

Results

## Generation and molecular analyses of transgenic parasite lines

To study expression and localization of IMC1a and variants of it in the parasite, we first generated a transgenic *P. berghei* line that expresses full-length IMC1a fused to a carboxy-terminal mCherry tag (Fig. 5.2A), named IMC1a/mCherry-WT. The *imc1a* gene targeting strategy employs double crossover homologous recombination, ensuring that its modifications are stable and non-reversible (Fig. 5.2A). To study the contribution of the cysteine motifs to IMC1a function, specific mutations were introduced by site-directed mutagenesis, removing either the entire N-terminal motif (named IMC1a/mCherry-Mutant 1), the entire C-terminal motif (named IMC1a/mCherry-Mutant 2), the cysteine doublet within the C-terminal motif (named IMC1a/mCherry-Mutant 3), or the single cysteine within the C-terminal motif (named IMC1a/mCherry-Mutant 4) (Fig. 5.2B). In addition, an IMC1a/mCherry targeting vector that contained a frame shift very near the 5' end of the coding sequence was used to generate an IMC1a null mutant parasite line (IMC1a/mCherry-KO) (Fig. 5.2B). After transfection of purified schizont preparations, pyrimethamine-resistant parasites were selected and cloned by limiting dilution. Confirmation of correct targeting and integration of the mCherry tag and selectable marker gene cassette into the *imc1a* locus was carried out with diagnostic PCR across the 5' and 3' integration sites using primer pairs P1/P2 and P3/P4, respectively (Fig. 5.2A), resulting in 4.3kb and 3.0kb products, respectively (Fig. 5.2C). The 4.3kb PCR product was digested with *Xho*1 (Mutant 1, Mutant 2 and Mutant 3) or *Nru*I (Mutant 4) to confirm the presence of the desired mutations (Fig. 5.2D). In addition, the absence of the unmodified *imc1a* allele in all clonal parasite lines was confirmed by diagnostic PCR with primer pair P1/P4 (Fig. 5.2A,C).

Life stage expression and subcellular localization of IMC1a

Strong mCherry-based fluorescence was detected in mature sporulating oocysts of parasite line IMC1a/mCherry-WT (Fig. 5.3A), in full agreement with the previously reported life stage expression of IMC1a (Khater *et al.*, 2004). This parasite

developed normally in mouse and mosquito, and was readily transmitted by sporozoite-infected mosquito bite, demonstrating that the mCherry tag does not interfere with normal IMC1a function. In sporozoites, the mCherry-based fluorescence was clearly concentrated at the cell periphery (Fig. 5.3A) which is consistent with the reported subcellular localization of IMC1a in the SPN (Khater *et al.*, 2004). Western blot analysis of sporozoite lysates using anti-mCherry antibodies detected one major band migrating at approximately 130kDa, corresponding to the IMC1a::mCherry fusion protein (Fig. 5.3B). Some smaller proteins of much lower intensity were also detected probably resulting from proteolytic processing (Fig. 5.3B). Measuring band intensities indicated that processing constitutes less than 10% and is therefore likely the result of low level degradation, rather than of specific proteolytic events with a biological role.

IMC1a/mCherry-KO parasites, as expected, did not exhibit mCherry fluorescence in oocysts or sporozoites (Fig. 5.3C), because the mCherry tag is not expressed due to an upstream frameshift (Fig. 5.2B). These oocysts displayed a phenotype comparable to that previously described for IMC1a null mutants (Khater *et al.*, 2004), producing numbers of sporozoites similar to its wildtype counterpart (mean midgut oocysts/sporozoites per mosquito IMC1a/mCherry-WT: 43/15,000; IMC1a/mCherry-KO: 52/17,000; n=10), but with abnormal size and shape (Fig. 5.3C).
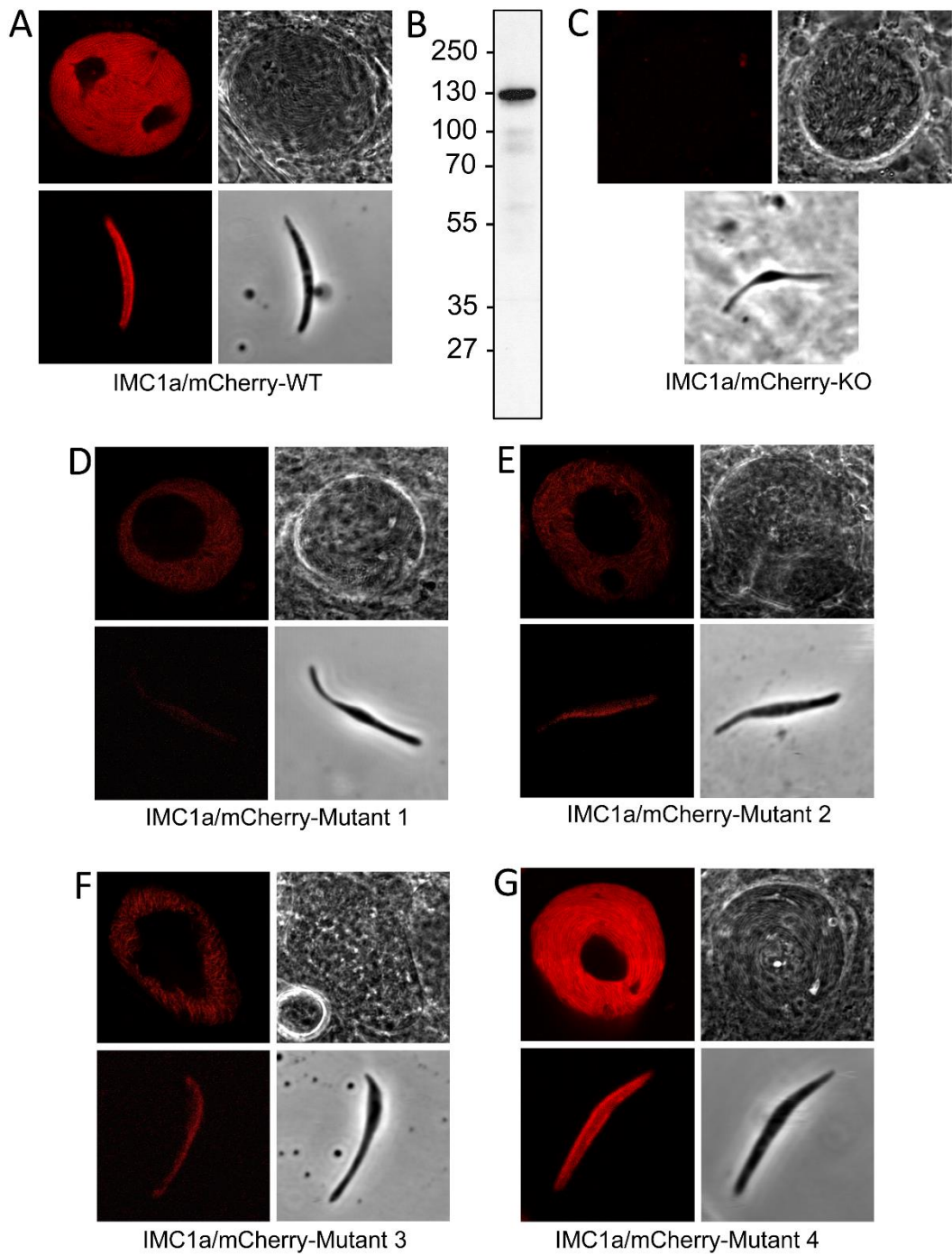
Figure 5.3. Fluorescence in oocysts and sporozoites of mCherry-tagged IMC1a-expressing parasite lines. A: Confocal fluorescence and brightfield images of a sporulating oocyst and sporozoite of parasite line IMC1a/mCherry-WT. **B**: Western blot of a sporozoite lysate of parasite line IMC1a/mCherry-WT (100,000 sporozoites loaded) using anti-mCherry antibodies, visualising the IMC1a::mCherry fusion protein. Size markers are shown on the left hand side. **C-G**: Confocal images of a sporulating oocyst and sporozoite of mutant parasite lines IMC1a/mCherry-KO (**C**); IMC1a/mCherry-Mutant 1 (**D**); IMC1a/mCherry-Mutant 2 (**E**); IMC1a/mCherry-Mutant 3 (**F**); IMC1a/mCherry-Mutant 4 (**G**). Confocal images were captured using the same confocal microscope settings.

The terminal cysteine motifs affect IMC1a protein level in the parasite

Having established the IMC1a/mCherry-WT and -KO phenotypes, we turned our attention to parasite lines IMC1a/mCherry-Mutant 1 and Mutant 2. Both mutants displayed mCherry-based fluorescence in mature oocysts and sporozoites (Figs 5.3D,E), demonstrating that the full-length IMC1a protein was being expressed, as expected. However, in both mutants the fluorescence levels were markedly lower compared to parasite line IMC1a/mCherry-WT (Fig. 5.3). These observations indicated that the removal of the amino- or carboxy-terminal cysteine motif from IMC1a had adversely affected either the stability of the alveolin, or the ability of its mCherry moiety to fluoresce. To distinguish between these possibilities, sporozoite samples from these parasite lines were analysed by western blot analysis, which revealed that relative to circumsporozoite protein (CSP), significantly reduced amounts of IMC1a::mCherry fusion protein were present in Mutant 2 and Mutant 1 (on average 21% and 10% of WT levels, respectively; n=3; P<0.001) (Fig. 5.4A). These reduced levels of IMC1a::mCherry fusion protein in the parasite explain the lower fluorescence levels observed in Mutant 1 and Mutant 2. Sporozoites of Mutant 1 had consistently lower levels of IMC1a than Mutant 2, although the differences were not statistically significant (P=0.09). The two bands migrating close together in Fig. 5.4A are full-length IMC1a::mCherry and a slightly smaller product (also observed in Fig. 5.3B) most likely the result of processing/degradation. The doublet is more obvious in this blot because it was overexposed to clearly reveal the lower amounts of IMC1a::mCherry proteins in the mutants (particularly Mutant 1). The difference in the relative intensities of the upper and lower band between Mutant 1 and Mutant 2 could reflect differences in their relative stability as a result of their different mutations.

To investigate whether the reduced IMC1a protein levels (Fig. 5.4A) could be the result of reduced transcription of the *imc1a* gene in the affected mutant parasite lines, we carried out reverse transcription-PCR analysis on sporulating oocysts. This was done with Mutant 1 - which shows the lowest IMC1a protein level - in direct comparson with the control parasite line IMC1a/mCherry-WT, and normalised against the reference tubulin 1 gene (*tub1*). Primers for *imc1a* amplified

a mRNA-specific 2.4kb product, and a gDNA-specific 2.8kb product (due to introns), while primers for *tub1* only amplified a mRNA-specific 0.35kb product (the product amplified from gDNA is 1.0kb due to introns (Al-Khattaf *et al.*, 2015)) (Fig. 5.4B). Measured band intensities normalised against the reference *tub1* gene showed that IMC1a/mCherry-Mutant 1 oocysts contained at least as much *imc1a* mRNA than its WT counterpart and, accordingly, the reduced levels of IMC1a protein present in Mutant 1, and by analogy in Mutant 2 (Fig. 5.4A), are unlikely to be caused by a reduced *imc1a* gene expression at the transcription level.
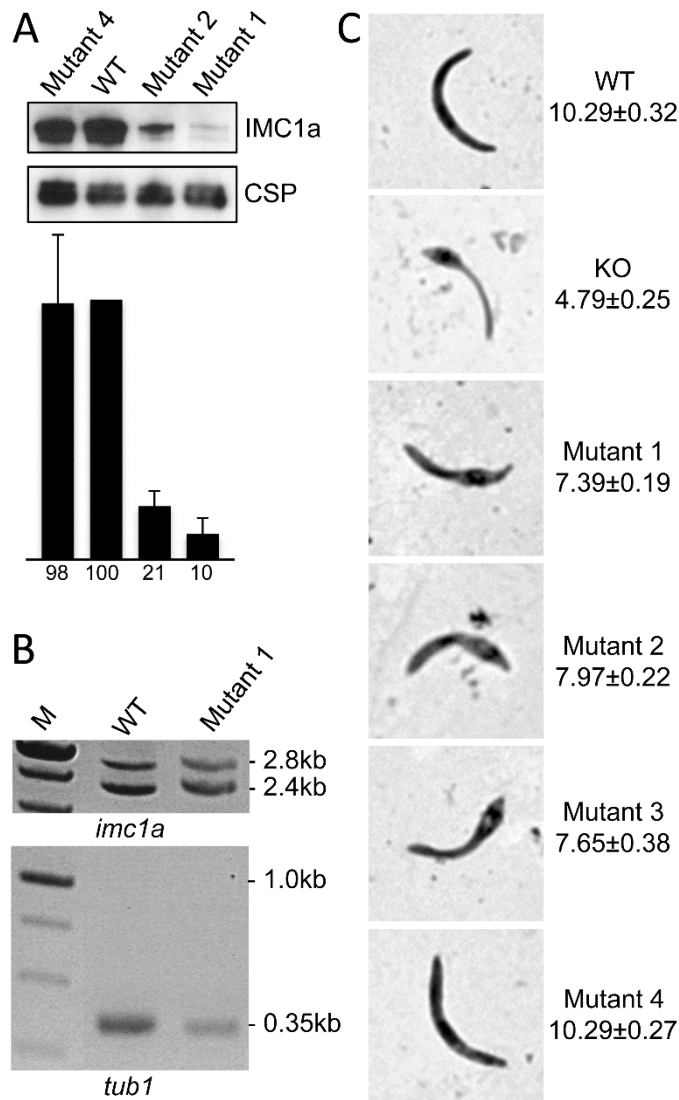
Figure 5.4. IMC1a protein levels and sporozoite shape of IMC1a cysteine mutants. A: Western blot of sporozoite lysates from parasite lines IMC1a/mCherry-WT, Mutant 1, Mutant 2 and Mutant 4, using anti-mCherry antibodies (top), or anti-CSP antibodies (bottom). Approximately 100,000 sporozoites were loaded for WT and Mutant 4, and 130,000 sporozoites for Mutant 1 and Mutant 2, to compensate for the smaller sporozoite sizes of the latter two. Histogram shows relative amounts of IMC1a, averaged over three independent measurements (WT set to 100%) and normalised against CSP loading controls. **B**: Reverse transcription PCR analysis of imc1a mRNA levels (relative to tub1 mRNA) in sporulating oocysts of parasite lines IMC1a/mCherry-WT and Mutant 1. **C**: Representative Giemsa-stained sporozoite images from parasite lines IMC1a/mCherry-WT, KO, and Mutants 1-4. Numbers give mean±sem footprint measurements in µm2 (n=27).

The terminal cysteine motifs of IMC1a affect sporozoite shape

Examination of sporozoites from IMC1a/mCherry-Mutant 1 and -Mutant 2 indicated that they had an abnormal shape (Figs 5.3, 5.4). Although this shape was similar to the shape of IMC1a null mutant sporozoites, it appeared less severe than is the case after a complete knockout of IMC1a expression (Figs 5.3, 5.4). Because of the variable and irregular shapes of the mutant sporozoites, their size was difficult to define by linear measurements of length and width. Thus, a more sensitive measure of the observed changes in sporozoite morphology was developed by determining their 'footprint', which gives a quantitative measure of the sporozoite's size independent of its shape. Footprint measurements showed that KO sporozoites are on average significantly smaller than WT sporozoites (P<0.0001, n=27), in fact less than half the normal size (Fig. 5.4C). Sporozoites of Mutant 1 and Mutant 2 had intermediate sizes, both being significantly smaller that WT sporozoites (P<0.0001, n=27), but significantly larger than KO sporozoites (P<0.0001, n=27) (Fig. 5.4C). Mutant 1 sporozoites were on average smaller than those of Mutant 2, albeit the differences were not statistically significant (P=0.07, n=27) (Fig. 5.4C). These observations demonstrate that mutations of the terminal cysteine motifs of IMC1a cause an intermediate phenotype with regards to sporozoite shape. We did not observe discernible shape/size differences between midgut- and salivary gland-derived sporozoites in our mutant lines, indicating that infectivity is similar across the sporozoite populations.

The double cysteine is more important than the single cysteine

To study the contribution of different cysteines within the motifs, we generated two more mutants of the C-terminal motif in which either its double cysteine (Mutant 3) or its single cysteine (Mutant 4) were substituted (Fig. 5.2B). Mutant 4 oocysts displayed bright fluorescence that was concentrated at the cortex of normal shaped sporozoites (Fig. 5.3G), and these parasites were indistinguishable from their IMC1a/mCherry-WT counterparts (Fig. 5.3). Indeed, footprint measurements confirmed that the average size of mutant 4 sporozoites was not significantly

different to that of IMC1a/mCherry-WT sporozoites (P=0.99, n=27) (Fig. 5.4C). Moreover, western analysis revealed that IMC1a::mCherry protein levels were not significantly reduced in Mutant 4 sporozoites compared to their WT counterparts, relative to CSP (Fig. 5.4A). In contrast to Mutant 4, Mutant 3 oocysts and sporozoites closely resembled those of Mutant 2 both in terms of shape, footprint (Fig. 5.4C) and fluorescent intensity (Fig. 5.3F). Overall, these results demonstrate that the double cysteine is the main contributor to the properties of the terminal cysteine motif.

Mutations of the terminal cysteine motifs of IMC1a affect sporozoite infectivity

In parallel to the assessments of IMC1a expression levels and sporozoite shape (Figs 5.3 and 5.4), we analyzed the effect of the various cysteine mutations on sporozoite infectivity. The reference parasite line IMC1a/mCherry-WT developed normally and gave rise to high numbers of salivary gland sporozoites (Table 5.1) that were readily transmissible by mosquito bite. In sharp contrast, and consistent with a previous report (Khater *et al.*, 2004), our IMC1a null mutant sporozoites were unable to reach the salivary glands in detectable numbers (Table 5.1). Salivary gland sporozoite numbers for Mutant 2 were consistently lower (3- to 4-fold) than those observed for IMC1a/mCherry-WT parasites (Table 5.1), pointing to a reduced infectivity to the salivary glands. Nonetheless, Mutant 2 sporozoites could be transmitted to naive mice by mosquito bite. After transmission, the phenotype of Mutant 2 remained the same with respect to fluorescence, sporozoite shape and infectivity (data not shown). In contrast to Mutant 2, salivary gland sporozoite numbers for Mutant 1 were consistently highly reduced (>10-fold) (Table 5.1), and we were repeatedly (n=5) unable to transmit this parasite by mosquito bite. Mutant 3 behaved similarly to Mutant 2 in terms of sporozoite infectivity, while Mutant 4 behaved like the IMC1a/mCherry-WT reference line (Table 5.1). These combined results demonstrate that Mutant 1, Mutant 2 and Mutant 3 possess intermediate phenotypes with regards to sporozoite infectivity.

Table 5.1. Effects of IMC1a mutations on *Plasmodium berghei* development in *Anopheles stephensi*

_____

Exp.	Parasite line IMC1a/mCherry-	Mean ± sem oocyst number per infected mosquito (n)[a]	Mean salivary gland sporozoite number per infected mosquito[b]
1	WT	39 ± 7 (20)	10,938
	KO	47 ± 8 (20)	0
2	WT	104 ± 42 (10)	6,556
	Mutant 1	97 ± 32 (10)	111
	Mutant 2	98 ± 27 (10)	2,800
3	Mutant 1	94 ± 13 (20)	260
	Mutant 2	133 ± 24 (20)	3,107
4	WT	109 ± 31 (10)	4,917
	Mutant 1	141 ± 50 (10)	224
	Mutant 4	120 ± 44 (10)	5,556
5	Mutant 2	34 ± 9 (20)	2,016
	Mutant 3	36 ± 9 (20)	2,750
6	WT	160 ± 33 (10)	16,600
	Mutant 2	192 ± 30 (10)	3,900
7	Mutant 1	47 ± 11 (10)	333
	Mutant 4	78 ± 25 (10)	9,900

_____

[a] n = Number of insects analysed.
[b] The same insects were analysed for both oocyst and sporozoite numbers. Oocyst counts were done on individual midguts, sporozoite counts were done on pooled salivary glands from n insects.

Discussion

In this study we have employed red fluorescent protein tagging in transgenic *P. berghei* parasites to confirm the subcellular localization and expression of the alveolin IMC1a in the SPN of sporozoites, and to study the function of its terminal cysteine residues. The results obtained show that mutagenesis of the conserved terminal cysteine motifs of IMC1a has a profound effect of the amount of IMC1a detectable in the cell (Fig. 5.4A). Because all transgenic parasite lines used here were generated with the same gene targeting strategy, and express IMC1a from the same, native *imc1a* promoter (Fig. 5.2A), the observed reductions in expression level are most likely a consequence of reduced protein stability. This is supported by the fact that *imc1a* transcript levels in Mutant 1 are not reduced (Fig. 5.4B). One possible explanation for the alveolin instability is that the removal of cysteines in the mutant proteins has changed their ability to form specific sulphur bridges, leading to a degree of misfolding and degradation by the proteasome. Arguing against this concept, however, is the localization of IMC1a in the cytoplasm, a reducing environment that disfavours formation of intra- or intermolecular sulphur bridges. Indeed, in non-reducing protein gels IMC1a migrates as a monomeric protein (Khater *et al.*, 2004). Another explanation for the observed alveolin instability is that the removal of cysteine residues in IMC1a adversely affected the ability of the proteins to be lipid modified. One of such modifications that occurs on cysteine residues is S-palmitoylation (Resh, 2013) and indeed several alveolins have been predicted to be palmitoylated (Anderson-White *et al.*, 2011b). *Plasmodium* proteomics studies (Bowyer *et al.*, 2011; Florens *et al.*, 2002; Hall *et al.*, 2005; Lasonder *et al.*, 2002; Pease *et al.*, 2013; Silvestrini *et al.*, 2010; Solyakov *et al.*, 2011; Treeck *et al.*, 2011) have detected at least six alveolins in blood stage parasites. Among these six, only two (IMC1c and IMC1g) possess conserved terminal cysteine motifs (Fig. 5.1). Compellingly, only IMC1c and IMC1g are detected in the blood stage palmitome (Jones *et al.*, 2012), providing strong support for a link between these motifs and palmitoylation. In fact, our results obtained with the IMC1a mutants are not without precedent: Protein instability and degradation was also shown for two known palmitoylated IMC-resident proteins (*Pf*GAP45 and

*Pf*MTIP) when their palmitoylation was prevented using palmitoylation inhibitors or mutagenesis of palmitoylation sites (Jones *et al.*, 2012). This adds further support to the view that IMC1a is palmitoylated via its terminal cysteine motifs. Palmitoylation of alveolins is thought to promote their association with the IMC via lipid anchoring into the IMC membranes. A reduced level of IMC1a palmitoylation could therefore adversely affect its targeting to the IMC and/or its recruitment to the SPN, which in turn could result in degradation of IMC1a. Palmitoylation could also be directly involved in IMC1a folding and stability (Resh, 2013).

Gene disruption studies of different *P. berghei* alveolins have revealed very similar loss-of-function phenotypes (Kaneko *et al.*, 2015; Khater *et al.*, 2004; Tremp and Dessens, 2011; Tremp *et al.*, 2008; Volkmann *et al.*, 2012), indicating that alveolins contribute to the function of the SPN by a similar mechanism. While co-expressed alveolins make distinct contributions to SPN function in a given zoite, these differences appear to be mainly quantitative. For example, null mutants sporozoites of the alveolin IMC1h have an abnormal shape and reduced infectivity not dissimilar from IMC1a null mutants (Tremp and Dessens, 2011). However, in contrast to the latter, IMC1h-KO sporozoites retain infectivity to the insect's salivary glands (Volkmann *et al.*, 2012). Re-examination of the IMC1h-KO sporozoite size with the footprint method developed here shows that they are in fact significantly larger than IMC1a null mutant sporozoites (footprint IMC1h-KO: 7.98 ± 0.44 μm^2; P<0.0001). Perhaps not surprisingly, these observations point to a correlation between sporozoite size and infectivity, which is corroborated by the results of the current IMC1a study.

The intermediate phenotypes of IMC1a/mCherry-Mutant 1 and Mutant 2 with regards to sporozoite shape and infectivity (Fig. 5.4, Table 5.1) indicate that the heavily depleted amount of IMC1a protein in their sporozoites remains at least partly functional. The low levels of IMC1a::mCherry in these mutants did not allow a definitive allocation of the fusion protein in the sporozoite SPN by fluorescence microscopy (Fig. 5.3). However, failure to localize to the functional site would arguably have resulted in a complete loss-of-function phenotype, which is clearly not the case. In further support for this notion, subcellular localization of *Pf*GAP45

lacking its palmitoylation site was shown to be unaffected, remaining at the IMC of developing merozoites (Anderson-White *et al.*, 2011b). In fact, these parasite lines are effectively IMC1a knockdowns, and combined with our observations that the severity of the phenotypes correlates well with the levels of IMC1a found in the parasite, this strongly indicates that IMC1a facilitates sporozoite morphogenesis and infectivity in a dose-dependent fashion. This demonstrates for the first time a link between the amount of alveolin in the zoite and its infectivity. Accordingly, SPN function in the cell is governed not only by the repertoire of co-expressed alveolins, but also by the level of their expression. Fitting with the nature of structural proteins, this finding suggests that the relative abundance of an alveolin in the cell may determine its relative contribution to the cortical cytoskeleton. In support of this concept, it is perhaps not a coincidence that knockout of the ookinete-expressed alveolin IMC1d has no detectable phenotype, and also has the lowest expression level of all ookinete-expressed alveolins examined by us (Al-Khattaf *et al.*, 2015; Tremp *et al.*, 2014; Tremp and Dessens, 2011; Tremp *et al.*, 2008). It was surprising to discover that just a fraction of IMC1a (10%-21% of WT level in Mutant 1 and Mutant 2, Fig. 5.4A) is sufficient to partially restore the phenotype of IMC1a null mutant parasites (Fig. 5.4C, Table 5.1), pointing to a non-linear correlation between alveolin level and phenotype, possibly due to the complexity of interactions with other alveolins and SPN components.

Studies with *Tg*IMC1, the *Toxoplasma gondii* orthologue of *Plasmodium* IMC1a, have revealed a specific proteolytic cleavage near the carboxy-terminus of the protein (Mann *et al.*, 2002). This cleavage coincides with, and is thought to be required for, the maturation of young parasites with a detergent-labile SPN into mature parasites with a detergent-resistant SPN. Furthermore, ablation of this cleavage through mutagenesis of certain C-terminal residues prevents the SPN to mature and become detergent-resistant (Mann *et al.*, 2002). In the case of *Plasmodium berghei* IMC1a, there is no evidence for a similar cleavage event. Western analysis of our parasite lines expressing IMC1a fused to a carboxy-terminal mCherry tag shows that sporozoites contain predominantly full-length IMC1a::mcherry fusion product (Fig. 5.3B), and that if such a cleavage occurred in

Plasmodium it would at best affect a very small proportion of the protein. This is likely to reflect specific differences between *Toxoplasma* and *Plasmodium*. One notable difference is the formation of *Plasmodium* sporozoites within a protective oocyst capsule, which arguably eliminates the need to develop within the protection of mechanically stable and rigid mother cell as is the case in *Toxoplasma* (Mann *et al.*, 2002). Despite this major difference between PbIMC1a and TgIMC1, there is also an interesting parallel between the two in that the double cysteine rather than the single cysteine in the motif is identified as the chief contributor. In *Tg*IMC1 one cysteine residue within the double cysteine is essential for the *Tg*IMC1 cleavage, while in IMC1a the double cysteine is responsible for the protein-stabilizing properties of the motif. If these alveolin orthologues are indeed post-translationally palmitoylated, the double cysteine would seem the more likely site for this modification. Further studies are underway to investigate this hypothesis.

Conflict of interest

The authors declare that they have no conflict of interest with the contents of this article.

Author contributions

AZT generated and analyzed parasite line IMC1a/mCherry-WT and provided technical assistance with other experiments. AE-H carried out site-directed mutagenesis. FSA-K generated all other constructs and parasite lines and performed and analyzed genotyping and phenotyping experiments. JTD was involved in all aspects of this study. All authors approved the final version of the manuscript.

5.6. References

Al-Khattaf, F. S., Tremp, A. Z., and Dessens, J. T. (2015) *Plasmodium* alveolins possess distinct but structurally and functionally related multi-repeat domains. *Parasitol Res* 115, 631-639

Anderson-White, B. R., Ivey, F. D., Cheng, K., Szatanek, T., Lorestani, A., Beckers, C. J., Ferguson, D. J., Sahoo, N., and Gubbels, M. J. (2011) A family of intermediate filament-like proteins is sequentially assembled into the cytoskeleton of Toxoplasma gondii. *Cellular microbiology*

Bannister, L. H., Hopkins, J. M., Fowler, R. E., Krishna, S., and Mitchell, G. H. (2000) A brief illustrated guide to the ultrastructure of *Plasmodium falciparum* asexual blood stages. *Parasitol Today* 16, 427-433

Bowyer, P. W., Simon, G. M., Cravatt, B. F., and Bogyo, M. (2011) Global profiling of proteolysis during rupture of *Plasmodium falciparum* from the host erythrocyte. *Mol Cell Prot* 10, M110 001636

Dessens, J. T., Beetsma, A. L., Dimopoulos, G., Wengelnik, K., Crisanti, A., Kafatos, F. C., and Sinden, R. E. (1999) CTRP is essential for mosquito infection by malaria ookinetes. *EMBO J* 18, 6221-6227

Florens, L., Washburn, M. P., Raine, J. D., Anthony, R. M., Grainger, M., Haynes, J. D., Moch, J. K., Muster, N., Sacci, J. B., Tabb, D. L., Witney, A. A., Wolters, D., Wu, Y., Gardner, M. J., Holder, A. A., Sinden, R. E., Yates, J. R., and Carucci, D. J. (2002) A proteomic view of the *Plasmodium falciparum* life cycle. *Nature* 419, 520-526

Gould, S. B., Tham, W. H., Cowman, A. F., McFadden, G. I., and Waller, R. F. (2008) Alveolins, a new family of cortical proteins that define the protist infrakingdom Alveolata. *Mol Biol Evol* 25, 1219-1230

Hall, N., Karras, M., Raine, J. D., Carlton, J. M., Kooij, T. W., Berriman, M., Florens, L., Janssen, C. S., Pain, A., Christophides, G. K., James, K., Rutherford, K., Harris, B., Harris, D., Churcher, C., Quail, M. A., Ormond, D., Doggett, J., Trueman, H. E., Mendoza, J., Bidwell, S. L., Rajandream, M. A., Carucci, D. J., Yates, J. R., 3rd, Kafatos, F. C., Janse, C. J., Barrell, B., Turner, C. M., Waters, A. P., and Sinden, R. E. (2005) A comprehensive survey of the *Plasmodium* life cycle by genomic, transcriptomic, and proteomic analyses. *Science* 307, 82-86

Herrmann, H., and Aebi, U. (2004) Intermediate filaments: molecular structure, assembly mechanism, and integration into functionally distinct intracellular Scaffolds. *Annu Rev Biochem* 73, 749-789

Jones, M. L., Collins, M. O., Goulding, D., Choudhary, J. S., and Rayner, J. C. (2012) Analysis of protein palmitoylation reveals a pervasive role in *Plasmodium* development and pathogenesis. *Cell Host Microbe* 12, 246-258

Kaneko, I., Iwanaga, S., Kato, T., Kobayashi, I., and Yuda, M. (2015) Genome-Wide Identification of the Target Genes of AP2-O, a Plasmodium AP2-Family Transcription Factor. *PLoS Pathogens* 11, e1004905

Khater, E. I., Sinden, R. E., and Dessens, J. T. (2004) A malaria membrane skeletal protein is essential for normal morphogenesis, motility, and infectivity of sporozoites. *J Cell Biol* 167, 425-432

Lasonder, E., Ishihama, Y., Andersen, J. S., Vermunt, A. M., Pain, A., Sauerwein, R. W., Eling, W. M., Hall, N., Waters, A. P., Stunnenberg, H. G., and Mann, M. (2002) Analysis of the *Plasmodium falciparum* proteome by high-accuracy mass spectrometry. *Nature* 419, 537-542

Mann, T., and Beckers, C. (2001) Characterization of the subpellicular network, a filamentous membrane skeletal component in the parasite *Toxoplasma gondii. Mol Biochem Parasitol* 115, 257-268

Mann, T., Gaskins, E., and Beckers, C. (2002) Proteolytic processing of TgIMC1 during maturation of the membrane skeleton of Toxoplasma gondii. *Journal Biol Chem* 277, 41240-41246

Morrissette, N. S., and Sibley, L. D. (2002) Cytoskeleton of apicomplexan parasites. *Microbiol Mol Biol Rev* 66, 21-38

Pease, B. N., Huttlin, E. L., Jedrychowski, M. P., Talevich, E., Harmon, J., Dillman, T., Kannan, N., Doerig, C., Chakrabarti, R., Gygi, S. P., and Chakrabarti, D. (2013) Global analysis of protein expression and phosphorylation of three stages of *Plasmodium falciparum* intraerythrocytic development. *J Prot Res* 12, 4028-4045

Resh, M. D. (2013) Covalent lipid modifications of proteins. *Curr Biol* 23, R431-435

Saeed, S., Carter, V., Tremp, A. Z., and Dessens, J. T. (2010) *Plasmodium berghei* crystalloids contain multiple LCCL proteins. *Mol Biochem Parasitol* 170, 49-53

Santos, J. M., Lebrun, M., Daher, W., Soldati, D., and Dubremetz, J. F. (2009) Apicomplexan cytoskeleton and motors: key regulators in morphogenesis, cell division, transport and motility. *Int J Parasitol* 39, 153-162

Sennepin, A. D., Charpentier, S., Normand, T., Sarre, C., Legrand, A., and Mollet, L. M. (2009) Multiple reprobing of Western blots after inactivation of peroxidase activity by its substrate, hydrogen peroxide. *Analytical biochemistry* 393, 129-131

Silvestrini, F., Lasonder, E., Olivieri, A., Camarda, G., van Schaijk, B., Sanchez, M., Younis Younis, S., Sauerwein, R., and Alano, P. (2010) Protein export marks the early

phase of gametocytogenesis of the human malaria parasite *Plasmodium falciparum*. *Mol Cell Prot* 9, 1437-1448

Solyakov, L., Halbert, J., Alam, M. M., Semblat, J. P., Dorin-Semblat, D., Reininger, L., Bottrill, A. R., Mistry, S., Abdi, A., Fennell, C., Holland, Z., Demarta, C., Bouza, Y., Sicard, A., Nivez, M. P., Eschenlauer, S., Lama, T., Thomas, D. C., Sharma, P., Agarwal, S., Kern, S., Pradel, G., Graciotti, M., Tobin, A. B., and Doerig, C. (2011) Global kinomic and phospho-proteomic analyses of the human malaria parasite *Plasmodium falciparum*. *Nat Comm* 2, 565

Treeck, M., Sanders, J. L., Elias, J. E., and Boothroyd, J. C. (2011) The phosphoproteomes of *Plasmodium falciparum* and *Toxoplasma gondii* reveal unusual adaptations within and beyond the parasites' boundaries. *Cell Host Microbe* 10, 410-419

Tremp, A. Z., Al-Khattaf, F. S., and Dessens, J. T. (2014) Distinct temporal recruitment of Plasmodium alveolins to the subpellicular network. *Parasitol Res* 113, 4177-4188

Tremp, A. Z., and Dessens, J. T. (2011) Malaria IMC1 membrane skeleton proteins operate autonomously and participate in motility independently of cell shape. *J Biol Chem* 286, 5383-5391

Tremp, A. Z., Khater, E. I., and Dessens, J. T. (2008) IMC1b is a putative membrane skeleton protein involved in cell shape, mechanical strength, motility, and infectivity of malaria ookinetes. *J Biol Chem* 283, 27604-27611

Volkmann, K., Pfander, C., Burstroem, C., Ahras, M., Goulding, D., Rayner, J. C., Frischknecht, F., Billker, O., and Brochet, M. (2012) The alveolin IMC1h is required for normal ookinete and sporozoite motility behaviour and host colonisation in *Plasmodium berghei*. *PloS One* 7, e41409

Waters, A. P., Thomas, A. W., van Dijk, M. R., and Janse, C. J. (1997) Transfection of malaria parasites. *Methods* 13, 134-147

Chapter 6

Palmitoylation of the

Plasmodium berghei alveolin IMC1c

occurs through its carboxy-terminal cysteine motif

and is functionally dispensable

Research Paper Cover Sheet

SECTION A – Student Details

Student	Fatimah Al-Khattaf
Principal Supervisor	Johannes Dessens
Thesis Title	Functional characterization of the alveolins, a family of cytoskeleton proteins of malaria parasites

SECTION C – Prepared for publication, but not yet published

Where is the work intended to be published?	Molecular and Biochemical Parasitology
Please list the paper's authors in the intended authorship order:	Al-Khattaf F, Tremp AZ, Dessens JT
Stage of publication	Not yet submitted

SECTION D – Multi-authored work

For multi-authored work, give full details of your role in the research included in the paper and in the preparation of the paper. (Attach a further sheet if necessary)	Student generated the mCherry-tagged IMC1c mutant parasite line and performed and analyszed genotyping and phenotyping experiments including palmitoylation assays. Student contributed to the preparation of the paper (text and figures).

Student Signature: _____   Date: _____

Supervisor Signature: _____   Date: _____

Palmitoylation of the *Plasmodium berghei* alveolin IMC1c occurs through its carboxy-terminal cysteine motif and is functionally dispensable

Fatimah S. Al-Khattaf, Annie Z. Tremp, and Johannes T. Dessens

Pathogen Molecular Biology Department, Faculty of Infectious and Tropical Diseases, London School of Hygiene and Tropical Medicine, Keppel Street, London WC1E 7HT, UK

Correspondence should be addressed to Johannes T. Dessens, LSHTM, Keppel Street, WC1E 7HT, London, UK, Tel.: +442079272865; Fax: +442076374314; E-mail: Johannes.Dessens@lshtm.ac.uk

Abstract

S-palmitoylation is a post-translational lipid modification that is widespread among *Plasmodium* proteins and functions as a key regulator of malaria parasite development in both vertebrate host and mosquito vector. Little is known about the contribution of palmitoylation to the function of individual parasite molecules. Alveolins form a conserved family of intermediate filament proteins in apicomplexan parasites that are characterized by conserved tandem repeat domains thought to be necessary for their filament-forming features. A subset of alveolins also possess conserved cysteine motifs situated near the ends of the proteins. The role of these motifs in alveolin function is unknown. Here, we use a modified acyl-biotin exchange protocol and transgenic *Plasmodium berghei* parasites to show that the alveolin IMC1c, a protein essential for asexual blood stage development, is palmitoylated on its carboxy-terminal cysteine motif. Mutant parasites lacking the cysteine motif in IMC1c displayed apparently normal development in mouse and mosquito, suggesting that the essential nature of protein palmitoylation at a cellular level may arise from cumulative small fitness gains at a molecular level, which are relatively insignificant when considered individually.

Introduction

Three invasive life stages: the ookinete, sporozoite and merozoite, feature among the many different developmental forms of the malaria parasite. These so-called 'zoites' are characterized by having secretory organelles (e.g. rhoptries and micronemes) as well as a specialized cortical structure termed the pellicle, which are required for their motile and invasive properties. A double membrane structure termed the inner membrane complex (IMC) situated directly underneath the plasma membrane defines the pellicle (Bannister *et al.*, 2000; Morrissette and Sibley, 2002; Santos *et al.*, 2009). In addition, a network of intermediate filaments termed the subpellicular network (SPN), which supports the pellicle membranes and provides mechanical strength (Mann and Beckers, 2001), is located on the cytoplasmic face of the IMC. Components of the SPN include a family of proteins termed alveolins (Khater *et al.*, 2004; Mann and Beckers, 2001). In the genus *Plasmodium*, 13 conserved and syntenic alveolin family members have been identified that are differentially expressed among the three zoites stages (Al-Khattaf *et al.*, 2015; Kaneko *et al.*, 2015). It has been shown in the rodent malaria species *P. berghei* that disruption of alveolins gives rise to morphological abnormalities that are accompanied by reduced tensile strength of the zoite stages in which they are expressed (Kaneko *et al.*, 2015; Khater *et al.*, 2004; Tremp and Dessens, 2011; Tremp *et al.*, 2008; Volkmann *et al.*, 2012). *Plasmodium* alveolins also have roles in parasite gliding motility (Khater *et al.*, 2004; Tremp and Dessens, 2011; Tremp *et al.*, 2008; Volkmann *et al.*, 2012) most likely by tethering components of the glideosome that reside in the IMC. Alveolins are characterised by having one or more highly conserved domains separated by regions of variable length and amino acid composition (Al-Khattaf *et al.*, 2015). We have recently shown that these conserved 'alveolin' domains are composed of tandem repeat sequences of typically 12 amino acid residues (Al-Khattaf *et al.*, 2015). In addition to these conserved domains, a subset of the alveolins also possess conserved cysteine motifs close to their amino- or carboxy-terminus. These motifs are made up of a single cysteine and a double cysteine that separated by a small number of other amino acids. The function of these cysteine motifs is hitherto unknown, but it is postulated

that they could act as substrates for S-palmitoylation to facilitate the tight connection between the IMC and SPN structures.

S-palmitoylation is a post-translational thioester linkage of the 16-carbon fatty acid palmitate to cysteine residues (Linder and Deschenes, 2007), a reaction that is catalyzed by palmitoyl-S-acyl-transferases (PATs). PATs are identifiable from having a Asp-His-His-Cys (DHHC) motif within a cysteine-rich domain, and at least 12 distinct putative PAT-encoding genes have been identified in *Plasmodium* spp. (Frenal *et al.*, 2013). Localization studies indicate that the subcellular distribution of many PATs restricted to distinct compartments including endoplasmic reticulum (e.g. DHHC7), IMC (e.g. DHHC3 and DHHC9), and rhoptries (e.g. DHHC7) (Frenal *et al.*, 2013). S-palmitoylation in *Plasmodium* affects over 400 proteins and is essential for parasite development both in the vertebrate host (Jones *et al.*, 2012) and in the mosquito vector (Santos *et al.*, 2015). However, little is known about the contribution of this lipid modification to the function of individual parasite proteins. Furthermore, most palmitoylation sites are poorly predictable. This study was aimed at investigating the potential contribution of palmitoylation to the function of the alveolin IMC1c in *P. berghei* (*Pb*IMC1c; PBANKA_120200), as well as the potential role of its cysteine motif in this process. *Pb*IMC1c and its orthologues have a single conserved cysteine motif at their carboxy-terminus and, in *P. falciparum*, the protein has been detected in the palmitoylated proteome of asexual blood stages (Jones *et al.*, 2012) indicating that it is indeed palmitoylated. *Pb*IMC1c is expressed in all three *Plasmodium* zoites where it displays a cortical localization consistent with that of the SPN, and is essential for asexual blood stage parasite development (Tremp *et al.*, 2014).

Results

Parasite line IMC1c/mCherry, which expresses full-length IMC1c fused to a carboxy-terminal red fluorescent protein tag (mCherry variant), was generated by double crossover homologous recombination (Figure 6.1A). IMC1c has a single cysteine motif at its carboxy-terminal end (Figure 6.1B) and to study its contribution to IMC1c function, a specific mutation substituting the three cysteines was introduced by site-directed mutagenesis (Figure 6.1B). To do so, plasmid pLP-IMC1c/mCherry (Tremp *et al.*, 2014) was PCR amplified with primers IMC1C-mut1-F (CTCGAGACAGGTACATGGAGAAGCTTAGGGGCCCTC) and IMC1C-Mut1-R (CCATGTACCTGTCTCGAGTCCAACTGGTTTAGCTTCTTCA) and circularized by in-fusion to give plasmid pLP-IMC1c/mCherry-Mutant 1. The mutation introduced a diagnostic *Xho*I restriction site at the same time. The presence of the mutation was confirmed by sequence analysis of the resulting plasmid DNA (data not shown). The resulting targeting vector was digested with *Kpn*I and *Sac*II to remove the plasmid backbone prior to transfection of purified *P. berghei* schizonts as described (Tremp *et al.*, 2014). Pyrimethamine-resistant parasites were selected and dilution cloned to give parasite line IMC1c/mCherry-Mutant 1. Diagnostic PCR across the 5'-integration site with primers IMC1c-long5'UTR-F (P3) (GGCTCTCAAATTCTTGGAAG) and pDNR-mCherry-R (P4) (AACGGGATCTTCTAGTTACTTGTACAGCTCGTCCATGC) gave rise to a 4.5kb product, as was the case for the corresponding IMC1c/mCherry line, demonstrating correct integration of the modified allele into the *imc1c* locus (Figure 6.1C, top panel). Moreover, the PCR product amplified from parasite line IMC1c/mCherry-Mutant 1 possessed the unique *Xho*I recognition sequence confirming that the cysteine motif mutation was indeed present (Figure 6.1D). Finally, the absence of the wildtype *imc1c* allele in the transgenic parasite lines was confirmed by diagnostic PCR with primers pDNR-IMC1c-F (P1) (ACGAAGTTATCAGTCGACGGTACCAAGTGCATTTAGTATGTTGTGGC) and IMC1c-3´R (P2) (TTAGAGCCGATTTTATCTTGTTACAC), amplifying an expected 2.3kb fragment from unmodified parental parasites, but not from the clonal transgenic IMC1c/mCherry lines (Figure 6.1C, bottom panel).
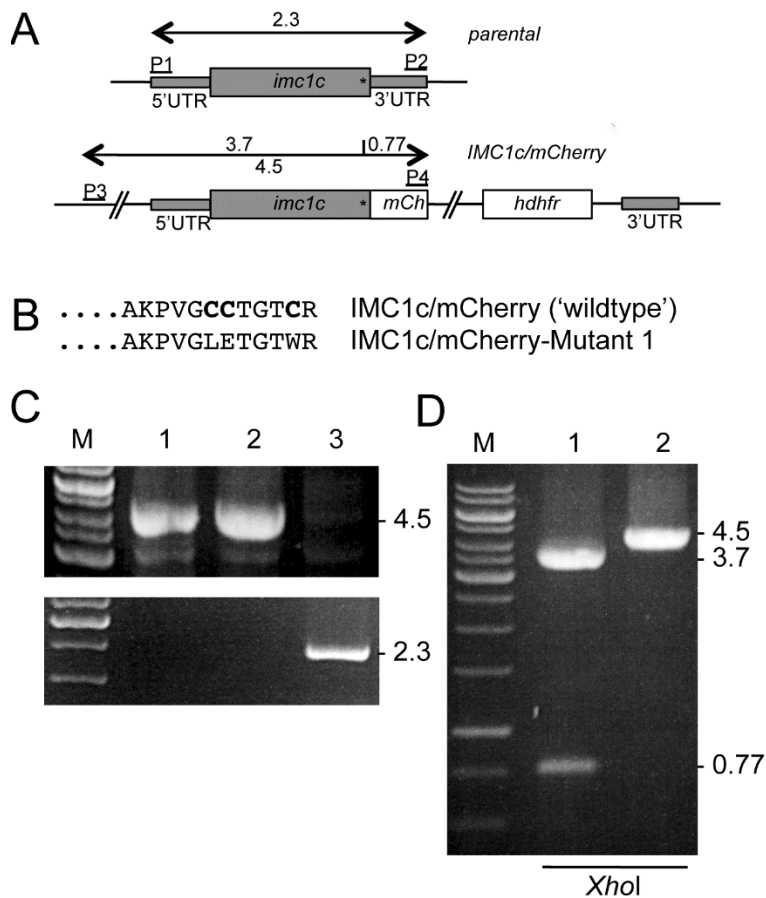
Figure 6.1. Generation and genetic analyses of mCherry-tagged PbIMC1c parasite lines. A: Schematic diagram of the unmodified (parental) and modified (IMC1c/mCherry) imc1c alleles. The imc1c gene is indicated with coding sequence (wide grey bars) and 5' and 3' untranslated regions (UTRs, narrow grey bars). Also indicated is the relative positions of the terminal cysteine motif (asterisk), the mCherry module (mCh); the hDHFR selectable marker gene cassette (hdhfr); and primers used for diagnostic PCR amplification (P1-P4). **B**: Amino acid sequences of the carboxy-terminal sequences of PbIMC1c in parasite lines IMC1c/mCherry (unmodified, wildtype sequence) and IMC1c/mCherry-Mutant 1. The conserved cysteines are marked in bold. **C**: PCR with primers P3 and P4 across the 5' integration site diagnostic for the presence of the mCherry-tagged pbimc1c alleles (top panel), and PCR with primers P1 and P2 diagnostic for the presence/absence of the unmodified pbimc1c allele (bottom panel), carried out on genomic DNA from clonal populations of parasite line IMC1c/mCherry-Mutant 1 (lane 1), IMC1c/mCherry (lane 2) and unmodified parental parasites (lane 3). **D**: XhoI restriction enzyme digestion of the PCR amplicon from C, diagnostic for the presence/absence of the carboxy-terminal cysteine motif mutation. Cleavage products of 3.7kb and 0.77kb are visible in parasite line IMC1c/mCherry-Mutant 1 (lane 1), but not in IMC1c/mCherry (lane 2), as expected.
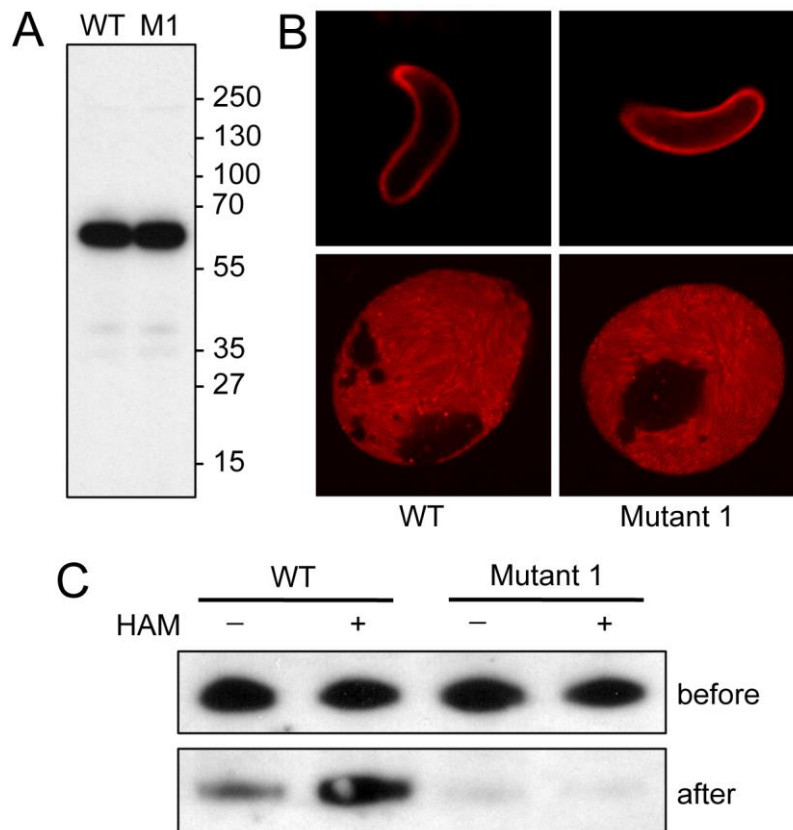
Parasite lines IMC1c/mCherry and IMC1c/mCherry-Mutant 1 developed normally in the mouse and displayed red fluorescence in the asexual blood stages and macrogametocytes when examined by UV microscopy (data not shown), similar to the fluorescence reported for parasite line IMC1c/GFP that expresses GFP-tagged IMC1c (Tremp *et al.*, 2014). Consistent with this observation, western blot analysis of blood stage parasites of both parasite lines using anti-mCherry antibodies revealed a strong band of approximately 60kDa, corresponding to the IMC1c::mCherry fusion proteins (Figure 6.2A). In the mosquito, too, parasite line IMC1c/mCherry-Mutant 1 developed normally and was indistinguishable from its wildtype counterpart in terms of IMC1c expression level (based on fluorescence intensity) and subcellular distribution: the latter was concentrated at the cortex of ookinetes and sporozoites consistent with a localization in the SPN/pellicle (Figure 6.2B). Moreover, both transgenic parasite lines were readily transmitted to naive mice by sporozoite-infected mosquito bite. These results demonstrate that the carboxy-terminal cysteine motif of *Pb*IMC1c is dispensable for normal protein function and parasite development in the mouse and mosquito.

Palmitoylation of IMC1c was assessed biochemically using a modification of the acyl-biotin exchange method (Wan *et al.*, 2007). Blood stage parasites from IMC1c/mCherry and IMC1c/mCherry-Mutant 1 were harvested and purified by red blood cell lysis and three washes in phosphate buffered saline (pH 7.4) to remove cellular debris. Parasite pellets were dissolved in lysis buffer (50mM Tris-HCl pH 7.2, 1% SDS, 1x protease inhibitor cocktail (PI, Sigma), 5mM EDTA, 1mM TCEP) and then treated with 40mM N-ethylmaleimide (NEM) overnight at 4°C with nutation to block free cysteines. SDS, TCEP and NEM were removed from the samples by buffer exchange on Zeba spin desalting columns (Thermo Scientific) equilibrated with hydroxylamine (HAM) buffer (1x PBS pH7.4, 1x PI, 5mM EDTA). Each sample was divided into two equal parts and to each was added an equal volume of HAM buffer supplemented with 2mM EZ-link HPDP-biotin (Thermo Fisher Scientific) and either 100mM HAM (labelled +HAM) or no HAM (labelled −HAM). Samples were incubated 2h at room temperature to allow palmitate-biotin exchange, after which HAM and unbound HPDP-biotin were removed by buffer exchange on Zeba spin

desalting columns equilibrated with HAM buffer supplemented with 0.1% Triton X-100. Streptavidin-agarose suspension (Sigma) was added and the mixture incubated for 1h at room temperature with nutation to allow binding to and subsequent pulldown of the biotinylated protein fraction. Agarose beads were collected by centrifugation, twice washed with HAM buffer plus 1% Triton X-100, and finally resuspended in an equal volume of 2x SDS polyacrylamide gel electrophoresis sample buffer supplemented with 1% β-mercaptoethanol to release biotinylated proteins from the streptavidin-agarose beads. Samples were heated at 70°C for 10min prior to fractionation through NuPage 4-12% Bis-Tris precast gels (Invitrogen).

Western analysis using anti-mCherry antibodies detected IMC1c::mCherry signal in the HAM-treated IMC1c/mCherry (WT) sample that was markedly stronger than in the HAM-negative control relative to pre-pulldown signals (Figure 6.2C). In the absence of HAM, palmitate-biotin exchange does not occur, and thus the increased signal in the HAM-positive sample indicates that *Pb*IMC1c is palmitoylated, which is consistent with the identification of IMC1c in the *P. falciparum* blood stage palmitoylated proteome (Jones *et al.*, 2012) (the signal in the HAM-negative sample is likely the result of some incomplete blocking of free cysteine residues by the earlier NEM treatment). In the IMC1c/mCherry-Mutant 1 samples IMC1c::mCherry signals were barely detectable in either –HAM and +HAM treatments (Figure 6.2C), demonstrating that *Pb*IMC1c is palmitoylated on its carboxy-terminal cysteine motif.

Figure 6.2. Phenotypic analyses of mCherry-tagged PbIMC1c parasite lines. A: Western blot using anti-mCherry antibodies of blood stage parasites from parasite line IMC1c/mCherry (WT) and IMC1c/mCherry-Mutant 1 (M1). Positions of molecular weight markers (PageRuler™ Prestained Protein Ladder +) are shown on the right hand side. **B**: Confocal fluorescence and brightfield images of ookinetes (top panels) and sporulating oocysts (bottom panels) of parasite lines IMC1c/mCherry WT and Mutant 1, showing cortical fluorescence. **C**: Western blot of blood stage parasite lysates of parasite lines IMC1c/mCherry (WT) and -Mutant 1 after acyl-biotin exchange in the absence (− HAM) or presence (+ HAM) of hydroxylamine, before and after pull-down with streptavidin-agarose beads.

Discussion

This study provides, to our knowledge, the first biochemical evidence linking palmitoylation of an alveolin to the terminal cysteine motifs that are present in a subset of these proteins. As IMC1c is an essential protein for blood stage parasites development (Tremp *et al.*, 2014), the lack of an apparent phenotype for the cysteine mutant reported here indicates that palmitoylation of this protein is in fact functionally dispensable. One reason for this functional redundancy could be the fact that *Plasmodium* zoites express multiple alveolin family members simultaneously (Al-Khattaf *et al.*, 2015), and assuming that they interact with each other within the SPN, palmitoylation of other alveolins could compensate for loss of IMC1c palmitoylation. Alternatively, it may be that palmitoylation of IMC1c only marginally enhances its function and hence contributes a fitness gain to the parasite that is too small to detect using our assays. The results shown here for IMC1c contrast with those reported for the sporozoite-expressed alveolin IMC1a: The equivalent mutation of the carboxy-terminal cysteine motif in IMC1a resulted in a marked reduction in IMC1a protein level in sporozoites, accompanied by significant reductions in sporozoite size and infectivity, which points to a role for this motif in alveolin stability (Chapter 5). Given the conserved nature of the alveolin cysteine motifs it is likely that IMC1a, like IMC1c, is palmitoylated on its carboxy-terminal cysteine motif and hence the markedly reduced IMC1a levels observed after mutating this palmitoylation site show that this alveolin is unstable without the lipid modification and degraded. Indeed, a similar phenomenon was described for the palmitoylated and IMC-resident proteins *Pf*MTIP and *Pf*GAP45 (Jones *et al.*, 2012).

What might explain the differences between IMC1a and IMC1c? Using quantitative mass spectrometry, Jones and colleagues (Jones *et al.*, 2012) showed that IMC1c in *P. falciparum* blood stage parasites is highly sensitive to treatment with the PAT inhibitor 2-BMP. Given that absence of palmitoylation does not result in degradation of IMC1c, as shown here (Figure 6.2A), its sensitivity to 2-BMP indicates that its palmitoylation status is highly dynamic (Jones *et al.*, 2012). Indeed, extensive palmitoyl cycling implies that IMC1c would spend a considerable part of its lifetime in a non-palmitoylated state and it makes sense therefore that it should

be stable in the absence of this lipid modification. Conversely, the instability of IMC1a, and proteins like GAP45, MTIP, in the enforced absence of palmitoylation implies that they are normally in a more stable state of palmitoylation. As this study shows, non-palmitoylated IMC1c remains biologically active. Likewise, IMC1a protein with mutated cysteine motifs remains functional, as inferred from the intermediate phenotypes of the IMC1a cysteine motif mutants (Chapter 5). These combined observations suggests that the anti-parasitic activity of PAT inhibitors like 2-BMP is perhaps not so much caused by changes in protein activity that may accompany imposed absence of palmitoylation, but rather by the resulting instability and degradation of a subset of PAT substrates.

Acknowledgements

References

Al-Khattaf FS, Tremp AZ, Dessens JT. *Plasmodium* alveolins possess distinct but structurally and functionally related multi-repeat domains. Parasitol Res. 2015;115:631-39.

Bannister LH, Hopkins JM, Fowler RE, Krishna S, Mitchell GH. A brief illustrated guide to the ultrastructure of *Plasmodium falciparum* asexual blood stages. Parasitol Today. 2000;16:427-33.

Frenal K, Tay CL, Mueller C, Bushell ES, Jia Y, Graindorge A, et al. Global analysis of apicomplexan protein S-acyl transferases reveals an enzyme essential for invasion. Traffic. 2013;14:895-911.

Jones ML, Collins MO, Goulding D, Choudhary JS, Rayner JC. Analysis of protein palmitoylation reveals a pervasive role in *Plasmodium* development and pathogenesis. Cell Host Microbe. 2012;12:246-58.

Kaneko I, Iwanaga S, Kato T, Kobayashi I, Yuda M. Genome-wide identification of the target genes of AP2-O, a *Plasmodium* AP2-family transcription factor. PLoS Pathogens. 2015;11:e1004905.

Khater EI, Sinden RE, Dessens JT. A malaria membrane skeletal protein is essential for normal morphogenesis, motility, and infectivity of sporozoites. J Cell Biol. 2004;167:425-32.

Linder ME, Deschenes RJ. Palmitoylation: policing protein stability and traffic. Nat Rev Mol Cell Biol. 2007;8:74-84.

Mann T, Beckers C. Characterization of the subpellicular network, a filamentous membrane skeletal component in the parasite *Toxoplasma gondii*. Mol Biochem Parasitol. 2001;115:257-68.

Morrissette NS, Sibley LD. Cytoskeleton of apicomplexan parasites. Microbiol Mol Biol Rev. 2002;66:21-38.

Santos JM, Kehrer J, Franke-Fayard B, Frischknecht F, Janse CJ, Mair GR. The *Plasmodium* palmitoyl-S-acyl-transferase DHHC2 is essential for ookinete morphogenesis and malaria transmission. Sci Rep. 2015;5:16034.

Santos JM, Lebrun M, Daher W, Soldati D, Dubremetz JF. Apicomplexan cytoskeleton and motors: key regulators in morphogenesis, cell division, transport and motility. Int J Parasitol. 2009;39:153-62.

Tremp AZ, Al-Khattaf FS, Dessens JT. Distinct temporal recruitment of *Plasmodium* alveolins to the subpellicular network. Parasitol Res. 2014;113:4177-88.

Tremp AZ, Dessens JT. Malaria IMC1 membrane skeleton proteins operate autonomously and participate in motility independently of cell shape. J Biol Chem. 2011;286:5383-91.

Tremp AZ, Khater EI, Dessens JT. IMC1b is a putative membrane skeleton protein involved in cell shape, mechanical strength, motility, and infectivity of malaria ookinetes. J Biol Chem. 2008;283:27604-11.

Volkmann K, Pfander C, Burstroem C, Ahras M, Goulding D, Rayner JC, et al. The alveolin IMC1h is required for normal ookinete and sporozoite motility behaviour and host colonisation in *Plasmodium berghei*. PLoS One. 2012;7:e41409.

Wan J, Roth AF, Bailey AO, Davis NG. Palmitoylated proteins: purification and identification. Nat Prot. 2007;2:1573-84.

Chapter 7

General Discussion

The body of work presented in this thesis has achieved significant advances in our understanding of the *Plasmodium* alveolins. For example, we have identified two alveolins, IMC1c and IMC1e, that are expressed in blood stage parasites and this study shows for the first time that alveolins are essential for blood stage parasite development (Chapter 3). This is important because it is blood stage infection that causes the clinical symptoms in malaria patients. Because the vital function of these two alveolins prevents the generation of knockout parasite lines in the conventional way, as this is dependent on drug selection in the mouse, we have not been able to determine the contribution of these two alveolins in ookinetes and sporozoites where they are also expressed. Disruption of IMC1e and IMC1c in ookinetes and sporozoites could be achieved by a 'promoter swapping' strategy, in which the native promoters are switched with that of another gene that is expressed in blood stage parasites, but not in the mosquito stages. This allows generation of parasites that are effectively mosquito stage-specific knockouts. It would be particularly interesting to test if the formation of normal-shaped ookinetes and sporozoites is possible in the absence of IMC1c, which we predict to be the case given that IMC1c is recruited to the SPN after the zoites have formed.

Chapter 3 also highlights surprising differences in alveolin gene expression in the sexual stages. While IMC1e is translationally repressed in gametocytes and expressed as protein only after fertilization, IMC1c is already expressed as protein in female gametocytes, and is expressed from both maternally and paternally-inherited alleles in the ookinete. IMC1c is nonetheless predicted to be translationally repressed (a phenomenon restricted to female gametocytes) and the observed protein expression of IMC1c in female gametocytes may be the first reported case of 'partial' or 'leaky' translational repression. Available transcriptome data (available via PlasmoDB) indicate that the alveolins IMC1l and IMC1m may have a different gene expression strategy in the sexual stages, because they appear to have high transcript levels only in ookinetes and are not predicted to be translationally repressed, unlike the other ookinete-expressed alveolins. The biological relevance of these different expression strategies is unclear and we can

shed light on this by studying GFP-tagged and knockout parasite lines of IMC1l and IMC1m.

Our studies have also revealed for the first time a level of redundancy among the alveolins, as the knockout of IMC1d did not show any apparent loss-of-function phenotypes (Chapter 4). Indeed, every alveolin studied so far has revealed interesting new aspects of this group of cytoskeletal proteins, and completing the functional characterization of the remaining family members (IMC1f, IMC1j, IMC1k) should be carried out and may provide further new insight into how this protein family operates in *Plasmodium*.

Chapters 5 and 6 of this thesis dealt with the conserved cysteine motifs found in a subset of the alveolins, and their suspected involvement with post-translational palmitoylation. Various proteomics studies predict six alveolins to be expressed in blood stage parasites (i.e. IMC1c, e, f, g, k and l), but only two (IMC1c and g) have been detected in the blood stage palmitome (Jones *et al.*, 2012). Only the latter two alveolins possess conserved cysteine motifs, providing compelling circumstantial evidence for a link between these motifs and palmitoylation. The results obtained with IMC1a show that removal of the cysteine motifs renders the protein unstable and prone to degradation (Chapter 5). Protein instability and degradation also appears to be the fate of at least two proteins that reside in the pellicle (GAP45, MTIP) when their palmitoylation is prevented either using PAT inhibitors or mutagenesis of palmitoylation sites (Jones *et al.*, 2012). This adds compelling support to the hypothesis that IMC1a is indeed palmitoylated via its terminal cysteine motifs. We do however not have direct biochemical evidence that IMC1a is a palmitoylated protein, and future studies will be carried out to address this using a biochemical approach such as ABE.

Our study in Chapter 6 presents the first conclusive link between the cysteine motif and palmitoylation, as we show that mutagenesis of the motif prevents palmitoylation. The results obtained from the IMC1a study indicates that the double cysteine rather than the single cysteine within the cysteine motif constitutes the palmitoylation site. This hypothesis could be tested by further

mutagenesis of the cysteine motif of IMC1c combined with the successful palmitoylation assay of IMC1c/mCherry blood stage parasites (Chapter 6), which should enable us to determine exactly which of the cysteine residues is/are palmitoylated. The question remains whether alveolins that do not naturally have a terminal cysteine motif can still be palmitoylated on other cysteines. This question could be addressed by carrying out the palmitoylation assay on for example parasite lines IMC1e/GFP (does not have a cysteine motif) and use anti-GFP antibodies to detect the fusion proteins in western blot. Conversely, a cysteine motifs could be artificially introduced into this alveolins by allelic replacement to see whether that changes its palmitoylation status (if not already palmitoylated) and if so what the effect is on parasite development.

A surprising result was the difference in behaviour of IMC1a and IMC1c upon mutagenesis of their carboxy-terminal cysteine motif. While IMC1a becomes unstable and is degraded, IMC1c remains stable and seemingly fully functional. We do know from studies in *P. falciparum* that the palmitoylation of IMC1c (and IMC1g) is severely affected by the PAT inhibitor 2-BMP, and this points to a highly dynamic palmitoylation status of this alveolin. In contrast, the instability of IMC1a in the absence of a palmitoyl group (Chapter 5) indicates that it is normally in a stable state of palmitoylation. IMC1a, like most of the alveolins that have been studied, is recruited to the SPN at an early stage of zoite formation. It is tempting to speculate that the palmitoylation dynamics of an alveolin have a bearing on its function/mode of action and perhaps stable palmitoylation is linked to early recruitment to the pellicle (e.g. IMC1a) while dynamic palmitoylation is linked to late pellicle recruitment as shown for IMC1c.

Our results showing that the alveolin domain is composed of tandem repeats of typically 12 amino acids (Chapter 4) has significantly advanced our understanding of alveolin structure, and supports the notion that there is an evolutionary link with articulins and plateins that are found in other protists. This knowledge could be used to generate 'synthetic' alveolins by tandemly linking variable numbers of consensus 12 amino acid repeat sequences. This could be tested by expressing

synthetic alvolins (with a GFP tag) in transgenic parasites and looking for SPN targeting. Moreover, it might be possible to rescue the phenotype of alveolin knockouts by replacing it with a synthetic version. The essential nature of the alveolins in malaria parasite development, their expression throughout the life cycle, and their absence in vertebrates makes them attractive drug targets for malaria treatment, prophylaxis and transmission control. Moreover, such drugs may be active against a broad range of other apicomplexan parasites, as well as against related pathogenic protozoans. In this context a better understanding of the core architecture of the alveolins and their assembly mechanisms is vital, and one aim should be to determine the atomic structure of the alveolins by X-ray crystallography.

References

Aikawa, M., Carter, R., Ito, Y., and Nijhout, M.M. 1984a. New observations on gametogenesis, fertilization, and zygote transformation in *Plasmodium gallinaceum*. *J Protozool*. 31:403-13.

Aikawa, M., Huff, C.G., and Sprinz, H. 1969. Comparative fine structure study of the gametocytes of avian, reptilian, and mammalian malarial parasites. *J Ultrastruct Res*. 26:316-31.

Aikawa, M., Schwartz, A., Uni, S., Nussenzweig, R., and Hollingdale, M. 1984b. Ultrastructure of *in vitro* cultured exoerythrocytic stage of *Plasmodium berghei* in a hepatoma cell line. *Am J Trop Med Hyg*. 33:792-9.

Al-Khattaf, F.S., Tremp, A.Z., and Dessens, J.T. 2015. Plasmodium alveolins possess distinct but structurally and functionally related multi-repeat domains. *Parasitol Res*. 115:631-39.

Aly, A.S., and Matuschewski, K. 2005. A malarial cysteine protease is necessary for *Plasmodium* sporozoite egress from oocysts. *J Exp Med*. 202:225-30.

Amino, R., Thiberge, S., Martin, B., Celli, S., Shorte, S., Frischknecht, F., and Menard, R. 2006. Quantitative imaging of *Plasmodium* transmission from mosquito to mammal. *Nat Med*. 12:220-4.

Anderson-White, B.R., Ivey, F.D., Cheng, K., Szatanek, T., Lorestani, A., Beckers, C.J., Ferguson, D.J., Sahoo, N., and Gubbels, M.J. 2011a. A family of intermediate filament-like proteins is sequentially assembled into the cytoskeleton of *Toxoplasma gondii*. *Cell Microbiol*. 13:18-31.

Anderson-White, B.R., Ivey, F.D., Cheng, K., Szatanek, T., Lorestani, A., Beckers, C.J., Ferguson, D.J., Sahoo, N., and Gubbels, M.J. 2011b. A family of intermediate filament-like proteins is sequentially assembled into the cytoskeleton of Toxoplasma gondii. *Cell Microbiol*.

Andrade, M.A., Perez-Iratxeta, C., and Ponting, C.P. 2001. Protein repeats: structures, functions, and evolution. *J Struct Biol*. 134:117-31.

Andrade, M.A., Ponting, C.P., Gibson, T.J., and Bork, P. 2000. Homology-based method for identification of protein repeats using statistical significance estimates. *J Mol Biol*. 298:521-37.

Arai, M., Billker, O., Morris, H.R., Panico, M., Delcroix, M., Dixon, D., Ley, S.V., and Sinden, R.E. 2001. Both mosquito-derived xanthurenic acid and a host blood-derived factor regulate gametogenesis of *Plasmodium* in the midgut of the mosquito. *Mol Biochem Parasitol*. 116:17-24.

Ausmees, N., Kuhn, J.R., and Jacobs-Wagner, C. 2003. The bacterial cytoskeleton: an intermediate filament-like function in cell shape. *Cell*. 115:705-13.

Bannister, L.H., Butcher, G.A., Dennis, E.D., and Mitchell, G.H. 1975. Studies on the structure and invasive behaviour of merozoites of *Plasmodium knowlesi*. *Trans R Soc Trop Med Hyg*. 69:5.

Bannister, L.H., Hopkins, J.M., Fowler, R.E., Krishna, S., and Mitchell, G.H. 2000. A brief illustrated guide to the ultrastructure of *Plasmodium falciparum* asexual blood stages. *Parasitol Today*. 16:427-33.

Bannister, L.H., Margos, G., and Hopkins, J.M. 2005. Making a home for *Plasmodium* post-genomics: Ultrastructural organization of the blood stages. *In* Molecular Approaches to Malaria. Sherman, I.W., editor. ASM Press, Washinton D.C. 24-49.

Bannister, L.H., and Mitchell, G.H. 1995. The role of the cytoskeleton in *Plasmodium falciparum* merozoite biology: an electron-microscopic view. *Ann Trop Med Parasitol*. 89:105-11.

Bannister, L.H., and Mitchell, G.H. 2009. The malaria merozoite, forty years on. *Parasitology*. 136:1435-44.

Barkhuff, W.D., Gilk, S.D., Whitmarsh, R., Tilley, L.D., Hunter, C., and Ward, G.E. 2011. Targeted disruption of *TgPhIL1* in *Toxoplasma gondii* results in altered parasite morphology and fitness. *PLoS One*. 6:e23977.

Baum, J., Richard, D., Healer, J., Rug, M., Krnajski, Z., Gilberger, T.W., Green, J.L., Holder, A.A., and Cowman, A.F. 2006. A conserved molecular motor drives cell invasion and gliding motility across malaria life cycle stages and other apicomplexan parasites. *J Biol Chem*. 281:5197-208.

Biegert, A., and Soding, J. 2008. De novo identification of highly diverged protein repeats by probabilistic consistency. *Bioinformatics*. 24:807-14.

Billingsley, P.F., and Hecker, H. 1991. Blood digestion in the mosquito, *Anopheles stephensi* Liston (Diptera: Culicidae): activity and distribution of trypsin, aminopeptidase, and alpha-glucosidase in the midgut. *J Med Entomol*. 28:865-71.

Billker, O., Shaw, M.K., Margos, G., and Sinden, R.E. 1997. The roles of temperature, pH and mosquito factors as triggers of male and female gametogenesis of *Plasmodium berghei in vitro. Parasitology*. 115 (Pt 1):1-7.

Blader, I.J., Coleman, B.I., Chen, C.T., and Gubbels, M.J. 2015. Lytic Cycle of Toxoplasma gondii: 15 Years Later. *Annu Rev Microbiol*.

Bowyer, P.W., Simon, G.M., Cravatt, B.F., and Bogyo, M. 2011. Global profiling of proteolysis during rupture of Plasmodium falciparum from the host erythrocyte. *Mol Cell Proteomics*. 10:M110 001636.

Brown, J.H., Cohen, C., and Parry, D.A. 1996. Heptad breaks in alpha-helical coiled coils: stutters and stammers. *Proteins*. 26:134-45.

Carter, V., Shimizu, S., Arai, M., and Dessens, J.T. 2008. PbSR is synthesized in macrogametocytes and involved in formation of the malaria crystalloids. *Mol Microbiol*. 68:1560-9.

Claudianos, C., Dessens, J.T., Trueman, H.E., Arai, M., Mendoza, J., Butcher, G.A., Crompton, T., and Sinden, R.E. 2002. A malaria scavenger receptor-like protein essential for parasite development. *Mol Microbiol*. 45:1473-84.

Cyrklaff, M., Kudryashev, M., Leis, A., Leonard, K., Baumeister, W., Menard, R., Meissner, M., and Frischknecht, F. 2007. Cryoelectron tomography reveals periodic material at the inner side of subpellicular microtubules in apicomplexan parasites. *J Exp Med*. 204:1281-7.

de Melo, E.J., and de Souza, W. 1997. A cytochemistry study of the inner membrane complex of the pellicle of tachyzoites of *Toxoplasma gondii. Parasitol Res*. 83:252-6.

Dearnley, M.K., Yeoman, J.A., Hanssen, E., Kenny, S., Turnbull, L., Whitchurch, C.B., Tilley, L., and Dixon, M.W. 2012. Origin, composition, organization and function of the inner membrane complex of *Plasmodium falciparum* gametocytes. *J Cell Sci*. 125:2053-63.

Dessens, J.T., Beetsma, A.L., Dimopoulos, G., Wengelnik, K., Crisanti, A., Kafatos, F.C., and Sinden, R.E. 1999. CTRP is essential for mosquito infection by malaria ookinetes. *Embo J*. 18:6221-7.

Dessens, J.T., Mendoza, J., Claudianos, C., Vinetz, J.M., Khater, E., Hassard, S., Ranawaka, G.R., and Sinden, R.E. 2001. Knockout of the rodent malaria parasite chitinase PbCHT1 reduces infectivity to mosquitoes. *Infect Immun*. 69:4041-7.

Dietrich, L.E., and Ungermann, C. 2004. On the mechanism of protein palmitoylation. *EMBO Rep*. 5:1053-7.

Dobrowolski, J.M., Carruthers, V.B., and Sibley, L.D. 1997. Participation of myosin in gliding motility and host cell invasion by *Toxoplasma gondii. Mol Microbiol*. 26:163-73.

Douradinha, B., Augustijn, K.D., Moore, S.G., Ramesar, J., Mota, M.M., Waters, A.P., Janse, C.J., and Thompson, J. 2011. *Plasmodium* Cysteine Repeat Modular Proteins 3 and 4 are essential for malaria parasite transmission from the mosquito to the host. *Malar J*. 10:71.

Drisdel, R.C., and Green, W.N. 2004. Labeling and quantifying sites of protein palmitoylation. *Biotechniques*. 36:276-85.

Dubremetz, J.F., and Elsner, Y.Y. 1979. Ultrastructural study of schizogony of *Eimeria bovis* in cell cultures. *J Protozool*. 26:367-76.

Engelmann, S., Silvie, O., and Matuschewski, K. 2009. Disruption of *Plasmodium* sporozoite transmission by depletion of sporozoite invasion-associated protein 1. *Eukaryot Cell*. 8:640-8.

Florens, L., Washburn, M.P., Raine, J.D., Anthony, R.M., Grainger, M., Haynes, J.D., Moch, J.K., Muster, N., Sacci, J.B., Tabb, D.L., Witney, A.A., Wolters, D., Wu, Y., Gardner, M.J., Holder, A.A., Sinden, R.E., Yates, J.R., and Carucci, D.J. 2002. A proteomic view of the *Plasmodium falciparum* life cycle. *Nature*. 419:520-6.

Fowler, R.E., Fookes, R.E., Lavin, F., Bannister, L.H., and Mitchell, G.H. 1998. Microtubules in *Plasmodium falciparum* merozoites and their importance for invasion of erythrocytes. *Parasitology*. 117 (Pt 5):425-33.

Frenal, K., Tay, C.L., Mueller, C., Bushell, E.S., Jia, Y., Graindorge, A., Billker, O., Rayner, J.C., and Soldati-Favre, D. 2013. Global analysis of apicomplexan protein S-acyl transferases reveals an enzyme essential for invasion. *Traffic*. 14:895-911.

Fukumoto, S., Xuan, X., Inoue, N., Igarashi, I., Sugimoto, C., Fujisaki, K., Nagasawa, H., Mikami, T., and Suzuki, H. 2003. Molecular characterization of a gene encoding a 29-kDa cytoplasmic protein of *Babesia gibsoni* and evaluation of its diagnostic potentiality. *Mol Biochem Parasitol*. 131:129-36.

Gould, S.B., Kraft, L.G., van Dooren, G.G., Goodman, C.D., Ford, K.L., Cassin, A.M., Bacic, A., McFadden, G.I., and Waller, R.F. 2011. Ciliate pellicular proteome identifies novel protein families with characteristic repeat motifs that are common to alveolates. *Mol Biol Evol*. 28:1319-31.

Gould, S.B., Tham, W.H., Cowman, A.F., McFadden, G.I., and Waller, R.F. 2008. Alveolins, a new family of cortical proteins that define the protist infrakingdom Alveolata. *Mol Biol Evol*. 25:1219-30.

Gubbels, M.J., Wieffer, M., and Striepen, B. 2004. Fluorescent protein tagging in *Toxoplasma gondii*: identification of a novel inner membrane complex component conserved among Apicomplexa. *Mol Biochem Parasitol*. 137:99-110.

Hall, N., Karras, M., Raine, J.D., Carlton, J.M., Kooij, T.W., Berriman, M., Florens, L., Janssen, C.S., Pain, A., Christophides, G.K., James, K., Rutherford, K., Harris, B., Harris, D., Churcher, C., Quail, M.A., Ormond, D., Doggett, J., Trueman, H.E., Mendoza, J., Bidwell, S.L., Rajandream, M.A., Carucci, D.J., Yates, J.R., 3rd, Kafatos, F.C., Janse, C.J., Barrell, B., Turner, C.M., Waters, A.P., and Sinden, R.E. 2005. A comprehensive survey of the *Plasmodium* life cycle by genomic, transcriptomic, and proteomic analyses. *Science*. 307:82-6.

Han, Y.S., and Barillas-Mury, C. 2002. Implications of Time Bomb model of ookinete invasion of midgut cells. *Insect Biochem Mol Biol*. 32:1311-6.

Han, Y.S., Thompson, J., Kafatos, F.C., and Barillas-Mury, C. 2000. Molecular interactions between *Anopheles stephensi* midgut cells and *Plasmodium berghei*: the time bomb theory of ookinete invasion of mosquitoes. *Embo J*. 19:6030-40.

Hegedus, D., Erlandson, M., Gillott, C., and Toprak, U. 2009. New insights into peritrophic matrix synthesis, architecture, and function. *Annu Rev Entomol*. 54:285-302.

Heger, A., and Holm, L. 2000. Rapid automatic detection and alignment of repeats in protein sequences. *Proteins*. 41:224-37.

Herrmann, H., and Aebi, U. 2004. Intermediate filaments: molecular structure, assembly mechanism, and integration into functionally distinct intracellular scaffolds. *Annu Rev Biochem*. 73:749-89.

Huber, M., Cabib, E., and Miller, L.H. 1991. Malaria parasite chitinase and penetration of the mosquito peritrophic membrane. *Proc Natl Acad Sci U S A*. 88:2807-10.

Huttenlauch, I., Geisler, N., Plessmann, U., Peck, R.K., Weber, K., and Stick, R. 1995. Major epiplasmic proteins of ciliates are articulins: cloning, recombinant expression, and structural characterization. *J Cell Biol*. 130:1401-12.

Huttenlauch, I., Peck, R.K., Plessmann, U., Weber, K., and Stick, R. 1998a. Characterisation of two articulins, the major epiplasmic proteins comprising the membrane skeleton of the ciliate *Pseudomicrothorax*. *J Cell Sci*. 111 (Pt 14):1909-19.

Huttenlauch, I., Peck, R.K., and Stick, R. 1998b. Articulins and epiplasmins: two distinct classes of cytoskeletal proteins of the membrane skeleton in protists. *J Cell Sci*. 111 (Pt 22):3367-78.

Huttenlauch, I., and Stick, R. 2003. Occurrence of articulins and epiplasmins in protists. *J Eukaryot Microbiol*. 50:15-8.

Janse, C.J., Ramesar, J., and Waters, A.P. 2006. High-efficiency transfection and drug selection of genetically transformed blood stages of the rodent malaria parasite *Plasmodium berghei*. *Nat Protoc*. 1:346-56.

Janse, C.J., and Waters, A.P. 2007. The exoneme helps malaria parasites to break out of blood cells. *Cell*. 131:1036-8.

Jones, M.L., Collins, M.O., Goulding, D., Choudhary, J.S., and Rayner, J.C. 2012. Analysis of protein palmitoylation reveals a pervasive role in Plasmodium development and pathogenesis. *Cell Host Microbe*. 12:246-58.

Kadota, K., Ishino, T., Matsuyama, T., Chinzei, Y., and Yuda, M. 2004. Essential role of membrane-attack protein in malarial transmission to mosquito host. *Proc Natl Acad Sci U S A*. 101:16310-5.

Kaneko, I., Iwanaga, S., Kato, T., Kobayashi, I., and Yuda, M. 2015. Genome-Wide Identification of the Target Genes of AP2-O, a Plasmodium AP2-Family Transcription Factor. *PLoS Pathog*. 11:e1004905.

Kappe, S.H., Kaiser, K., and Matuschewski, K. 2003. The *Plasmodium* sporozoite journey: a rite of passage. *Trends Parasitol*. 19:135-43.

Kariu, T., Yuda, M., Yano, K., and Chinzei, Y. 2002. MAEBL is essential for malarial sporozoite infection of the mosquito salivary gland. *J Exp Med*. 195:1317-23.

Kaushal, D.C., Carter, R., Howard, R.J., and McAuliffe, F.M. 1983. Characterization of antigens on mosquito midgut stages of *Plasmodium gallinaceum*. I. Zygote surface antigens. *Mol Biochem Parasitol*. 8:53-69.

Khan, S.M., Franke-Fayard, B., Mair, G.R., Lasonder, E., Janse, C.J., Mann, M., and Waters, A.P. 2005. Proteome analysis of separated male and female gametocytes reveals novel sex-specific Plasmodium biology. *Cell*. 121:675-87.

Khater, E.I., Sinden, R.E., and Dessens, J.T. 2004. A malaria membrane skeletal protein is essential for normal morphogenesis, motility, and infectivity of sporozoites. *J Cell Biol*. 167:425-32.

Kloetzel, J.A., Baroin-Tourancheau, A., Miceli, C., Barchetta, S., Farmar, J., Banerjee, D., and Fleury-Aubusson, A. 2003a. Cytoskeletal proteins with N-terminal signal peptides: plateins in the ciliate *Euplotes* define a new family of articulins. *J Cell Sci*. 116:1291-303.

Kloetzel, J.A., Baroin-Tourancheau, A., Miceli, C., Barchetta, S., Farmar, J., Banerjee, D., and Fleury-Aubusson, A. 2003b. Plateins: a novel family of signal peptide-containing articulins in euplotid ciliates. *J Eukaryot Microbiol*. 50:19-33.

Kono, M., Herrmann, S., Loughran, N.B., Cabrera, A., Engelberg, K., Lehmann, C., Sinha, D., Prinz, B., Ruch, U., Heussler, V., Spielmann, T., Parkinson, J., and Gilberger, T.W. 2012. Evolution and architecture of the inner membrane complex in asexual and sexual stages of the malaria parasite. *Mol Biol Evol*. 29:2113-32.

Kudryashev, M., Lepper, S., Stanway, R., Bohn, S., Baumeister, W., Cyrklaff, M., and Frischknecht, F. 2010. Positioning of large organelles by a membrane- associated cytoskeleton in Plasmodium sporozoites. *Cell Microbiol*. 12:362-71.

Kudryashev, M., Munter, S., Lemgruber, L., Montagna, G., Stahlberg, H., Matuschewski, K., Meissner, M., Cyrklaff, M., and Frischknecht, F. 2012. Structural basis for chirality and directional motility of *Plasmodium* sporozoites. *Cell Microbiol*.

Lasonder, E., Ishihama, Y., Andersen, J.S., Vermunt, A.M., Pain, A., Sauerwein, R.W., Eling, W.M., Hall, N., Waters, A.P., Stunnenberg, H.G., and Mann, M. 2002. Analysis of the *Plasmodium falciparum* proteome by high-accuracy mass spectrometry. *Nature*. 419:537-42.

Linder, M.E., and Deschenes, R.J. 2007. Palmitoylation: policing protein stability and traffic. *Nat Rev Mol Cell Biol*. 8:74-84.

Lindner, S.E., Swearingen, K.E., Harupa, A., Vaughan, A.M., Sinnis, P., Moritz, R.L., and Kappe, S.H. 2013. Total and putative surface proteomics of malaria parasite salivary gland sporozoites. *Mol Cell Proteomics*. 12:1127-43.

Lopez-Barragan, M.J., Lemieux, J., Quinones, M., Williamson, K.C., Molina-Cruz, A., Cui, K., Barillas-Mury, C., Zhao, K., and Su, X.Z. 2011. Directional gene expression and antisense transcripts in sexual and asexual stages of Plasmodium falciparum. *BMC Genomics*. 12:587.

Luckhart, S., Vodovotz, Y., Cui, L., and Rosenberg, R. 1998. The mosquito *Anopheles stephensi* limits malaria parasite development with inducible synthesis of nitric oxide. *Proc Natl Acad Sci U S A*. 95:5700-5.

Mair, G.R., Braks, J.A., Garver, L.S., Wiegant, J.C., Hall, N., Dirks, R.W., Khan, S.M., Dimopoulos, G., Janse, C.J., and Waters, A.P. 2006. Regulation of sexual development of *Plasmodium* by translational repression. *Science*. 313:667-9.

Mann, T., and Beckers, C. 2001. Characterization of the subpellicular network, a filamentous membrane skeletal component in the parasite *Toxoplasma gondii. Mol Biochem Parasitol*. 115:257-68.

Mann, T., Gaskins, E., and Beckers, C. 2002. Proteolytic processing of TgIMC1 during maturation of the membrane skeleton of *Toxoplasma gondii. J Biol Chem*. 277:41240-6.

Marrs, J.A., and Bouck, G.B. 1992. The two major membrane skeletal proteins (articulins) of *Euglena gracilis* define a novel class of cytoskeletal proteins. *J Cell Biol*. 118:1465-75.

Meis, J.F., and Ponnudurai, T. 1987. Ultrastructural studies on the interaction of Plasmodium falciparum ookinetes with the midgut epithelium of Anopheles stephensi mosquitoes. *Parasitol Res*. 73:500-6.

Meis, J.F., Pool, G., van Gemert, G.J., Lensen, A.H., Ponnudurai, T., and Meuwissen, J.H. 1989. Plasmodium falciparum ookinetes migrate intercellularly through Anopheles stephensi midgut epithelium. *Parasitol Res*. 76:13-9.

Meis, J.F., Verhave, J.P., Jap, P.H., and Meuwissen, J.H. 1985. Transformation of sporozoites of *Plasmodium berghei* into exoerythrocytic forms in the liver of its mammalian host. *Cell Tissue Res*. 241:353-60.

Menard, R. 2001. Gliding motility and cell invasion by Apicomplexa: insights from the *Plasmodium* sporozoite. *Cell Microbiol*. 3:63-73.

Mercier, C., Adjogble, K.D., Daubener, W., and Delauw, M.F. 2005. Dense granules: are they key organelles to help understand the parasitophorous vacuole of all apicomplexa parasites? *Int J Parasitol*. 35:829-49.

Moon, R.W., Taylor, C.J., Bex, C., Schepers, R., Goulding, D., Janse, C.J., Waters, A.P., Baker, D.A., and Billker, O. 2009. A cyclic GMP signalling module that regulates gliding motility in a malaria parasite. *PLoS Pathog*. 5:e1000599.

Morrissette, N.S., Murray, J.M., and Roos, D.S. 1997. Subpellicular microtubules associate with an intramembranous particle lattice in the protozoan parasite *Toxoplasma gondii. J Cell Sci*. 110 (Pt 1):35-42.

Morrissette, N.S., and Sibley, L.D. 2002. Cytoskeleton of apicomplexan parasites. *Microbiol Mol Biol Rev*. 66:21-38; table of contents.

Mota, M.M., Pradel, G., Vanderberg, J.P., Hafalla, J.C., Frevert, U., Nussenzweig, R.S., Nussenzweig, V., and Rodriguez, A. 2001. Migration of *Plasmodium* sporozoites through cells before infection. *Science*. 291:141-4.

Myung, J.M., Marshall, P., and Sinnis, P. 2004. The *Plasmodium* circumsporozoite protein is involved in mosquito salivary gland invasion by sporozoites. *Mol Biochem Parasitol*. 133:53-9.

Pasvol, G. 2010. Protective hemoglobinopathies and Plasmodium falciparum transmission. *Nat Genet*. 42:284-5.

Pease, B.N., Huttlin, E.L., Jedrychowski, M.P., Talevich, E., Harmon, J., Dillman, T., Kannan, N., Doerig, C., Chakrabarti, R., Gygi, S.P., and Chakrabarti, D. 2013. Global analysis of protein expression and phosphorylation of three stages of Plasmodium falciparum intraerythrocytic development. *J Proteome Res*. 12:4028-45.

Pradel, G., Garapaty, S., and Frevert, U. 2002. Proteoglycans mediate malaria sporozoite targeting to the liver. *Mol Microbiol*. 45:637-51.

Raabe, A.C., Billker, O., Vial, H.J., and Wengelnik, K. 2009. Quantitative assessment of DNA replication to monitor microgametogenesis in *Plasmodium berghei. Mol Biochem Parasitol*. 168:172-6.

Raibaud, A., Lupetti, P., Paul, R.E., Mercati, D., Brey, P.T., Sinden, R.E., Heuser, J.E., and Dallai, R. 2001. Cryofracture electron microscopy of the ookinete pellicle of *Plasmodium gallinaceum* reveals the existence of novel pores in the alveolar membranes. *J Struct Biol*. 135:47-57.

Raine, J.D., Ecker, A., Mendoza, J., Tewari, R., Stanway, R.R., and Sinden, R.E. 2007. Female inheritance of malarial lap genes is essential for mosquito transmission. *PLoS Pathog*. 3:e30.

Resh, M.D. 1999. Fatty acylation of proteins: new insights into membrane targeting of myristoylated and palmitoylated proteins. *Biochim Biophys Acta*. 1451:1-16.

Resh, M.D. 2013. Covalent lipid modifications of proteins. *Curr Biol*. 23:R431-5.

Roth, A.F., Wan, J., Bailey, A.O., Sun, B., Kuchar, J.A., Green, W.N., Phinney, B.S., Yates, J.R., 3rd, and Davis, N.G. 2006. Global analysis of protein palmitoylation in yeast. *Cell*. 125:1003-13.

Saeed, S., Carter, V., Tremp, A.Z., and Dessens, J.T. 2010. *Plasmodium berghei* crystalloids contain multiple LCCL proteins. *Mol Biochem Parasitol*. 170:49-53.

Saeed, S., Tremp, A.Z., and Dessens, J.T. 2012. Conformational co-dependence between *Plasmodium berghei* LCCL proteins promotes complex formation and stability. *Mol Biochem Parasitol*. 185:170-3.

Santos, J.M., Kehrer, J., Franke-Fayard, B., Frischknecht, F., Janse, C.J., and Mair, G.R. 2015. The Plasmodium palmitoyl-S-acyl-transferase DHHC2 is essential for ookinete morphogenesis and malaria transmission. *Sci Rep*. 5:16034.

Santos, J.M., Lebrun, M., Daher, W., Soldati, D., and Dubremetz, J.F. 2009. Apicomplexan cytoskeleton and motors: key regulators in morphogenesis, cell division, transport and motility. *Int J Parasitol*. 39:153-62.

Sennepin, A.D., Charpentier, S., Normand, T., Sarre, C., Legrand, A., and Mollet, L.M. 2009. Multiple reprobing of Western blots after inactivation of peroxidase activity by its substrate, hydrogen peroxide. *Anal Biochem*. 393:129-31.

Shahabuddin, M., and Kaslow, D.C. 1994. *Plasmodium*: parasite chitinase and its role in malaria transmission. *Exp Parasitol*. 79:85-8.

Sherman, I.W. 2005. The life of *Plasmodium*: an overview. *In* Molecular Approaches to Malaria. Sherman, I.W., editor. ASM Press, Washington D.C. 3-11.

Silvestrini, F., Lasonder, E., Olivieri, A., Camarda, G., van Schaijk, B., Sanchez, M., Younis Younis, S., Sauerwein, R., and Alano, P. 2010. Protein export marks the early phase of gametocytogenesis of the human malaria parasite Plasmodium falciparum. *Mol Cell Proteomics*. 9:1437-48.

Sinden, R.E. 1978. Cell Biology. *In* Rodent Malaria. Peters, R.K.-K.a.W., editor. Academic Press, London. 85-168.

Sinden, R.E., Alavi, Y.I.H., Butcher, G.A., Dessens, J.T., Raine, J.D., and Trueman, H.E. 2004. Ookinete Cell Biology. *In* Malaria Parasites: Genomes and Molecular Biology. Waters, A.P. and Janse, C., editors. Caister Academic press, Wymondham.

Sinden, R.E., and Billingsley, P.F. 2001. *Plasmodium* invasion of mosquito cells: hawk or dove? *Trends Parasitol*. 17:209-12.

Sinden, R.E., and Garnham, P.C. 1973. A comparative study on the ultrastructure of *Plasmodium* sporozoites within the oocyst and salivary glands, with particular reference to the incidence of the micropore. *Trans R Soc Trop Med Hyg*. 67:631-7.

Sinden, R.E., and Matuschewski, K. 2005. The Sporozoite. *In* Molecular Approaches to Malaria. Sherman, I.W., editor. ASM Press, Washington, D.C. 169-190.

Sinden, R.E., and Strong, K. 1978. An ultrastructural study of the sporogonic development of *Plasmodium falciparum* in *Anopheles gambiae. Trans R Soc Trop Med Hyg*. 72:477-91.

Soldati, D., and Meissner, M. 2004. *Toxoplasma* as a novel system for motility. *Curr Opin Cell Biol*. 16:32-40.

Solyakov, L., Halbert, J., Alam, M.M., Semblat, J.P., Dorin-Semblat, D., Reininger, L., Bottrill, A.R., Mistry, S., Abdi, A., Fennell, C., Holland, Z., Demarta, C., Bouza, Y., Sicard, A., Nivez, M.P., Eschenlauer, S., Lama, T., Thomas, D.C., Sharma, P., Agarwal, S., Kern, S., Pradel, G., Graciotti, M., Tobin, A.B., and Doerig, C. 2011. Global kinomic and phospho-proteomic analyses of the human malaria parasite Plasmodium falciparum. *Nat Commun*. 2:565.

Sultan, A.A., Thathy, V., Frevert, U., Robson, K.J., Crisanti, A., Nussenzweig, V., Nussenzweig, R.S., and Menard, R. 1997. TRAP is necessary for gliding motility and infectivity of *Plasmodium* sporozoites. *Cell*. 90:511-22.

Tewari, R., Rathore, D., and Crisanti, A. 2005. Motility and infectivity of *Plasmodium berghei* sporozoites expressing avian *Plasmodium gallinaceum* circumsporozoite protein. *Cell Microbiol*. 7:699-707.

Tomas, A.M., Margos, G., Dimopoulos, G., van Lin, L.H., de Koning-Ward, T.F., Sinha, R., Lupetti, P., Beetsma, A.L., Rodriguez, M.C., Karras, M., Hager, A., Mendoza, J., Butcher, G.A., Kafatos, F., Janse, C.J., Waters, A.P., and Sinden, R.E. 2001. P25 and P28 proteins of the malaria ookinete surface have multiple and partially redundant functions. *Embo J*. 20:3975-83.

Treeck, M., Sanders, J.L., Elias, J.E., and Boothroyd, J.C. 2011. The phosphoproteomes of Plasmodium falciparum and Toxoplasma gondii reveal unusual adaptations within and beyond the parasites' boundaries. *Cell Host Microbe*. 10:410-9.

Tremp, A.Z., Al-Khattaf, F.S., and Dessens, J.T. 2014. Distinct temporal recruitment of Plasmodium alveolins to the subpellicular network. *Parasitol Res*. 113:4177-88.

Tremp, A.Z., Carter, V., Saeed, S., and Dessens, J.T. 2013. Morphogenesis of Plasmodium zoites is uncoupled from tensile strength. *Mol Microbiol*. 89:552-64.

Tremp, A.Z., and Dessens, J.T. 2011. Malaria IMC1 membrane skeleton proteins operate autonomously and participate in motility independently of cell shape. *J Biol Chem*. 286:5383-91.

Tremp, A.Z., Khater, E.I., and Dessens, J.T. 2008. IMC1b is a putative membrane skeleton protein involved in cell shape, mechanical strength, motility, and infectivity of malaria ookinetes. *J Biol Chem*. 283:27604-11.

Vanderberg, J., and Rhodin, J. 1967. Differentiation of nuclear and cytoplasmic fine structure during sporogonic development of *Plasmodium berghei. J Cell Biol*. 32:C7-10.

Vlachou, D., Zimmermann, T., Cantera, R., Janse, C.J., Waters, A.P., and Kafatos, F.C. 2004. Real-time, *in vivo* analysis of malaria ookinete locomotion and mosquito midgut invasion. *Cell Microbiol*. 6:671-85.

Volkmann, K., Pfander, C., Burstroem, C., Ahras, M., Goulding, D., Rayner, J.C., Frischknecht, F., Billker, O., and Brochet, M. 2012. The alveolin IMC1h is required for normal ookinete and sporozoite motility behaviour and host colonisation in *Plasmodium berghei. PLoS One*. 7:e41409.

Wan, J., Roth, A.F., Bailey, A.O., and Davis, N.G. 2007. Palmitoylated proteins: purification and identification. *Nat Protoc*. 2:1573-84.

Wang, Q., Fujioka, H., and Nussenzweig, V. 2005. Exit of *Plasmodium* sporozoites from oocysts is an active process that involves the circumsporozoite protein. *PLoS Pathog*. 1:e9.

Waters, A.P., Thomas, A.W., van Dijk, M.R., and Janse, C.J. 1997. Transfection of malaria parasites. *Methods*. 13:134-47.

WHO. 2015. World Malaria Report 2015.

Yeoh, S., O'Donnell, R.A., Koussis, K., Dluzewski, A.R., Ansell, K.H., Osborne, S.A., Hackett, F., Withers-Martinez, C., Mitchell, G.H., Bannister, L.H., Bryans, J.S., Kettleborough, C.A., and Blackman, M.J. 2007. Subcellular discharge of a serine protease mediates release of invasive malaria parasites from host erythrocytes. *Cell*. 131:1072-83.

Yeoman, J.A., Hanssen, E., Maier, A.G., Klonis, N., Maco, B., Baum, J., Turnbull, L., Whitchurch, C.B., Dixon, M.W., and Tilley, L. 2011. Tracking Glideosome-associated protein 50 reveals the development and organization of the inner membrane complex of *Plasmodium falciparum. Eukaryot Cell*. 10:556-64.

Ying, P., Shakibaei, M., Patankar, M.S., Clavijo, P., Beavis, R.C., Clark, G.F., and Frevert, U. 1997. The malaria circumsporozoite protein: interaction of the conserved regions I and II-plus with heparin-like oligosaccharides in heparan sulfate. *Exp Parasitol*. 85:168-82.

Yuda, M., Yano, K., Tsuboi, T., Torii, M., and Chinzei, Y. 2001. von Willebrand Factor A domain-related protein, a novel microneme protein of the malaria ookinete highly conserved throughout *Plasmodium* parasites. *Mol Biochem Parasitol*. 116:65-72.

Zieler, H., and Dvorak, J.A. 2000. Invasion *in vitro* of mosquito midgut cells by the malaria parasite proceeds by a conserved mechanism and results in death of the invaded midgut cells. *Proc Natl Acad Sci U S A*. 97:11516-21.